UNIVERSITY OF GENOVA

PHD PROGRAM IN BIOENGINEERING AND ROBOTICS

Coupling Robot-aided assessment and surface electromyography to evaluate wrist and forearm muscles activity, muscle fatigue and its effect on proprioception

by

Maddalena Mugnosso

Thesis submitted for the degree of *Doctor of Philosophy* (32° cycle)

December 2019

Prof. Pietro Morasso	Supervisor
Dr. Jacopo Zenzeri	Supervisor

Thesis Jury:

Prof. Domenico Campolo, *Nanyang Technological University*	External examiner
Prof. Angelo Basteris, *Southern Denmark University*	External examiner
Prof. Maura Casadio, *University of Genoa*	External examiner

Dibris

Department of Informatics, Bioengineering, Robotics and Systems Engineering

A mio nonno

Declaration

I hereby declare that except where specific reference is made to the work of others, the contents of this dissertation are original and have not been submitted in whole or in part for consideration for any other degree or qualification in this, or any other university. This dissertation is my own work and contains nothing which is the outcome of work done in collaboration with others, except as specified in the text and Acknowledgements. This dissertation contains fewer than 65,000 words including appendices, bibliography, footnotes, tables and equations and has fewer than 150 figures.

Maddalena Mugnosso
January 2020

Acknowledgements

First, I'd like to thank my supervisor Prof. Pietro Morasso for his guidance and mentorship and my supervisor Jacopo Zenzeri for all his patience and teaching over the past three years.
I would also like to thank all of my present and past colleagues of the RBCS unit, who shared with me this amazing journey filling it with passion for science and happy moments.
In particular, thanks Francesca for all your encouragement and tips throughout my PhD and thanks Amel for your constant presence and support.
I would also like to thank and acknowledge all of our colleagues at the Brock University, Prof. Michael Holmes, Garrick Forman, Davis Forman, Ashley Reece, Kailynn Mannella and Robert Kumar not only for their precious help with experiments and analysis presented in this thesis but also for being exceptional hosts.
Finally, a huge thanks to my family and all of my friends, for their unconditional love.

Pubblications

Journal Articles

M. Mugnosso, F. Marini, M.W.R. Holmes, P. Morasso, J. Zenzeri. “Muscle fatigue assessment during robot-mediated movements”. J. Neuroeng. Rehabil. 15, 119. doi:10.1186/s12984-018-0463-y

M. Mugnosso, J. Zenzeri, C.M.L. Hughes, F. Marini.“Coupling robot-aided assessement and surface electromyography (sEMG) to evaluate the effect of muscle fatigue on wrist position sense”. Frontiers in human neuroscience, 2019, 13: 396. doi: 10.3389/fnhum.2019.00396.

R. Iandolo, F. Marini, M. Semprini, M. Laffranchi, M. Mugnosso, A. Cherif, L. De Michieli, M. Chiappalone, J. Zenzeri. “Perspectives and challenges in robotic neurorehabilitation”. Applied Sciences. 2019, 9, 3183; doi:10.3390/app9153183

M. Mugnosso, F. Marini, L. Doglio, C. Panicucci, C. Bruno, P. Moretti, P. Morasso, J. Zenzeri. "Robot-aided assessment of peripheral muscular fatigue in children with neuromuscular disorders.” In preparation for J. Neuroeng. Rehabil.

D.A. Forman, G.N. Forman, E.J. Avila-Mireles, M. Mugnosso, J. Zenzeri, B. Murphy, M.W.R. Holmes. “Characterizing forearm muscle activity during dynamic wrist flexion-extension movement using a wrist robot”. Under review for J. of Biomechanics

D.A. Forman, G.N. Forman, E.J. Avila-Mireles, M. Mugnosso, J. Zenzeri, B. Murphy, M.W.R. Holmes. “Characterizing forearm muscle activity during dynamic wrist radial-ulnar movement using a wrist robot”. Under Review for J. of Biomechanics

A. Reece, F. Marini, M. Mugnosso, G. Frost, P. Sullivan, M. Zabihhosseinian, J. Zenzeri, M.W.R. Holmes. Investigating the Effects of Subclinical Neck Pain, Cervical Treatment, and Neck Muscle Fatigue on Wrist Joint Position Sense. Submitted to Journal of Manipulative and Physiological Therapeutics

Conferences Proceedings

M. Mugnosso, F. Marini, P. Morasso, J. Zenzeri. A novel method for muscle fatigue assessment during robot-based tracking tasks. In International Conference on Rehabilitation Robotics (ICORR); 2017 (pp. 84–9).

M. Mugnosso, F. Marini, L. Doglio, C. Panicucci, C. Bruno, P. Moretti, P. Morasso, J. Zenzeri. Quantitative Muscle Fatigue Assessment in Neuromuscular Disorders: A Pilot Study on Duchenne Pediatric Subjects. In International Conference on NeuroRehabilitation; 2018 (pp. 459-463).

Other conferences and symposia

M. Mugnosso, F. Marini, P. Morasso, L. Doglio, C. Bruno, P. Moretti and J. Zenzeri. Un nuovo test per la valutazione della fatica muscolare in pazienti con patologie neuromuscolari. Congresso Nazionale SIMFER 2017. October 2017. Genova.

M. Mugnosso, F. Marini, P. Morasso, J. Zenzeri. How to determine muscle fatigue from superficial forearm muscles: a novel robot-based protocol. PACE Workshop. October 2017. Genova.

M. Mugnosso, F. Marini, L. Doglio, C. Panicucci, C. Bruno, P. Moretti, P. Morasso, J. Zenzeri. Robot-aided assessment of peripheral muscular fatigue in children with neuromuscular disorders. XVIII Congresso Nazionale Associazione Italiana Miologia. June 2018. Genova.

M. Mugnosso, F. Marini, L. Doglio, C. Panicucci, C. Bruno, P. Moretti, P. Morasso, J. Zenzeri. Coupling robotic tasks and surface electromyography to assess muscle fatigue in children with neuromuscular diseases. XXI International Society of Electrophysiology and Kinesiology Congress. June 2018. Dublin.

M. Mugnosso, F. Marini, L. Doglio, C. Panicucci, C. Bruno, P. Moretti, P. Morasso, J. Zenzeri. Coupling a robotic task and sEMG to assess muscle fatigue in children with neuromuscular disorders. Workshop Innovation in Rehabilitation Technologies. March 2019. Genova.

D.A. Forman, G.N. Forman, M. Mugnosso, J. Zenzeri, B. Murphy, M.W.R. Holmes. The influence of isometric wrist flexor/extensor fatigue on hand tracking performance using a haptic wrist robot. XXVII Congress of the International Society of Biomechanics. July 2019. Calgary

K. Mannella, G.N. Forman, M. Mugnosso, J. Zenzeri, M.W.R. Holmes. The effects of grip force on wrist kinematics in response to sudden perturbations. XXVII Congress of the International Society of Biomechanics. July 2019. Calgary

Abstract

Sensorimotor functions and an intact neural control of muscles are essential for the effective execution of movements during daily living tasks. However, despite the ability of human sensorimotor system to cope with a great diversity of internal and external demands and constraints, these mechanisms can be altered as a consequence of neurological disorders, injuries or just due to excessive effort leading to muscle fatigue.

A precise assessment of both motor and sensory impairment is thus needed in order to provide useful cues to monitor the progression of the disease in pathological populations or to prevent injuries in case of workers.

In particular, considering muscle fatigue, an objective assessment of its manifestation may be crucial when dealing with subjects with neuromuscular disorders for understanding how specific disease features evolve over time or for testing the efficacy of a potential therapeutic strategy. Indeed, muscle fatigue accounts for a significant portion of the disease burden in populations with neuromuscular diseases but, despite its importance, a standardized, reliable and objective method for fatigue measurement is lacking in clinical practice. The work presented in this thesis investigates a practical solution through the use of a robotic task and parameters extracted by surface electromyography signals.

Moreover, a similar approach that combines robot-mediated proprioception test and muscle fatigue assessment has been developed and used in this thesis to objectively investigate the influence of muscle fatigue on position sense.

Finally, the effect of posture on muscle activity, from a perspective of injuries prevention, has been examined. Data on adults and children have been collected and quantitative and objective information about muscle activity, muscle fatigue and joint sensitivity were obtained gaining useful insight both in the clinical context and in the prevention of workplace injuries.

A novel method to assess muscle fatigue has been proposed together with the definition of an easy readable indicator that can help clinicians in the assessment of the patient. As for the impact of fatigue on the sensorimotor system, results obtained showed a decrease in wrist proprioceptive acuity which led also to a decline in the performance of a simple tracing task.

Regarding the adoption of different muscle strategies depending on postures, results showed that muscle activity of forearm muscles was overall similar regardless from the postures.

Table of contents

List of figures

List of tables

Nomenclature

Acronyms / Abbreviations

AP	Action Potential
ARV	Average Rectified Value
GUI	Graphical User Interface
CAF	Central Activation Failure
CNS	Central Nervous System
CV	Conduction Velocity
DIC	Dorsal Intercarpal
DNS	Direct Numerical Simulation
DoF	Degree of Freedom
DRC	Dorsal Radiocarpal
EDC	Extensor Digitorum Communis
EMG	Electromyography
FDS	Flexor Digitorum Superficialis
MAP	Muscle Action Potential
MDF	Median Frequency
MNF	Mean Frequency
MU	Motor Unit

MVC Maximal Voluntary Contraction

NMJ Neuromuscular Junction

PSD Power Spectral Density

RMS Root Mean Square

ROM Range of Motion

SR Sarcoplasmic Reticulum

Part I

Section One

Introduction

Assessment of disability represents the first step in developing a rehabilitation treatment plan. A systematic approach to evaluate both motor and sensory impairment can provide important cues on the disability itself, on its progression and on the efficacy of the adopted therapies to consequently adapt and modify the rehabilitation protocols in the most efficient way. The implementation of clinical tests on robotic platforms allows for collection of large normative datasets through standard and accurate procedures that yields reliable data at a high resolution (Balasubramanian et al., 2012). The adoption of robotic technologies in the clinical routine could thus improve the quality of the therapeutic approach allowing to detect even subtle changes among patients or rehabilitative sessions and then tailor the therapy on each patient needs in a highly precise way. Moreover, considering the wide range of parameters of physical properties and subject's performance that can be measured during a variety of behaviors in a highly controlled sensory and motor environment, the advantages of robotic devices are not limited to the clinical practice. Indeed, through the development of ad-hoc sensorimotor tasks, robotic devices have provided fundamental insights about motor control and motor learning strategies (Morasso, 1981; Patton and Mussa-Ivaldi, 2004) which continue to motivate further scientific researches.

Starting from these considerations, the studies presented in this thesis exploited the use of robotic devices and surface electromyography to propose effective solutions for objective clinical assessments and to address still open scientific questions.

In particular, given the great impact on voluntary motor control of proprioception and the complexity of muscle fatigue, these two topics are the core of my thesis. Furthermore, all the studies targeted wrist joint and forearm muscles mainly for two reasons: most of the robotic devices developed for rehabilitation and the related studies have targeted the proximal part of the upper limb (shoulder and elbow (Maciejasz et al., 2014)) while only few projects currently exist for the distal upper arm (Gupta et al., 2008; Marini et al., 2017b); wrist and forearm muscles are often exposed to high solicitations (Amini, 2011) that can lead to injuries; unveiling their muscular strategies could help in the prevention of injuries in workplace and in the reduction of ergonomic risk factors for workers.

Chapter one presents the human wrist and forearm muscles from an anatomical and biomechanical perspective.

Chapter two presents an overview of proprioception sense and of muscle fatigue in order to better understand the rationale behind the methodologies adopted in the following experimental studies. It also shows further details about methods presenting the robotic

device used in this thesis.

Chapter three presents three studies carried out to propose an objective muscle fatigue assessment test. The first experiment involved healthy subjects and aimed to prove the repeatability of the test. Next, the second experiment has been conducted to validate the proposed test on a wider healthy population. Finally, we tested subjects with neuromuscular disorders to investigate the feasibility of the test in the clinical practice.

Chapter four presents three experiments involved in the investigation of the alterations of wrist proprioception sense as a consequence of muscle fatigue. In the first study, muscle fatigue was induced by a high fatigue dynamic task while in the second one, muscle fatigue was caused by isometric contractions. Finally, the third experiment investigated changes in wrist proprioception acuity in relation with muscle fatigue or pain in a different body segment.

Chapter five reports an investigation of potential changes in forearm muscle strategies due to different forearm postures. Subjects performed the experiment with their forearm rotated into three different postures in the pronation-supination plane. In addition, seven postures were taken into account as an extension of the previous study.

Finally, **Chapter six** presents the conclusions that could be drawn from the studies included in this thesis.

Chapter 1

The human wrist and forearm muscles

1.1 Introduction

Upper limb structures play a crucial role in our everyday life allowing us both to perform fine movements or to exert a large amount of force. The complexity of the joints and of the muscles in the upper limb reflects the variety of functions they can execute. Among the upper limb joints, the wrist joint, controlled by the muscles in the forearm, is capable of an impressive arc of motion yet retaining a remarkable degree of stability (Volz et al., 1980). Unfortunately, its functionality is often affected as a consequence of neurological disorders or orthopedic impairment. Therefore, in the last decades innovative upper limb robotic devices have been developed in order to effectively help clinicians during the rehabilitation (see (Iandolo et al., 2019) for a review). In the following sections, anatomical and biomechanical aspects of wrist joint and forearm are presented.

1.2 Forearm muscles and Wrist Joint

1.2.1 Forearm

Structure

The forearm is the portion of the arm distal to the elbow and proximal to the wrist. Two bones, the ulna (located medially) and the radius (which runs parallel to it, laterally) form the forearm. These two bones are held together by the intervening interosseous membrane (Figure 1.1). The interosseous membrane and the fibrous intermuscular septa divide the forearm into two compartments: an anterior or ventromedial compartment that contains

the flexor muscles and a posterior or dorsolateral one that contains the extensor muscles. Considering both the compartments, there are twenty muscles that work together to move the elbow, forearm, wrist and digits of the hand and that can be classified either as intrinsic or extrinsic muscles (Mitchell and Whited, 2019):

- the intrinsic muscles function to move the forearm by pronating and supinating the radius and ulna;
- the extrinsic muscles flex and extend the digits of the hand.

One muscle, the brachioradialis, traverses the elbow joint, running from the arm to the wrist, helping to flex the elbow.

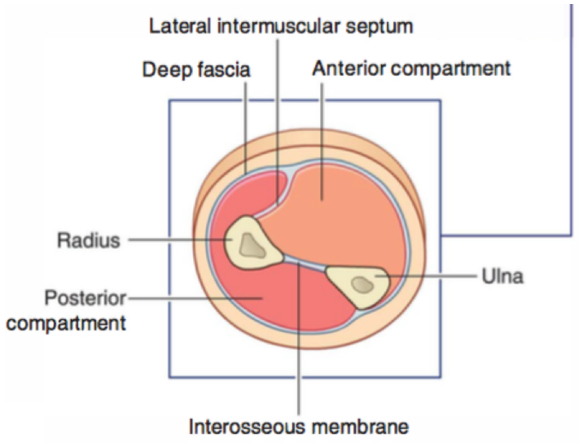

Figure 1.1 Cross section of human forearm muscle. Extracted from (www.memorangapp.com, 2019)

Muscles of the anterior forearm

The anterior compartment of the forearm houses four superficial, one intermediate and three deep muscles. All of the four superficial muscles - the flexor carpi radialis longus, the palmaris longus, the flexor carpi ulnaris, and the pronator teres (shown in Figure 1.2, Panel A)- originate primarily from the medial epicondyle of the humerus, known as the common flexor tendon. The final attachment site for the pronator teres is the middle portion of the radius while the palmaris longus attaches to the flexor retinaculum of the wrist (a fibrous band that covers the carpal bones on the palmar side of the hand near the wrist). Both the flexor carpi radialis and flexor carpi ulnaris insert on the bases of the second and fifth metacarpals, respectively (Lung and Siwiec, 2018). The flexor carpi radialis longus primarily functions to

flex and radially deviate the wrist while also providing minor contribution to elbow flexion and forearm pronation. The flexor carpi ulnaris functions to flex and ulnar deviate the wrist while also providing minor contribution to elbow flexion.
The intermediate layer contains just one muscle – the flexor digitorum superficialis- that crosses the wrist through the carpal tunnel and inserts at the proximal interphalangeal joint at the base of the middle phalanx of digits two through five.
The deep layer of the flexor side of the forearm contains the flexor digitorum profundus, the flexor pollicis longus, and the pronator quadratus. Both the flexor digitorum profundus originates on the proximal three-fourths of the ulna, and the flexor pollicis longus originates on the anterior radius. The flexor digitorium profundus runs with the tendons of the flexor digitorum superficialis and the median nerve through the carpal tunnel to insert on the distal phalanx of digits two through five in the hand (Lung and Burns, 2019). The pronator quadratus originates on the distal anteromedial ulna and inserts on the distal anterolateral radius. It allows for pronation of the forearm.

Muscles of the posterior forearm

Seven superficial and five deep muscles occupy the posterior forearm.
As with the anterior superficial compartment, the majority of the superficial muscles of the posterior compartment – namely the extensor carpi radialis brevis, extensor carpi radialis longus, extensor digitorum, extensor digiti minimi, extensor carpi ulnaris, and anconeus - arise from a common extensor tendon that is the lateral epicondyle of the humerus (as shown in Figure 1.2, Panel B). The extensor carpi radialis longus and brevis attach to the proximal portion of the second and third metacarpals. The tendons of the extensor digitorum run under the extensor retinaculum and divide to attach to the extensor hoods of the middle and distal phalanx of each of the digits two through five. The extensor digiti minimi runs along with the extensor digitorum and inserts into the extensor hood of the fifth digit. The seventh muscle of the superficial layer is the brachioradialis that originates at the lateral supracondylar ridge of the humerus and it attaches on the flexor side of the wrist immediately proximal to the radial styloid (Mitchell and Whited, 2019).
The deep compartment of the extensor side of the forearm contains the adductor pollicis longus, the extensor pollicis longus and brevis, the extensor indicis, and the supinator. Three of the muscles originate from the ulna, the adductor pollicis longus, the extensor pollicis longus, and the extensor indicis. These three muscles extend into the dorsum of the hand and attach to the digits. The adductor pollicis longus connects at the base of the first metacarpal and to the trapezium of the wrist. The extensor pollicis longus runs along the forearm to

the wrist where it makes a sharp turn at Lister's tubercle and finally attaches to the distal phalanx of the thumb. Extensor indicis runs with the extensor digitorum tendon and joins the second digit at the extensor hood. Extensor pollicis brevis and the supinator originate from the radius. Extensor pollicis brevis runs with the abductor in the forearm and connects to the base of the proximal phalanx of the first digit.
The supinator is unique because it starts on the lateral epicondyle of the humerus along with the radius before wrapping around the back of the arm to connect to the radius at the same location at pronator teres (Mitchell and Whited, 2019). This muscle allows for the supination of the forearm (Kerkhof et al., 2018).

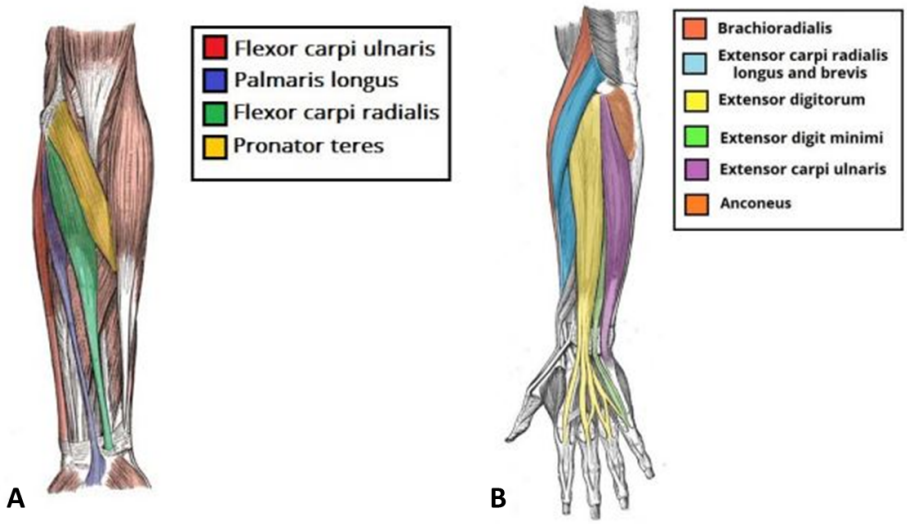

Figure 1.2 Forearm muscles of the anterior compartment (Panel A) and posterior compartment (Panel B). Extracted from (www.teachmeanatomy.com, 2019)

1.2.2 Wrist joint

The wrist joint, also referred to as the radiocarpal joint, is a condyloid synovial joint of the distal upper limb that connects and serves as a transition point between the forearm and hand. Its function is to provide the range of motion necessary to facilitate functional use of the hand while maintaining a physiologic level of stability (Erwin and Varacallo, 2018).

Structure

The above mentioned function is possible thanks to the osseous articular components creating a condyloid joint. A condyloid joint is a modified ball and socket joint that permits simul-

taneous movement in two perpendicular planes, in this case, dorsopalmar and radioulnar (Kauer, 1980). The joint itself is formed through the articulations between the distal radius and the scaphoid, lunate, and triquetrum (Figure1.3, Panel A).
Surrounding the wrist joint is a dual layered joint capsule, which is common amongst all synovial joints:

- the outer layer is fibrous and attaches to the radius, ulna, and carpal bones;
- the inner layer forms a synovial membrane which secretes synovial fluid and lubricates the joint.

The proximal articulation forms a concave shape composed of a combination between the distal end of the radius and articular disk. The distal articulation is convex and composed of the scaphoid, lunate, and triquetrum bones of the proximal hand.
Note that the ulna is not part of the wrist joint itself, as it articulates with the distal via the distal radioulnar joint (Lewis et al., 1970).

1.2.3 Ligaments

The stability of the wrist joint is accomplished thanks to four ligaments: the palmar and dorsal radiocarpal ligaments and the ulnar and radial collateral ligaments (Erwin and Varacallo, 2018).
The palmar radiocarpal ligaments connect the radius to both the proximal and distal rows of carpal bones and are the strongest supporting structures (Figure 1.3, Panel B).
The dorsal radiocarpal ligament is similar to the palmar ligament except that it is located on the dorsal side of the wrist joint.
Besides stability, palmar and dorsal radiocarpal ligaments also ensure that the hand and forearm move together during supination and pronation respectively.
The ulnar collateral ligament runs from the ulnar styloid process to the triquetrum and pisiform bones, and the radial collateral ligament runs from the radial styloid process to the scaphoid and trapezium bones.
The collateral ligaments work together to prevent excessive lateral joint displacement thus providing stability.

1.2.4 Movements

The forearm muscles and the complex structure detailed above, allows for motion of wrist joint in two planes: radial ulnar deviation and palmar flexion and extension (Kijima and

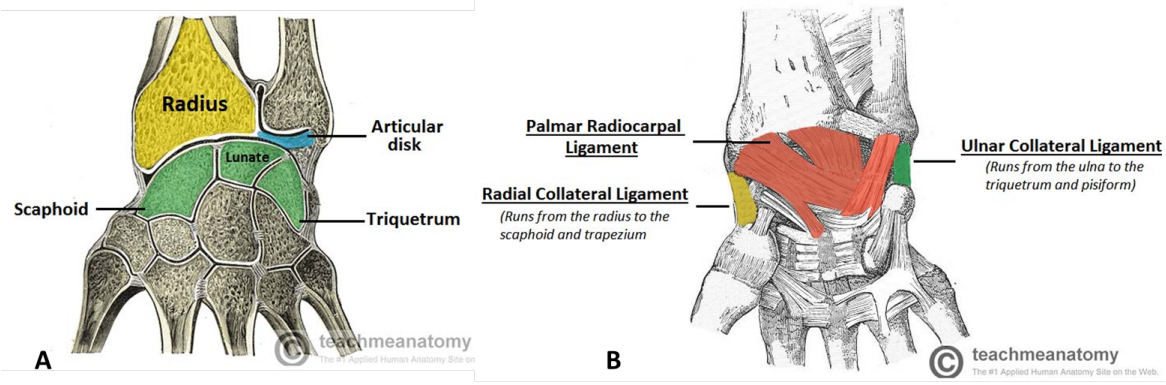

Figure 1.3 Articular surfaces (Panel A) and palmar view of ligaments (Panel B) of the wrist joint. Extracted from (www.teachmeanatomy.com, 2019)

Viegas, 2009). The center of motion for these planes of movement is located within the proximal and palmar pole of the capitate. However, since the wrist plays an essential role in the transmission of forearm prono/supination movements, this can be considered as a third DoF of the wrist. Fifteen muscles of the forearm cross the wrist joint and perform the following movements (shown in 1.4):

- Flexion – Produced mainly by the flexor carpi ulnaris, flexor carpi radialis, with assistance from the flexor digitorum superficialis;
- Extension – Produced mainly by the extensor carpi radialis longus and brevis, and extensor carpi ulnaris, with assistance from the extensor digitorum;
- Adduction – Produced by the extensor carpi ulnaris and flexor carpi ulnaris;
- Abduction- Produced by the abductor pollicis longus, flexor carpi radialis, extensor carpi radialis longus and brevis;
- Supination - In part occurs via the supinator muscle, which is found swirling around upper posterior region of the radius. With cohesive synergy applied with the biceps brachii, supination can occur;
- Pronation - The pronator teres and the pronator quadrus are responsible for cohesive synergetic contraction that leads to pronation.

The remaining forearm muscles cross both the wrist joint and interphalangeal joints acting as prime movers for digit movements (Bawa et al., 2000). Between them, the Flexor Digitorum Superficialis (FDS) and Extensor Digitorum Communis (EDC) contribute significant

forces and moments about the wrist (Moore et al., 1993) while their primary action is digit movements.

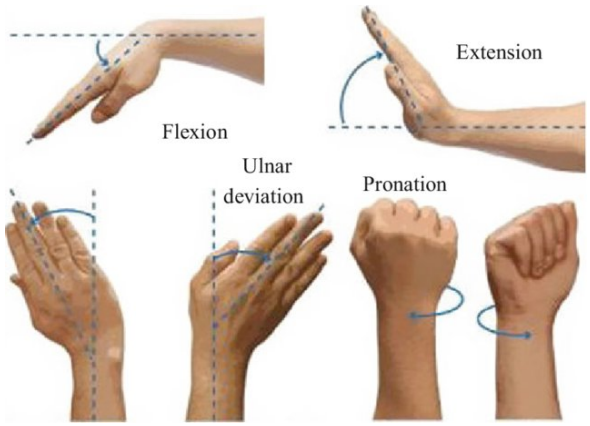

Figure 1.4 Movements of the wrist joint. Extracted from (Romero-Ángeles et al., 2019)

Chapter 2

Sensorimotor functions: a focus on proprioception and muscle fatigue

2.1 Introduction

The wrist is capable of a wide repertoire of gestures and fine movements, not only thanks to its complex structure and the muscles detailed in the previous chapter, but mainly thanks to the sensorimotor system. Indeed, the integration of multimodal sensory information, both from the external world or from proprioception, plays a crucial role in the correct elicitation of signals to recruit muscles and perform the right movements.
However, despite the ability of human sensorimotor system to cope with a great diversity of internal and external demands and constraints, these mechanisms can be altered as a consequence of neurological disorders, injuries or just due to excessive effort leading to muscle fatigue.
In particular, upper limb is one of the most often affected body parts in neurological population with 70% of stroke survivors (Meyer et al., 2014) and 66% of people with Multiple Sclerosis (Spooren et al., 2012) presenting upper extremity impairment. Similarly, due to their importance in carrying out tasks and their overuse, forearm and wrist are often exposed to high solicitations which can result in muscle fatigue or impairments (Amini, 2011).
Therefore gaining insight into sensorimotor functions of wrist joint, with a particular focus on proprioception, and into muscle activity, focusing on fatigue, can provide crucial information both to optimize rehabilitative protocols in case of neurological populations and to prevent injuries in case of workers.

2.2 Wrist proprioception

As mentioned above, proprioception is critical for meaningful interactions with our surrounding environment helping with the planning of movements, sport performance, playing a musical instrument and ultimately helping us avoid an injury.
Indeed, focusing on wrist, proprioception allows a fine control of this joint guarantying the equilibrium of both static and dynamic functions. Whereas static stability is determined by articular congruency and the ligamentous restraints (detailed in section 1.2.3), dynamic stability is achieved by the neuromuscular and proprioceptive influences on the wrist joint (Linscheid and Dobyns, 2002).

2.2.1 Definitions

The term "proprioception" is derived from the Latin "proprius"—belonging to one's own, and "-ception"—to perceive, that is, the ability to sense and perceive one self.
Proprioception is the ability of a joint to determine its position in space, detect precision movement and kinesthesia, and contribute to dynamic joint stability (Swanik et al., 1997). Human proprioception can be divided in three different submodalities: kinesthesia, joint position sense, and neuromuscular control(Riemann and Lephart, 2002).

- Kinaesthesia is the awareness of motion of human body. It refers to the ability to appreciate joint movement, including the duration, direction, amplitude, speed, acceleration and timing of movements (Sherrington, 1907);

- Joint Position Sense is our sense of joint/limb positioning. Joint position sense determines the ability of a person to perceive a presented joint angle and then, after the limb has been moved, to actively or passively reproduces the same joint angle;

- The neuromuscular sense is an unconscious proprioception sense. It allows the feed-forward anticipatory control of muscles around a joint, as well as the ability to unconsciously retain an adequate posture and maintain joint stability and equilibrium.

The two former senses are controlled consciously through cortical interactions, whereas the latter is primarily an unconscious reflex control of a joint at the spinal and cerebellar level (Hagert, 2010). Furthermore, although the conscious senses are primarily influenced by afferent information from muscle spindles and, to an extent, cutaneous receptors, the latter is in addition supported by information from intra-articular nerve endings.

2.2.2 Wrist proprioception mechanisms

All the three submodalities of proprioception arise from the sum of neural inputs from the joint capsules, ligaments, muscles, tendons, and skin, in a multifaceted system, which influences behavior regulation and motor control of the body (Blanche et al., 2012).

The neurological basis of proprioception comes primarily from afferent sensory receptors,

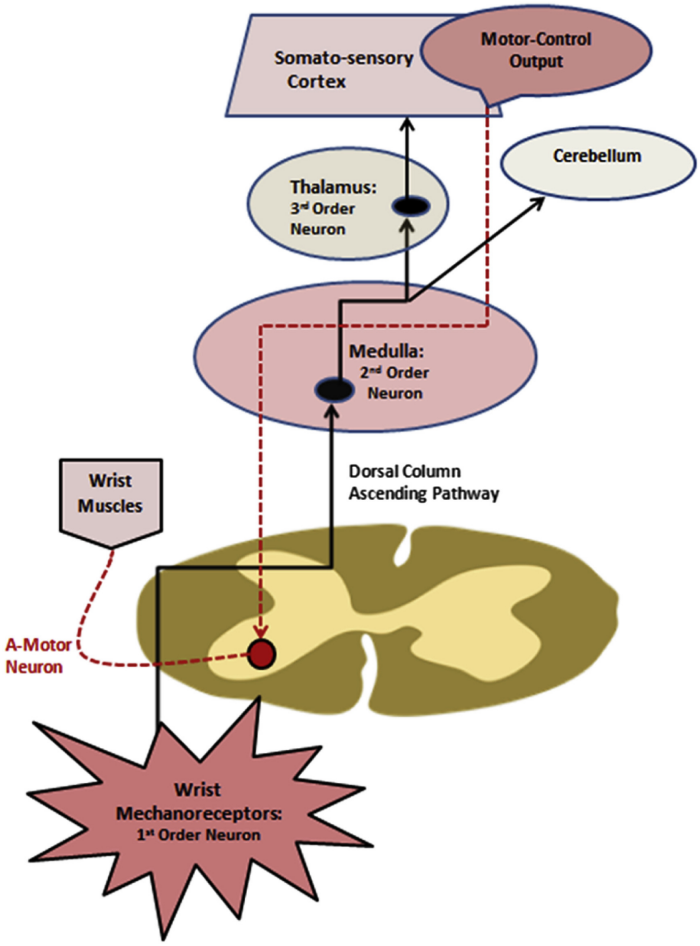

Figure 2.1 Diagram of ascending wrist proprioceptive input leading to descending motor control output. Extracted from (Karagiannopoulos and Michlovitz, 2016)

called mechanoreceptors, located in joints and muscles. These mechanoreceptors allow for the identification of limb position and movement via transmitting a specialized neural signal proportional to the degree of the deformation or changes occurred in muscle, skin or joint stretch. These information are transmitted to the dorsal horn of the spinal cord up to the central nervous system and to the primary motor and sensory cortices (as shown in Figure2.1) where the conscious awareness of joint motion in generated (Hagert, 2010).

In addition, some information is transmitted to the cerebellum, which is the primary local-

ization for the complex integration of somatosensation and proprioception, and concerns the unconscious neuromuscular control of a joint. Hence, proprioception is basically a continuous loop of feedforward and feedback inputs between sensory receptors throughout the body and the nervous system.

Mechanoreceptors and receptors

Several types of mechanoreceptors can be found in the wrist, each of them has peculiar characteristics allowing to detect different aspects of motion and thus to achieve a fine proprioception sense.
Mechanoreceptors are imbedded within static (i.e. skin, joint capsule, ligaments) and dynamic (i.e. musculotendineous) tissues and respond to various types of mechanical deformation applied to their host membrane (Karagiannopoulos and Michlovitz, 2016).
Wrist static proprioceptive feedback is derived from the Meissner corpuscles, Merkel discs, Ruffini endings, Pacinian corpuscle, and Golgi-like ending receptors.
The predominant mechanoreceptor type found in wrist ligaments is the Ruffini ending. The Ruffini ending, also referred to as dendritic or spray ending, is a slowly adapting, low-threshold receptor, which is constantly reactive during joint motion (Grigg and Hoffman, 1996). The Ruffini endings have been found to react to axial loading and tensile strain in the ligament, but not to perpendicular compressive joint forces, revealing their importance in signaling joint position and rotation, rather than direct pressure. These characteristics determine the regulation of stiffness and preparatory control of the muscles around the joint.
Contrary to the Ruffini ending, the Pacini corpuscle is a rapidly adapting, highthreshold receptor sensitive to joint acceleration/deceleration that is able to sense mechanical disturbances occurring even at a distance (Macefield, 2005). Pacini corpuscle is sensitive to compressive but not tensile forces therefore it senses sudden joint perturbations, and signals during possibly noxious joint motions. The Pacini corpuscle is not always present in the wrist suggesting that these functions are of minor importance in wrist neuromuscular stability (Hagert et al., 2009).
The Golgi-like receptor is a type of spray ending, belonging to the same family as the Ruffini ending, that is silent in the immobile joint and only active at the extremes of joint motion. The Golgi-like receptor has, so far, only been identified in the large dorsal wrist ligaments, the dorsal radiocarpal (DRC) and dorsal intercarpal (DIC) ligaments, which traverse both the radiocarpal and midcarpal joints (Hagert et al., 2005). Although the DRC is considered important in stabilizing the wrist in flexion and pronation (Viegas et al., 1999), the DIC is attributed importance in maintaining transverse stability of the proximal carpal row, as well

as indirect stability of the dorsal midcarpal joint space.
As for the wrist joint dynamic proprioceptive feedback, it is derived from muscle spindles and Golgi tendon organs.
The muscle spindle exists within a muscle midportion and it encapsulates its own intrafusal fibers (Proske et al., 2000). Wrapped around the middle of these fibers are the spiral terminals of a large sensory neuron, the type Ia axon. To one side of these spiral terminals are the terminals of a smaller sensory neuron, the type II axon. Both types of nerve endings are sensitive to stretch thus they send feedback about muscle contraction and length changes to the brain. In particular, the type I axons signal both the rate of change in muscle length and the length change itself, making them responsive to muscle vibration while type II axons terminals are only position sensors (Proske et al., 2000).
The Golgi tendon organ is another encapsulated receptor that exists within the musculotendinous muscle region and is linked to multiple muscle fibers through collagen tendon strands. It constantly senses and conveys both static and dynamic changes in extrafusal muscle fiber tension via its Ib afferent fiber. In particular Golgi tendon organ is sensitive to muscle contraction: in the resting state it is silent, while when the muscle fiber contracts, it pulls on the tendon strand and stretches it. This stretches the nerve ending of the Ib axon to generate nerve impulses. Golgi tendon organ offers a protective mechanism against excessive contractile muscle forces.

2.3 Muscle fatigue

Whether in the context of athletic competition, manual labor or patients with various neuromuscular diseases, fatigue is a commonly experienced phenomenon with important consequences. Indeed muscle fatigue can affect task performance (Monjo et al., 2015), posture-movement coordination (Vafadar et al., 2012), position sense and can be a highly debilitating symptom in several pathologies (Zwarts et al., 2008). Therefore gaining insight into muscle function capabilities with a particular focus on localized muscle fatigue, is a crucial research goal that can lead to reduce ergonomic risk factors for workers or to optimize therapeutic treatments in pathological populations.

2.3.1 Definitions

In literature there exist a variety of definitions of fatigue, however these share three unifying points: I) there is a decline in one or more of the biological systems; II) the decline is

reversible; III) the decline may or may not occur before an observable performance or task failure occurs.
The first point usually refers to the decline in force, velocity or power of the biological system, usually with reference to muscle performance.
The second point, reversibility, distinguishes fatigue from injury or disease when muscle performance might be impaired for a period of time.
The latter point is an important consideration as it establishes the decline in performance often observed during a maximal "all-out" effort compared to the fatigue which might be progressively experienced during a prolonged exercise task (Williams and Ratel, 2009). Indeed, some definitions associated fatigue with the notion of a "break point", thus identifying fatigue with the inability to sustain an exercise. However, many neurophysiological mechanisms are perturbed before the body feels the effect of fatigue and these changes sometimes constitute advance warning of fatigue (Boyas and Guével, 2011). Furthermore, the initial state of the neuromuscular system (e.g. energy reserves, ion concentrations and the arrangement of contractile proteins) is altered as soon as exercise starts. Fatigue then would begin almost at the onset of the exercise and would develop progressively until the muscle is no longer able to perform the requested task (Boyas and Guével, 2011).
Considering all these aspects, neuromuscular fatigue represents "any exercise induced reduction in force or power regardless of whether the task can be sustained or not" (Bigland-Ritchie and Woods, 1984). Neuromuscular fatigue is a complex phenomenon that occurs due to the impairment of one or several physiological processes which enable the contractile proteins to generate force. In order to better understand them and the mechanisms that are believed to cause the impairment that lead to fatigue at the cellular level, a brief overview about skeletal muscle cell, motor unit and mechanisms of contraction will follow.

2.3.2 Skeletal muscle cell

The architecture of skeletal muscle is characterized by a very particular and well-described arrangement of muscle fibers (also referred to as myofibers or muscle cells) and associated connective tissue. Each skeletal muscle has three layers of connective tissue (epimysium, endomysium and perimysium) which enclose it and provide structure to the muscle as a whole, and also organize the muscle fibers within the muscle into distinct patterns. The epimysium covers the outside surface of each muscle. It allows a muscle to contract and move independently and powerfully while maintaining its structural integrity. The perimysium collects bundles of fibers into fascicles in a cross-pattern adding stability to the structure.

Inside each fascicle, each muscle fiber is encased in a thin connective tissue layer of collagen and reticular fibers called the endomysium. Arteries and veins run through the endomysium (Gowitzke and Milner, 1988). Indeed, it contains the extracellular fluid, known as sarcoplasm, which in turn contains nourishing sources (such as lipid or glycogen), organelles (such as nuclei, mitochondria etc.), enzymes (such as myosin adenosine triphosphate, etc.). The sarcoplasm also contains a membranous system that assists muscle in the conduction of the signals coming from the CNS. This system encompasses the sarcoplasmic reticulum (SR), lateral sacs and transverse tubules (T-tubules).
The SR runs longitudinally along fibers and, at specific locations long the myofibril, bulges into lateral sacs. Orthogonal to the SR and associated with sacs are the T-tubules, which are branched invaginations of the sarcolemma as shown in Figure 2.2. The rapid transmission of the activation signal from the sarcolemma to the contractile apparatus is facilitated by the connection between the SR and T-tubules.

A single muscle fiber (with approximate dimensions of 100 μm in diameter and 1 cm

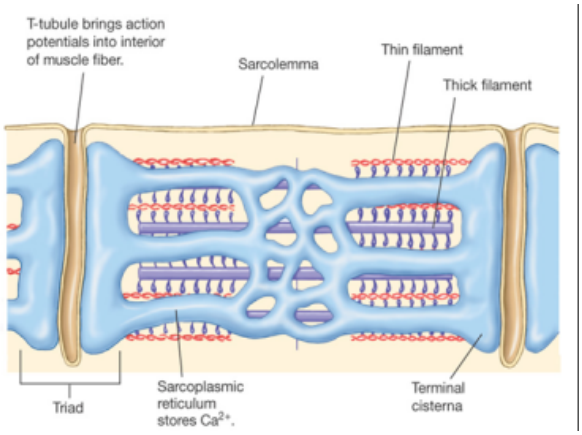

Figure 2.2 The SR runs longitudinally along fibers and orthogonal to the T-tubules. Extracted from (Silverthorn, 2015)

in length) is surrounded by a thick excitable cell membrane called sarcolemma (Frontera and Ochala, 2015). These individual fibers may be broken down into clusters of individual myofibrils, which are tiny hairlike strands. Each myofibril consists of aggregates of myosin and actin filaments. The absence (partial or complete). or dysfunction of one of these proteins may result in damage to the sarcolemma, muscle weakness, and atrophy. For example, this complex is the location of the protein dystrophin that is partially or completely absent in some types of neuromuscular disorders such as Duchenne and Becker muscular dystrophies (Thomas, 2013).
Myosin and actin filaments forms the sarcomere, while repeating sections of sarcomere

compose the myofibrils. Within the sarcomere, there are areas where only actin resides (I bands) and areas where myosin overlaps the actin fibers (A bands). In the middle of the I-band there is a thin structure, called Z-line, orthogonal to the filaments. Also the A-band has a thin central structure, the M-line, with a high electronic density. The sarcomere includes, then, the zone of myofibrils from one Z band to the next one. The actin filament is a thin fiber with two negatively charged molecules that spiral around each other. The myosin filament is a much thicker filament with "globular heads" on it. These filaments are also negatively charged. In the resting state, these two filaments lie next to each other, mutually repelled by their negative charges.

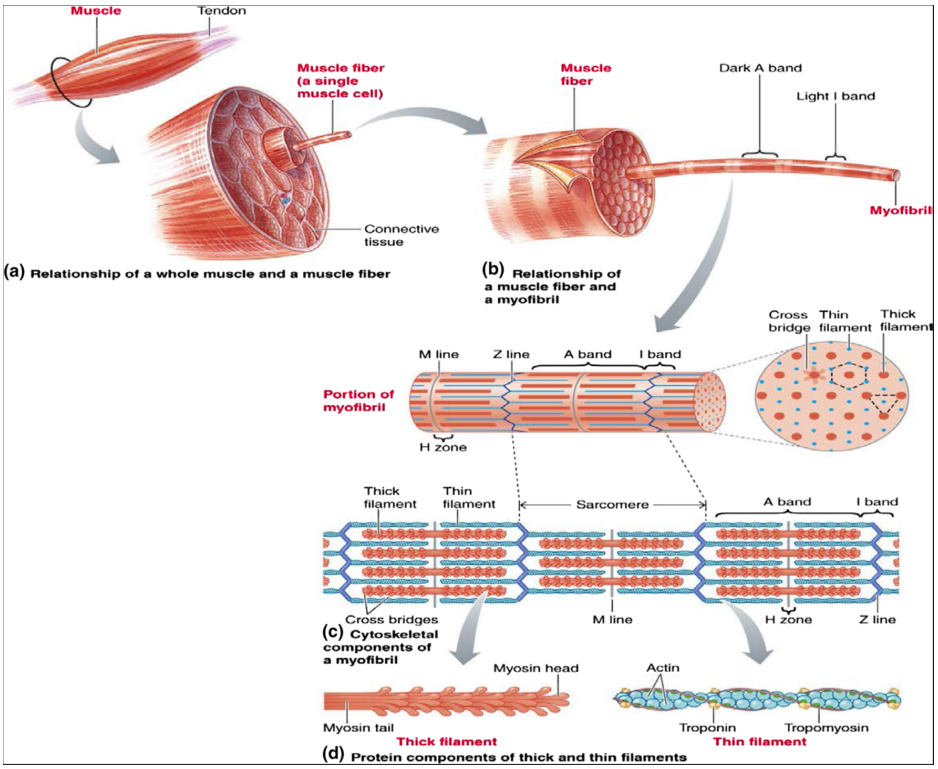

Figure 2.3 Structure of skeletal muscle. Extracted from (Frontera and Ochala, 2015)

2.3.3 Motor unit type

Different molecular composition of the myofibrils determines the heterogeneity of mechanical and energetic properties of the muscle fibers. Similarly, there exists a wide variation in the morphological and electrophysiological properties of the motoneuron. Interestingly, the muscle fibers that are innervated by a particular motoneuron show nearly identical biochemical, histochemical, and contractile characteristics. Such properties allow the definition

of the different types of motor unit (MU). A MU consists of an α-motoneuron in the spinal cord and of the muscle fibers it innervates. Earlier studies (Burke, 2011) identified three types of motor units based on physiological properties such as speed of contraction and fatigability (sensitivity to fatigue):

- fast-twitch, fatigable (FF or type IIb);
- fast-twitch, fatigue-resistant (FR or type IIa);
- slow-twitch (S or type I), which is most resistant to fatigue.

Motor units were believed to be recruited in a relatively stable order according to Henneman's size principle, from those with slow conduction velocity producing small forces to those with fast conduction velocity producing large forces (Henneman and Desmedt, 1981). This principle links motor neuron properties (i.e. small size, long after hyperpolarization, and low axonal conduction velocity) with properties of muscle fibers (small twitch force, long contraction times, slow fiber conduction velocity and low fatigability).

2.3.4 Muscle contractions

Voluntary muscles activation depends on smooth flow of nerve impulses in the major sensory and motor system. Sensory signals from skin, cardiorespiratory systems, muscles, and joints, and special senses (skin, eyes, and ears), provide afferent input. This information is processed by the primary motor cortex which activates brainstem motor nuclei and anterior horn cells in the spinal cord (efferent pathway) (Figure 2.4). Signal from lower motor neurons reaches muscle through peripheral nerves and the neuromuscular junction (NMJ). Within the muscle, a series of metabolic events then provides chemical energy for contraction (Chaudhuri and Behan, 2004) (see Figure 2.5). The muscles cells are activated by the α-motoneurons. At the neuromuscular endplate, acetylcholine (Ach) is released from the end terminals of the motoneuron. ACh binds to receptors on the surface membrane of the muscle cells. This attachment triggers the opening of the Na^+/K^+ channels and the influx of Na+ into and the efflux of K+ from the muscle fiber. The movement of these ions results in the development of the end-plate potential that can trigger the generation of a muscle fiber action potential (AP). This process is referred to as neuromuscular propagation (Enoka and Duchateau, 2008).
Once an AP has been generated, several processed, known as excitation-contraction coupling contribute to the generation of force. Eight major processes are involved in this conversion phenomenon and in particular:
(1) the action potential is conducted along the surface of the muscles cells (sarcolemma) (2)

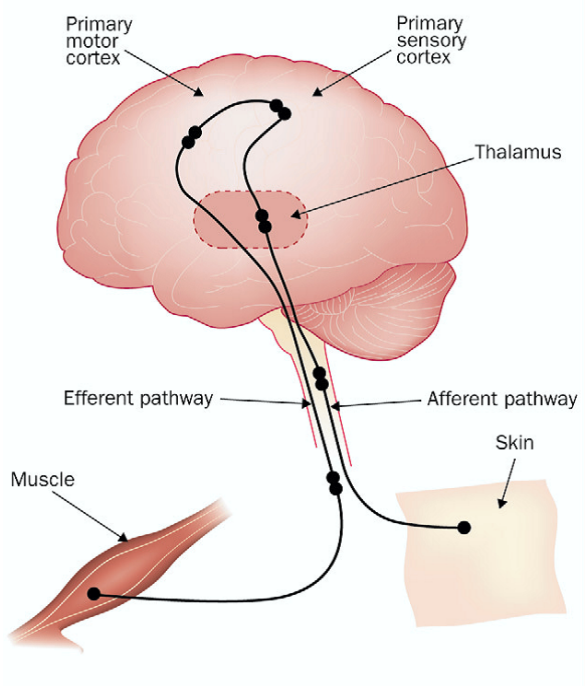

Figure 2.4 Integration of sensory and motor pathways for voluntary contractions. Extracted from (Chaudhuri and Behan, 2004)

and along the T-tubule system. This system consists of invaginations of the surface membrane that form a fine network of tubules that surround each myofibril. Thus, the t-tubules contain extracellular fluid. They also contain voltage-activated Na^+ and K^+ channels and hence they can conduct action potentials.
3) When the AP propagated along the sarcolemma down the T-tubules and into the interior of muscle fiber, it triggers an increase in Ca2+ conductance, which corresponds to an opening of ryanodine receptors (RyRs) located in the sarcoplasmatic reticulum (SR).
(4) The SR is the intracellular Ca^{2+} storage space, and when RyRs open, Ca^{2+} is released from the SR into the cytosol (myoplasm); (5) Myoplasm is in direct contact with the myofibrils of the skeletal muscle cell. Myofibrils are composed by actin and myosin filaments organized in long series of sarcomeres. When Ca^{2+} increases in myoplasm, it binds to troponin. 6) The binding of Ca2+ to troponin moves tropomyosin away from the myosin-binding site on actin. 7) The two contractile proteins, actin and myosin, can thus interact (cross-bridge cycle). This process involves the use of ATP by the globular head of myosin to attach actin. 8) Hydrolysis of ATP into ADP and Pi causes a rotation of the head of the protein toward the tail and the pulling on the compliant arm of the cross-bridge (Huxley, 2000). The consequence of this pull is a relative movement of thin and thick filaments and the shortening of the sarcomere.

Since the displacement of the myosin head occurs while actin and myosin are connected, both the filaments slide one with respect to the other and exert a force on the cytoskeleton (sliding filament theory of muscle contraction) (Huxley, 2000).
As long as Ca^{2+} ions remain in the sarcoplasm to bind to troponin, which keeps the actin-binding sites "unshielded," and as long as ATP is available to drive the cross-bridge cycling and the pulling of actin strands by myosin, the muscle fiber will continue to shorten to an anatomical limit.
Muscle contraction usually stops when signaling from the motor neuron ends, which repolarizes the sarcolemma and T-tubules, and closes the voltage-gated calcium channels in the SR. Ca^{2+} ions are then pumped back into the SR, which causes the tropomyosin to reshield (or re-cover) the binding sites on the actin strands. A muscle also can stop contracting when it runs out of ATP and becomes fatigued.

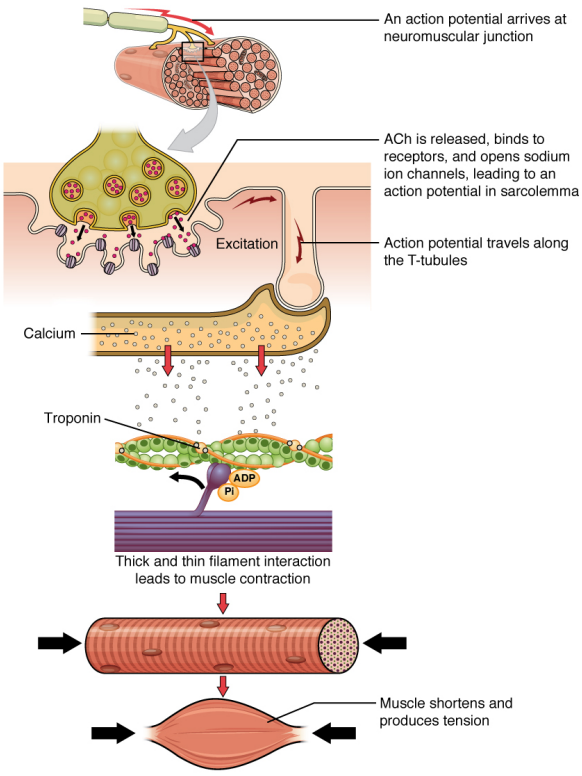

Figure 2.5 Contraction of a Muscle Fiber. A cross-bridge forms between actin and the myosin heads triggering contraction. As long as Ca2+ ions remain in the sarcoplasm to bind to troponin, and as long as ATP is available, the muscle fiber will continue to shorten. Extracted from (OpenStaxCollege, 2013).

2.3.5 Muscle fatigue mechanisms

Any interruption or alteration of this complex chain of events can lead to a decrease in force generation typical of muscle fatigue. In particular fatigue may be due to alterations in:

1. activation of the primary motor cortex;
2. propagation of the command from the central nervous system (CNS) to the motorneurons (the pyramidal pathways);
3. activation of the MUs and muscles;
4. neuromuscular propagation (including propagation at the NMJ);
5. excitation-contraction coupling;
6. availability of metabolic substrates;
7. state of the intracellular medium;
8. performance of the contractile apparatus;
9. blood flow.

Considering these sites, it is possible to distinguish between central fatigue (1 to 3) and peripheral fatigue (4 to 9) (Boyas and Guével, 2011).

Central Muscle fatigue

Central fatigue can be defined as the decrease of voluntary activation of the muscle by the nervous system. When submaximal central activation occurs, a central activation failure (CAF) is said to be present and the muscle receive a suboptimal input. As a consequence the muscle will not be able to develop its maximal force capacity (Zwarts et al., 2008). The presence of CAF, and therefore central fatigue, can be evaluated with the technique of twitch interpolation: during maximal voluntary contraction (MVC) of a specific muscle, an electrical stimulation is applied to the motor nerve or motor endplate. If the electrical stimulation will result in an increased exertion of force, it indicates that the voluntary activation was not really maximal. This means that some MUs are either not recruited or do not fire often enough for the muscle fibers to generate maximal force (Taylor and Gandevia, 2001).
One of the causes of this weakness in central command during prolonged exercise could be the decreased excitation supplied by the motor cortex (Gandevia, 1998).

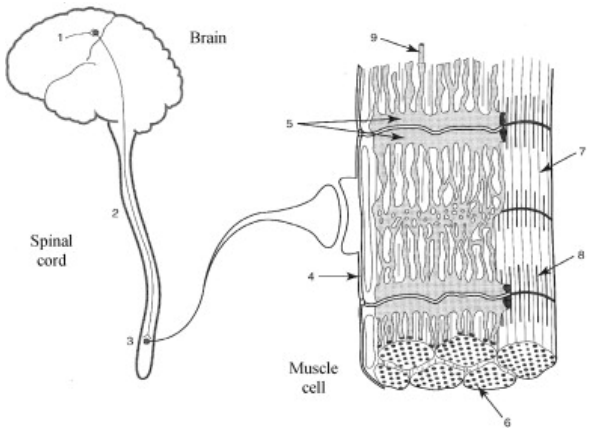

Figure 2.6 Sites which can contribute to neuromuscular fatigue. Fatigue may be due to alterations in: (1) activation of the primary motor cortex; (2) propagation of the command from the central nervous system to the motoneurons (the pyramidal pathways); (3) activation of the motor units and muscles; (4) neuromuscular propagation (including propagation at the neuromuscular junction); (5) excitation-contraction coupling; (6) availability of metabolic substrates; (7) state of the intracellular medium; (8) performance of the contractile apparatus; (9) blood flow. Extracted from (Boyas and Guével, 2011).

This supraspinal fatigue can be identified by means of magnetic or electrical stimulation of the motor cortex (Taylor and Gandevia, 2001). In fact, the stimulation of the motor cortex artificially activates the motor cortex neurons and thus the muscles they innervate (Rothwell, 1997). Similarly to the twitch interpolation, the subject is asked to perform short MVCs at regular intervals during sustained, submaximal, isometric exercise. The response is measured at the output site by recording the force or the electrical muscle response. If the stimulation induced an increase in peak force during the maximal contraction, it indicates the presence of supraspinal fatigue, which may be due to submaximal excitation by the motor cortex (Taylor et al., 1996). This supraspinal fatigue can be linked to accumulation of certain brain neurotransmitters, such as serotonin, dopamine, glutamate, acetylcholine, adenosine and gamma-aminobutyric acid, or other substances such as ammonium ions and glycogen.
At the spinal level, central fatigue may be caused by several mechanisms. Firstly, the inhibitory afferents from intramuscular receptors appear to be involved in the decrease in motoneuron activity. In fact, the activity of the alpha motoneurons can be inhibited by group III and IV muscle afferents (metaboreceptors) which in turn are stimulated by ischaemia (Lagier-Tessonnier et al., 1993), hypoxaemia (Arbogast et al., 2000) and the extracellular accumulation of potassium (K^+) and lactate (Luc Darques et al., 1998; Rotto and Kaufman, 1988). Similarly, group Ia and II afferents (neuromuscular spindles) may limit the alpha motoneuron activity (Bongiovanni and Hagbarth, 1990; Gandevia, 2001). Indeed, these

neuromuscular spindles, explained in section 2.2.2, are oriented parallel to the muscle fibers and its sensitivity can be reduced by structural changes in muscle (e.g. variations in stiffness) resulting from repeated contractions or stretching.

Peripheral Muscle fatigue

Muscle fatigue has mostly been studied at the peripheral level where the fatigue-induced electrochemical alterations may be observable locally at the cellular level and the mechanical ones at the muscle-tendon complex (Allen et al., 2008; Fitts, 2008). Concerning the electrochemical changes, peripheral fatigue affects the neuromuscular transmission that is the transformation of the nerve action potential (AP) into a muscle action potential (MAP). This transformation takes place at the neuromuscular junction when the sum of the excitatory and inhibitory presynaptic potentials reaches or exceeds the muscle cells' excitability threshold. During fatigue, this mechanism can be altered by (Boyas and Guével, 2011):

- insufficient propagation of the nerve potential at the nerve endings;
- a failure of the coupling between excitation and neurotransmitter secretion in the synaptic gap;
- neurotransmitter depletion;
- reduced neurotransmitter release;
- a decrease in the sensitivity of the post-synaptic acetylcholine receptors and the post-synaptic membrane (Allen et al., 2008; Sieck and Prakash, 1995).

During sustained contraction, fatigue may decrease the excitability of small-diameter axons which in turn may lead to their inactivation and in a decrease in the amount of neurotransmitter released in the synaptic gap (Krnjević and Miledi, 1959). Moreover, the amplitude of motor end-plate potentials decreases during fatiguing exercise, as a result of a decrease in the quantity of neurotransmitter (acetylcholine) released by each nerve ending. In addition, several factors alter the transformation of the nervous excitation into muscle force and fatiguing exercise may contribute to this changes (Allen et al., 1992): the propagation of the MAP along the sarcolemma and the transverse tubules, the sarcoplasmatic reticulum's permeability to Ca^{2+}, the movement of Ca^{2+} inside the sarcoplasma, the active efflux of Ca^{2+} from the SR, Ca^{2+} binding to troponin and the myosin-actin interaction associated with the work performed by the crossbridges.
A reduction in blood flow is another mechanism involved in fatigue: muscle contraction

often compresses the blood vessels decreasing the blood supply to the active muscles (Wright et al., 1999). The limitation of the blood supply reduces the oxygen supply and induces a rapid accumulation of the metabolites associated with muscle contraction. In fact, muscle contractions activate ATPases and promote glycolysis thus leading to an increase in intracellular metabolites such as H^+, lactate and Pi. The accumulation of H^+ lowers the pH, thus potentially interfering with SR Ca^{2+} release, troponin C sensitivity to Ca^{2+} and cross-bridge cycling and resulting in impaired muscle force (Wan et al., 2017). Similarly increased Pi substantially impairs myofibrillar performance, decreases SR Ca^{2+} release and therefore contributes to the decreased activation (Allen and Trajanovska, 2012).
Among mechanical factors, peripheral fatigue seems to influence the force transmission from the muscle to the tendon insertion point by altering the mechanical properties of the MTC and other tissues surrounding a joint (e.g. altered viscoelasticity and stiffness of the system). These electrochemical and mechanical events concur to generate afferent feedback to the spinal cord, which then modulates motor drive and final force output (Cè et al., 2019).

2.3.6 Peripheral muscle fatigue assessment

Electromyography (EMG) is the recording of electrical signals that are sent from motoneurons to muscle fibers (action potentials) while they propagate along the sarcolemma, from the neuromuscular junction to the extremities of the muscle fibers (Enoka and Duchateau, 2008). The biochemical and physiological changes in muscles during fatiguing contractions, described in the section above, can be detected from the myoelectric signals recorded on the surface of the skin above the muscle concerned.
Indeed, the properties of surface electromyography signals (sEMG) are related to these changes:

- muscle fiber conduction velocity (CV) decreases due to changes in intracellular pH. As a consequence, the frequency content of the sEMG signal shift towards lower frequency. Furthermore, this downward shift could be attributed to a shift in dominance from fast-twitch fiber to slow-twitch fiber as a result of the fatigability of the fast-twitch fibers, or a combination of these factors.

- A gradual additional recruitment of new MUs occurs resulting in an increase in the amplitude of the signal (Arendt-Nielsen et al., 1989).

It is important to highlight that both of the two characteristics must be considered jointly, in the so-called Joint Analysis of EMG spectrum and amplitude (JASA)(Luttmann

et al., 2000), when investigating muscle fatigue. Accordingly, simultaneous consideration of amplitude and spectrum of a surface EMG can provide information on whether EMG changes are fatigue-induced or force-related. Briefly four cases can be distinguished:

- if the EMG amplitude increases and EMG spectrum shifts towards higher frequencies, muscle force increase is the probable cause;
- if the EMG amplitude decreases and EMG spectrum shifts towards lower frequencies, muscle force decrease is the probable cause;
- if the EMG amplitude increases and EMG spectrum shifts towards lower frequencies, this is considered to be result of muscle fatigue;
- if the EMG amplitude decreases and the EMG spectrum shifts towards higher frequencies, this is considered to be recovery from previous muscle fatigue.

For this purpose, a series of parameters which capture the changes in amplitude or in frequency content of the sEMG signals has been proposed.

Time domain parameters

The most commonly used parameters in the analysis of the raw EMG signal in the time domain are the average rectified value (ARV) (also called mean absolute value MAV) and the root-mean-square value (RMS). The ARV measures the average of the absolute signal value while the RMS is a measure of the signal power (Merletti et al., 2003). They are defined by the following equations:

$$ARV = \frac{1}{N}\sum_{i=1}^{N}|x_i| \tag{2.1}$$

$$RMS = \sqrt{\frac{1}{N}\sum_{i=1}^{N}x_i^2} \tag{2.2}$$

where x_i is the ith sample of an EMG signal and N is the number of samples in the epoch. However, several authors prefer the RMS (De Luca, 1997; Merletti et al., 2003), since it can also be used to obtain a moving average for processing raw EMG signals.

Frequency domain parameters

The most common frequency-dependent features in sEMG analysis are the mean frequency (MNF), the median frequency (MDF), or normalized higher spectral moments. The MNF is the average frequency of the power spectrum and it is defined as its first-order moment (Arendt-Nielsen and Mills, 1985; Eberstein and Beattie, 1985; Mortimer et al., 1970). It indicates the shift of the Power Spectral Density (PSD) of the sEMG signal toward lower frequencies and it is evaluated as follows (Kwatny et al., 1970):

$$F_{Mean} = \frac{\int_0^{\frac{f_s}{2}} fP(f)\,\mathrm{d}f}{\int_0^{\frac{f_s}{2}} P(f)\,\mathrm{d}f} \tag{2.3}$$

where f_s is the sampling frequency, and $P(f)$ is the PSD of the signal.

The MDF, instead, is the frequency which divides the spectrum into two regions of equal power (Kupa et al., 1995; Merletti and Roy, 1996). The MDF and MNF coincide if the spectrum is symmetric with respect to its center line, but are usually different reflecting the skewness of the power spectrum. Further the standard deviation of the MDF is higher than the one of MNF.
Finally, regarding higher spectral moments, the normalized index proposed by Dimitrov and colleagues (Dimitrov et al., 2006) is expressed by the ratio between the spectral moments of order (-1) and the spectral moment of order k, with k ranging from 1 to 5 as below:

$$DI = \log \frac{\int_{f_1}^{f_2} f^{-1}P(f)\,\mathrm{d}f}{\int_{f_1}^{f_2} f^{k}P(f)\,\mathrm{d}f} \tag{2.4}$$

where f_1 and f_2 determine the bandwidth of the signal (lowest and highest frequency respectively), k is the order of spectral moment and $P(f)$ is the PSD as in the previous indicator.
The frequency content of a signal can be determined by performing a Fourier transform to reveal its individual frequency components. The fast Fourier transform (FFT), a method for calculating the discrete Fourier transform, is suitable for use in stationary signals. EMG signals, which are non-stationary, should be represented in both the time and frequency domains. Therefore, the short time Fourier transform (STFT), which analyses a small temporal section of the signal, can be used to determine the frequency and phase evolution of the EMG signal over time. The time and frequency resolution depend upon the sampling

rate and the temporal length of the signal section. Due to the inverse relationship between time and frequency in the Fourier transform, it follows that the higher the time resolution the lower the frequency resolution will be and vice versa.

Although sEMG has been applied in many studies of localised muscle fatigue, it is not without its limitations, in particular, in studies of dynamic muscle contractions.

2.4 Wrist Robotic Device

In the present thesis, the potentiality of the sEMG parameters to asses muscle fatigue (presented in the previous sections) has been exploited together with the use of a robotic device. In details, the robotic device is an end-effector robot and it has been designed for the wrist neurorehabilitation of patients with neurological or orthopedic disabilities (Figure 2.7).
The device, called Wristbot, has been developed in the Motor Learning, Assistive and Rehabilitation Robotics laboratory of the Italian Institute of Technology (IIT). The robot allows movements along the three wrist articulations, with a range of motion similar to a typical human subject: $\pm 62^{\circ}$ in flexion-extension, $45^{\circ}/40^{\circ}$ in radial-ulnar deviation, and $\pm 60^{\circ}$ for pronation-supination movements (Masia et al., 2009).
It is provided with four brushless motors that allow guidance and assistance of wrist movements in the three above-mentioned planes, with a maximum torque of 1.53 Nm in flexion-extension, 1.63 Nm in radial-ulnar deviation, and 2.77 Nm in pronation-supination movements. In addition, these motors are chosen to provide accurate haptic rendering to compensate for the weight and inertia of the device, thus allowing free smooth movements.
Angular rotations on the three axes are acquired by means of high-resolution incremental encoders with a maximum error of 0.17°, thus making Wristbot an optimal tool to assess the rehabilitative process in an objective and precise way.
Another peculiarity of the Wristbot is the possibility to provide assistive or perturbative forces that automatically adapt to the level disability and performances of the patient.
An intuitive graphical user interface (GUI) allows the therapist to choose the desired exercises and to set a wide range of parameters to continuously tailor the therapy to the patient's needs. As for the interaction with patients, they are requested to hold the handle of the Wristbot to perform wrist movements and execute the task presented on a monitor. In fact, a virtual reality environment is integrated into the system in order to provide stimulating visual feedback and engaging interaction. The main advantages of the Wristbot are its programmability and multi-functionality, which allow for a highly personalized therapy. In addition, the quantitative functional assessment provided by the device constitutes a valuable tool to support clinicians in the choice of the optimal therapy.
The development of robotic tasks using the robot Wristbot was a fundamental technological objective not only to fulfill the experimental studies of my PhD's project but also with the purpose to promote the technology transfer of the device in the market. Indeed, the acquired knowledge could be used to improve and expand the portfolio of rehabilitation and assessment protocols implemented with Wristbot.

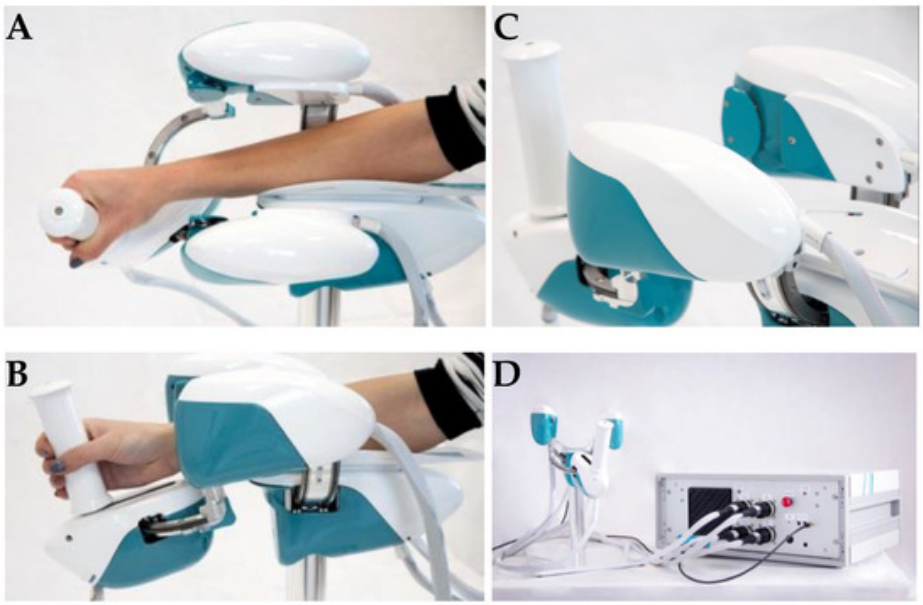

Figure 2.7 Lateral view of Wristbot during combined movements in the flexion–extension and pronation–supination DoFs (Panel A) and movements in the radial–ulnar deviation DoF (Panel B); posterior–lateral view of the handle of Wristbot (Panel C) and a frontal view (Panel D). Extracted from (Iandolo et al., 2019)

Part II

Section Two

Chapter 3

Coupling kinematic and sEMG parameters for muscle fatigue assessment

3.1 Introduction

It is of crucial importance to take into account muscle fatigue for the design of efficient rehabilitation protocols (Poyil et al., 2017) and fatigue assessment can provide crucial information about skeletal muscle functions for many patients with neuromuscular impairments. Muscle fatigue is a typical symptom (Angelini and Tasca, 2012) of several neuromuscular diseases (e.g. Duchenne, Becker Muscular Dystrophies, and spinal muscular atrophy) and fatigue itself accounts for a significant portion of the disease burden.
A systematic approach to assess muscle fatigue might provide important cues on the disability itself, on its progression and on the efficacy of adopted therapies. Indeed, therapeutic strategies are now under deep investigation and a lot of effort has been devoted to accelerate the development of drugs targeting these disorders (Shimizu-Motohashi et al., 2016). In particular, promising results have been reported in case of subjects such as patients with Duchenne Muscular Dystrophy (DMD) or with Becker Muscular Dystrophy (BMD). In details, these two dystrophinopathies are progressive diseases which affect 1 in 19.000 live male births in case of BMD and 1 in 3.500 in case of DMD (Romitti et al., 2009). They are due to mutations in the gene encoding the dystrophin protein. The mutations cause a reduced amount or shortened functional dystrophin in Becker Muscular Dystrophy and its absence in patients with Duchenne Muscular Dystrophy. The alteration or absence of the dystrophin

causes in turn a progressive muscle wasting starting from proximal limb muscles to those in distal, and from the lower to the upper part of the body. As a consequence, exhaustion during daily activities and fatigue are among the most common symptoms of DMD or BMD patients, significantly and negatively impacting their quality of life (Bushby et al., 1999). Therefore, the need for an objective tool to measure muscle fatigue is impelling and of great relevance.

Currently, muscle fatigue is evaluated in clinical practice by means of qualitative rating scales like the 6-min walk test (6MWT) (McDonald et al., 2010) or through subjective questionnaires administered to the patient (e.g. the Multidimensional Fatigue Inventory (MFI), the Fatigue Severity Scale (FSS), and the Visual Analog Scale (VAS)) (McDonald et al., 2010). During the 6MWT patients have to walk, as fast as possible, along a 25 meters linear course and repeat it as often as they can for 6 min: 'fatigue' is then defined as the difference between the distance covered in the sixth minute compared to the first. Obviously, such a measure is only applicable to ambulant patients and this is a strong limitation to clinical investigation because a patient may lose ambulatory ability during a clinical trial, resulting in lost ability to perform the primary clinical endpoint (Mayhew et al., 2013). It should also be considered that neuromuscular patients, e.g. subjects with Duchenne Muscular Dystrophy, generally lose ambulation before 15 years of age (Bushby et al., 2010), excluding a large part of the population from the measurement of fatigue through the 6MWT. Since neuromuscular patients often experience a progressive weakness also in the upper limb, reporting of muscle fatigue in this region is common. A fatigue assessment for upper limb muscles could be used to monitor patients across different stages of the disease. Actually, clinical scales for the assessment of upper limb are available (Arnould et al., 2004; Jebsen et al., 1969) but none of these were specifically designed for Duchenne or Becker Muscular Dystrophy. As a consequence, the scales do not reflect the difficulties related to the specific pattern and progression of such diseases as pointed out by a review of (Mazzone et al., 2012) and do not address the assessment of fatigue.

As for the questionnaires, the MFI is a 20 items scale designed to evaluate five dimensions of fatigue (general fatigue, physical fatigue, reduced motivation, reduced activity, and mental fatigue) (Smets et al., 1995). Similarly, the FSS questionnaire contains nine statements that rate the severity of fatigue symptoms and the patient has to agree or disagree with them (Krupp et al., 1989). The VAS is even more general: the patient has to indicate on a 10 cm line ranging from "no fatigue" to "severe fatigue" the point that best describes his/her level of fatigue (Wolfe et al., 1996). Despite the ease to administer, such subjective assessments of fatigue may not correlate with the actual severity or characteristics of fatigue, and may

provide just qualitative information with low resolution, reliability and objectivity.
Considering various levels of efficacy among the methods currently used in clinical practice, research should focus on the development of an assessment tool for muscle fatigue, that is easy and fast to administer, even to patients with a high level of impairment. Such a tool, should provide clear results, be easy to read and understand by a clinician, be reliable and objectively correlated with the physiology of the phenomenon.
As reported in the previous chapter (section 2.3.6), surface electromyography (sEMG) is a noninvasive and widely used technique to evaluate muscle fatigue. Certain characteristics of the sEMG signal can be indicators of muscle fatigue. For example during sub-maximal tasks, muscle fatigue will associate with decreases in muscle fiber conduction velocity and frequency and increases in amplitude of the sEMG signal (Cifrek et al., 2009). The trend and rate of change will depend on the intensity of the task: generally, sEMG amplitude has been observed to increase during sub-maximal efforts and decrease during maximal efforts. It has been reported that there is a significantly greater decline in the frequency content of the signal during maximal efforts compared to sub-maximal (Carr et al., 2016). Accordingly, spectral (i.e. mean frequency) and amplitude parameters (i.e. Root Mean Square (RMS)) of the signals, can be used to measure muscle fatigue (González-Izal et al., 2010; Kahl and Hofmann, 2016). However, the context of contraction type and intensity must be specified for a proper interpretation.
A significant problem with the majority of existing protocols is that they rely on quantifying maximal voluntary force loss, maximum voluntary muscle contraction (MVC) (Hug et al., 2009; Oda and Kida, 2001) or high fatiguing dynamic tasks (González-Izal et al., 2010) that cannot be reliably performed in clinical practice, especially in the case of pediatric subjects. Actually, previous works pointed out that not only the capacity to maintain MVC can be limited by a lack of cooperation (Ratel et al., 2006), but also, that sustaining a maximal force in isometric conditions longer than 30 s reduces subject's motivation leading to unreliable results (Halin et al., 2003). Besides, neuromuscular patients might have a high level of impairment and low residual muscular function thus making even more difficult, as well as dangerous for their muscles, sustaining high levels of effort or the execution of MVC. In order to overcome this issue, maximal muscle contractions can be elicited by magnetic (Lou et al., 2010) or electrical stimulation (Gregory and Bickel, 2005). Although such procedures allow to bypass the problem mentioned above, these involve involuntary muscle activation and not physiological recruitment of motor units (Vøllestad, 1997). Moreover, these methods can be uncomfortable for patients and can require advanced training, therefore they are not commonly included in clinical fatigue assessment protocols.

As for the above mentioned problem with children motivation, work by (Naughton et al., 1992) showed that the test-retest coefficient of variation of fatigue index during a Wing-Gate test significantly decreased when using a computerized feedback game linked to pedal cadence. Such results suggest that game-based procedures may ensure more consistent results in children assessment.

In recent years, the assessment of sensorimotor function has been deepened thanks to the introduction of innovative protocols administered through robotic devices (De Santis et al., 2015; Marini et al., 2016b; Mugnosso et al., 2017). These methods have the ambition to add meaningful information to the existing clinical scales and can be exploited as a basis for the implementation of a muscle fatigue assessment protocol. In order to fill the gap between the need of a quantitative clinical measurement protocol of muscle fatigue and the lack of an objective method which does not demand a high level of muscle activity, we proposed a new method based on a robotic test, which is fast and easy to administer. Further, we decided to address the analysis of muscle fatigue on the upper limb as to provide a test suitable to assess patients from the beginning to the late stages of the disease, regardless of walking ability. Moreover, we focused on an isolated wrist flexion-extension tasks to assess wrist muscle fatigue. This ensured repeatability of the tests and prevented the adoption of compensatory movements or poor postures that may occur in multisegmental tasks, involving the shoulder-elbow complex.

In the previous chapter muscle fatigue has been defined and an overview of the mechanisms involved in its manifestation has been presented. In the following paragraphs I reported the method that we developed to assess muscle fatigue. In particular, firstly the method has been applied on adult healthy subjects to preliminary test its feasibility and the repeatability of the results (paragraph 3.2); then we tested it on a larger adult control population (paragraph 3.3). Finally, to test the feasibility of the method with children with neuromuscular disorders, we run pilot experiments on pediatric subjects with Duchenne Muscular Dystrophy and Becker Muscular Dystrophy as well as healthy children (paragraph 3.4).

The most relevant and novel features of the proposed test include the ability to perform the test regardless of the subjects' capability and strength, the objectivity and repeatability of the data it provides, and the simplicity and minimal time required to administer.

3.2 A novel method for muscle fatigue assessment during robot-based tasks. Part I

3.2.1 Introduction

In order to fill the gap between the need of a quantitative clinical measurement protocol of fatigue, and the available EMG-based techniques which request a good level of muscular functions, we propose a robotic test for the wrist joint, easy and fast to administer, and we evaluated performance of the two muscles involved in the task (*Flexor* and *Extensor carpi radialis*).
The aims of the proposed protocol, and its innovative aspects, were mainly two.
Firstly, to extract objective information about muscle condition and fatigue level from movements which could be performed whatever level of subjects' capability.
Secondly, to use a a fully backdrivable robotic platform which allowed to minimize task variability, make the test repeatable and provide haptic interaction resulting in a viscous field.
In this work we preliminary tested our method on 9 healthy participants and we analyzed the sensitivity of the chosen indicators of performance, looking at both the spectrum and the amplitude of muscular activity through the task.

3.2.2 Methods

Experimental setup

The experiment was carried out at the Motor Learning, Assistive and Rehabilitation Robotics Lab of the Istituto Italiano di Tecnologia (Genoa, Italy). The device used for this study is Wristbot a 3 Degrees Of Freedom (DoFs) manipulandum, developed for motor control studies and rehabilitation of the human wrist (paragraph 2.4).

Experimental Protocol

Subjects sat on a chair with their forearm strapped to the robot support, with a correct alignment between the axes of the mechanical structure and the wrist's anatomical ones, and they held the handle of the robot (see Figure 3.1). The proposed task consisted in a haptic tracking: starting from a central position, subjects were asked to execute a flexion-extension movement with their dominant right wrist, in order to track a target moving along a horizontal trajectory in a viscous force field. Task instructions emphasized tracking accuracy in order to force subjects keeping a constant speed and therefore a constant level of the viscous field

magnitude. Movement's excursion varied between 55° of extension to 65° of flexion, each movement lasted 2 seconds and target followed a minimum jerk trajectory with an average velocity of 60°/sec. Target and wrist actual position were represented on a computer screen placed in front of the robot with two animated features. The experienced viscous force was proportional to a preset damping coefficient (B) and to wrist angular speed ($\dot{\theta}$) according to the following equation:

$$F = -B\dot{\theta} \tag{3.1}$$

The damping parameter B was set taking into account the gender differences in grip strength. Grip strength of each subject has been evaluated, prior to the experiment, using a hand held hydraulic dynamometer (in the Baseline 7-Piece Hand Evaluation Kit, Fabrication Enterprises Inc) in order to verify the greater hand grip strength of male subjects with respect to female subjects as indicated in literature (Bäckman et al., 1995; Leyk et al., 2007; Phillips et al., 2000). Then, we chose a value of B equal to 22.2 N/rad for women and 27.7 N/rad for men. The experimental protocol consisted of three robotic sessions performed on three

Figure 3.1 Experimental setup. Participant sitting on a chair with the forearm secured to the Wristbot while performing the wrist rotation reaching task. The visual targets of the reaching task are shown on a dedicated screen.

different days, in order to assure a proper rest between them. Each session consisted of 150 cycles (1 cycle = 1 flexion + 1 extension). Nine right-handed healthy volunteers (4 males and 5 females; age 26.4±2.5 years of age) took part to the experiment. The research conformed to the ethical standards laid down in the 1964 declaration of Helsinki, which protect research

subjects and the protocol was approved by the regional ethical committee. The subjects signed a consent form that conforms to these guidelines.

Data Analysis

Wrist joint rotations, recorded from the robot encoders, were converted to angular displacements and used to compute angular velocities. Then all these values were processed with a sixth-order Savitzky-Golay low-pass filter (10 Hz cut-off frequency) and re-sampled at the EMG sample rate by linear interpolation. EMG data were band-pass filtered (5-350 Hz), rectified and low-pass filtered (20 Hz cut-off frequency). EMG signals and kinematic data were synchronized through a trigger signal sent from the robot to the EMG base unit to assure association between each muscle activation and the corresponding movement. We segmented EMG signals in order to calculate fatigue indexes just when the muscle was actually active, i.e. we considered *Flexor Carpi Radialis* just during flexion movements and vice versa *Extensor carpi radialis* during extension movements. To assess fatigue, we chose three different standard EMG measures, two in the frequency and one in the time domain (previously presented in section 2.3.6):

- *Mean Frequency* (F_{Mean}) (Kwatny et al., 1970). It indicates the shift of the Power Spectral Density (PSD) of the sEMG signal toward lower frequencies and it is evaluated following the equation 2.3.

- *Dimitrov Index* (Dimitrov et al., 2006). It quantifies the spectral changes of muscle EMG during fatigue using different spectral moments and it is calculated as the ratio between them (see equation 2.4) We used the order of spectral $K = 5$ (González-Izal et al., 2010). We chose to introduce the *DI* because the spectral moment of order -1 emphasizes increments in low frequencies in the sEMG spectrum while spectral moments of order greater than 1 emphasize the effect of decrements in high frequencies (Arabadzhiev et al., 2005). As such, the *DI* achieves higher sensitivity under both isometric and dynamic contractions than conventional parameters.

- Finally, we evaluated the averaged *Root Mean Square (RMS)* of the sEMG data, obtained according to the following equation by the mean of the squares of the instantaneous values of the processed EMG signal (see equation 2.2).

To best describe development of fatigue throughout task duration, data across the 150 trials for flexion (*Flexor Carpi Radialis* muscle) and extension (*Extensor Carpi Radialis* muscle) were fitted using a 3rd order polynomial function, based on mean least squares approximation.

From the fitted curve of the Mean Frequency (F_{Mean}) we evaluated the Onset of Fatigue (OF) as the movement during which the F_{Mean} has a decrement of 50% of the difference between the first and the minimum values.

3.2.3 Results

Figure 3.2 shows the mean trend over the three sessions of Mean Frequency, Dimitrov Index and RMS for the two muscles of the nine subjects (continuous line for *Flexor* muscle, dashed line for *Extensor* muscle), statistics of the fitting (goodness (R^2) and RMSE), are reported in Table 3.1. The curves relative to the *Flexor* muscle do not precisely follow the proposed trend for three subjects (S3, S6 and S8) while the chosen model predicts the behavior of the *Extensor* muscle in a good way for all the subjects with the exception of S9. Moreover, Figure 3.2 clearly shows the decreasing pattern of the Mean Frequency curve, obtained by the average of the curves of the three sessions, which is steep during the first third of the task and reaches a plateau during the last third. Similarly the mean curves of the DI and the RMS change throughout the task (increase as expected for these indicators), the most gradually, the most the movement is close to the end of the task. Exception is made by subject 4 who does not present a monotonic trend for neither *Flexor* nor *Extensor*. For this subject, despite the three indicators have the expected trend for the first half of the experiment,they present the opposite behavior at the end of the task.

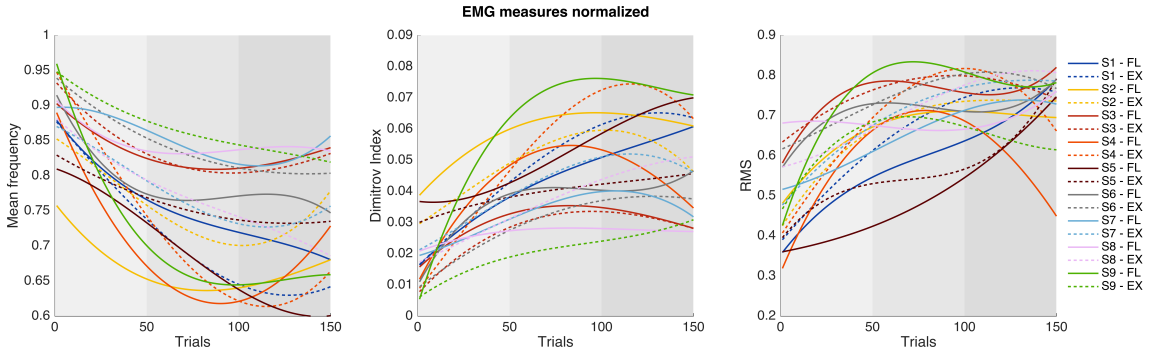

Figure 3.2 Trend of the normalized EMG indicators for *flexor*(continuous line) and *extensor* muscle (dashed line). Mean of the three sessions for the nine subjects.

Figure 3.3 shows the Onset of Fatigue for the nine subjects. Different markers indicate the three sessions. The plot highlights consistency of the indicator, and shows how fatigue arises at a similar moment for the three repetitions of the task, and how it happens in the first third of the experiment in most of the cases both for the *Flexor* and *Extensor* muscle.

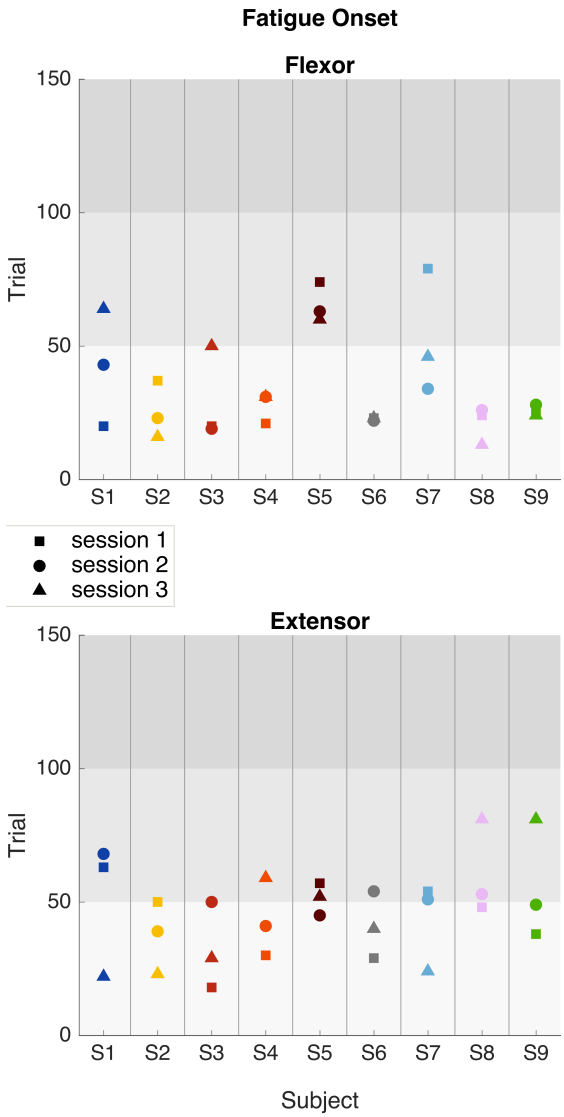

Figure 3.3 Onset of Fatigue for the nine subjects and the three sessions, top and bottom panel reports data of the *Flexor* and *Extensor* muscle respectively. Grey areas divide each session (light gray first 50 trials, medium gray for trials between 100 and 150, dark gray for the last 50 trials of the session). Marker shapes indicate the session number, different colors describe the nine subjects. Vertical lines separate each subject.

Subjects 5 is the only one presenting the Onset of Fatigue later in time for the *Flexor* muscle. Considering the mean value of the OF of the three sessions for each subject, the OF occurs on average at the movement 34.67 ± 5 (average value $\pm$ standard error) for the *Flexor* muscle and 46.2 ± 3 for the *Extensor* muscle. Figure 3.4 provides information about changes in the slope of the fitted curve of the Dimitrov Index during task execution. Purple colors indicate higher slope, conversely, if the slope of a trial is depicted in orange it indicates milder values.

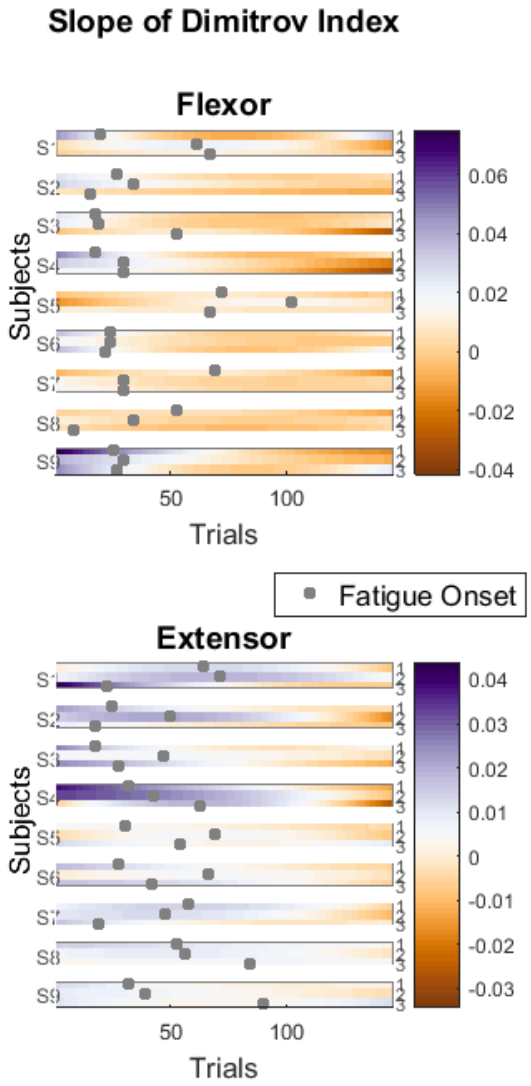

Figure 3.4 Changes of the fitting curve of the DI during task execution. Purple colors indicate higher slope, conversely, if the slope of a trial is depicted in orange it indicates milder values. The grey dots mark the trial corresponding to the fatigue onset. Top and bottom panels are related to *flexor*and *extensor* respectively; subjects are indicated on the left, session number on the right side.

The grey dots mark the trial corresponding to the Onset of Fatigue. Top and bottom panels are related to *Flexor* and *Extensor* respectively; subjects are indicated on the left, session number on the right side. It is evident how the slope decreases after the Onset of Fatigue and in general highlights how the DI curve stabilizes to a plateau going towards the end of the task. Finally, Figure 3.5 shows changes in RMS slope before and after the *OF*. Left panel: *Flexor* muscle, right panel: *Extensor* muscle. Different marker shapes indicate the three

Table 3.1 Goodness of fit (R^2) and RMSE of *Mean Frequency* curves for each subject. Goodness higher than 0.6 is underlined.

	Flexor		*Extensor*	
	R^2	RMSE	R^2	RMSE
S1	<u>0.78</u>	0.054	<u>0.89</u>	0.041
S2	0.52	0.058	<u>0.74</u>	0.051
S3	0.44	0.051	0.54	0.040
S4	<u>0.70</u>	0.066	<u>0.82</u>	0.054
S5	<u>0.66</u>	0.080	0.53	0.076
S6	0.34	0.052	0.61	0.046
S7	<u>0.60</u>	0.060	<u>0.76</u>	0.051
S8	0.12	0.053	<u>0.76</u>	0.045
S9	<u>0.79</u>	0.049	0.42	0.061

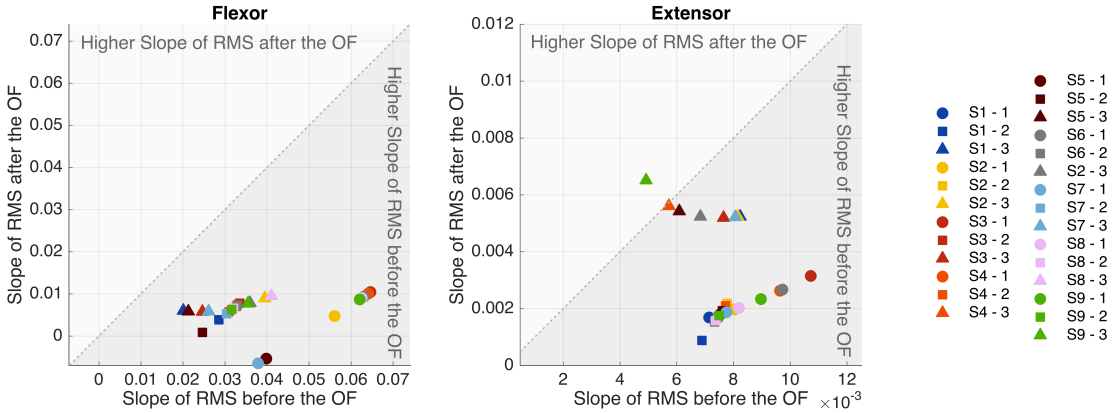

Figure 3.5 Changes in RMS slope before and after the Onset of Fatigue (*OF*). Left panel: *flexor*muscle, right panel: *extensor*muscle. Different marker shapes indicate the three sessions for all the 9 subjects (depicted with different colors)

sessions for all the 9 subjects (depicted with different colors). Data points which fall above the equality line (dashed grey line) indicate higher slope of the RMS after the *OF*, conversely, data points which fall below the diagonal line of identity indicate that the RMS stopped increasing after the *OF*. Overall, results are consistent for all the nine subjects showing a lower slope of the RMS after the Onset of Fatigue.

3.2.4 Discussion

The method presented in this work is a first attempt to quantitatively measure muscle fatigue in a clinical variegated setting. Our goals were to validate the feasibility of the method and ascertain the sensitivity and reliability of the indicators chosen to evaluate subjects' performance. As shown in the previous sections, the method is simple and easy to administer. The method is not based on MVC, as the majority of the existing protocols. Therefore, also participants who are not able to sustain MVCs could potentially perform the test. These advantages could promote the adoption of the method in clinical practice. Moreover, such protocol can be tailored on the specific abilities (or disabilities) of patients customizing the robotic task properties appropriately (i.e. the damping of the viscous field, the range of motion, the ideal requested speed etc.). Furthermore, the three sEMG-based measures (Mean Frequency, Dimitrov index and RMS) and the proposed indicator (Onset of Fatigue (*OF*)) resulted to objectively describe muscle fatigue. The DI brings similar results of the Mean Frequency but it could be more sensitive when the subject is not able to perform well isometric and dynamic contractions, e.g. when he/she is affected by a neuromuscular disease (Dimitrov et al., 2006).

Almost all subjects highlighted a consistent trend of the three indicators during the task (i. e. the Mean Frequency decreases over time while the DI and the RMS increase). However in the last part of the task (starting about after 100 trials) the trend resulted to be inverted, that may be related, from a physiological perspective, to a de-recruitment of fatigued motor unit in charge of the movement, in favor of the recruitment of new motor units of different muscles (Dimitrova et al., 2009). This result puts in light a lack of our method, which imposes the number of trials to perform. A better procedure would be, in future, to let the subject perform as many trials as possible, or stop the task according to an online control of the sEMG signals, and evaluate the number of trials as a measure of performance (Octavia et al., 2015). Overall results confirmed the sensitivity of the *OF* as a measure of the time in which fatigue occurs. The final purpose of the test is to be used with pathological populations. Indeed, an eventual shift in time of the *OF* during different testing sessions would add information about the progression of the disease. The repeatability of the method was assessed by repeating three times the proposed test. Results provided the evidence of similar performance and trend of the indicators over time thus suggesting the repeatability of the test. Finally, to check the generalization capabilities of the method we tested two different muscles (*extensor* and *Flexor Carpi Radialis*) and, due to similar indicators' behavior obtained, we can predict reliable results when the muscles involved in the specific task are others. During the progression of the disease the symptoms of muscle fatigue become more severe and this will result in

a significant change in the slope of the indicators fitting curves and in the *OF* permitting to supervise better an eventual clinical intervention. The proposed test resulted to be easily performed and well accepted by the subjects, laying down the basis for further improvements with the aim of implementing it in rehabilitation practice where clinicians strongly claim the need of an assessment tool for fatigue assessment in childhood, adulthood and with elderly people.

3.3 A novel method for muscle fatigue assessment during robot-based tasks. Part II

3.3.1 Introduction

As an extension and consolidation of the preliminary study (paragraph 3.2), in this section I present the results obtained with 40 healthy subjects tested with a novel improved version of the robot-based assessment protocol. In particular, in the first version of the test we used a pure viscous force field. This type of force is proportional to velocity. This choice could reduce the repeatability of the results in case of patients who are not able to sustain the same speed from the beginning to the end of the test. In the present study, we decided to implement an elastic force field to overcome this issue. A small contribution of viscous force was added to reduce the damping of the inertia of the robot. In addition, the resistive force field was applied just in one direction (flexion direction or extension direction) to reduce the effort required to perform the test. Therefore, in order to analyze the behavior and the characteristics of both the flexor and extensor muscles, subjects were divided into two groups. In the first group, the resistive force was applied by the robot only during flexion movements, whereas, in the second group, the force was applied only during extension movements.

3.3.2 Methods

Participants

Forty healthy subjects with no history of motor disorders were enrolled in the study. All participants were right-handed according to the Edinburgh Handedness Inventory (Oldfield, 1971). The study was approved by the Ethics Committee of the regional health authority, Azienda Sanitaria Locale Genovese (ASL) N.3 (Protocol number 311REG2014 approved on 09/12/2015), and all participants signed a written informed consent. Experiments were carried out at the Motor Learning, Assistive and Rehabilitation Robotics Lab of the Istituto Italiano di Tecnologia (Genoa, Italy). Participants were randomly divided into two equal groups: *Flexion Group* (*FG*) (5 male and 15 females, mean age 31.4 $\pm$ 6.3 years); and *Extension Group* (*EG*) (8 male and 12 females, mean age 25.5 $\pm$ 3.9 years). Moreover, the maximum grip force of each subject was evaluated using a hand held hydraulic dynamometer (Baseline 7-Piece Hand Evaluation Kit, Fabrication Enterprises Inc). Subject demographics are summarized in Table 3.2.

Table 3.2 Subject details for the *Flexion Group* (*FG*) and the *Extension Group* (*EG*): Sex, Age and hand grip Force.

	FG			*EG*		
	Sex	Age	Force [Kg]	Sex	Age	Force [Kg]
S1	F	26	21	F	21	32
S2	F	22	24	M	30	38
S3	F	26	26	M	25	40
S4	F	34	30	M	23	40
S5	F	22	25	F	33	22
S6	F	26	32	M	22	40
S7	M	35	38	F	31	36
S8	F	27	31	F	25	40
S9	M	35	40	F	26	20
S10	F	40	24	F	30	35
S11	F	37	15	F	25	35
S12	M	40	39	F	24	36
S13	F	34	25	F	30	26
S14	F	30	35	M	19	36
S15	M	43	42	M	19	34
S16	F	33	34	M	22	43
S17	F	24	36	F	26	34
S18	M	32	39	M	28	43
S19	F	37	22	F	26	27
S20	F	25	35	F	26	30

Task and procedures

The experimental design involved a motor task where subjects sat in front of a three degrees of freedom wrist robotic manipulandum, (Wristbot , see 1.3 for more details), holding the handle with their right hand (Figure 3.1). Subjects' forearm was strapped to the robot support in order to avoid forearm movements and to have a correct alignment between the axes of the mechanical structure and the anatomical ones. The experimental setup was complemented by a 6-axis force/torque sensor (Optoforce HEX-58-RE-400N) mounted on the handle in order to evaluate the efficiency of the robot in terms of provided torque. The task consisted of a series of continuous target reaching movements interacting with a visco-elastic force generated by the Wristbot (Figure 3.6). Grasping the handle of the robot, subjects were requested to perform flexion and extension movements with their wrist in order to reach flexion-extension targets, presented alternately at an angular distance of $\theta_e = 48^\circ$ or $\theta_f = -48^\circ$ with respect to the neutral wrist position. The elastic force experienced by *FG* subjects opposed flexion

movements and facilitated extension movements and it was implemented as a virtual spring whose equilibrium angle was $\theta = \theta_e = 48°$. In the case of the *EG* subjects the elastic force opposed extension movements and facilitated flexion movements, by means of a virtual spring whose equilibrium angle was $\theta = \theta_f = -48°$. In both cases, a small viscous force was added to compensate the inertia of the hand:

$$\begin{cases} F_{FG} = -k(\theta - \theta_e) - b\dot{\theta} \\ F_{EG} = +k(\theta - \theta_f) + b\dot{\theta} \end{cases} \tag{3.2}$$

where k is the stiffness coefficient of the force-field and b the corresponding viscous coefficient. The stiffness parameter k was set, prior to the experiment, taking into account the significant grip force difference between male and female subjects (see Table 3.2). Mean female grip force was 30% less than that of males, which is in agreement with what is reported in the literature (Bäckman et al., 1995; Phillips et al., 2000). More specifically, the following values of the visco-elastic parameters were chosen: k = 22.2 N/rad for female subjects, k = 27.7 N/rad for males, and b = 1.77 Ns/rad for all subjects. In order either to avoid a possible fatigue recovery between one movement and to limit the variability between movement duration, targets had to be reached within a fixed time. In particular, a visual and an auditory feedback was provided: the target color changed and a sound was produced if the subject did not reach the target within a duration of 1.5 s. Besides, the minimum

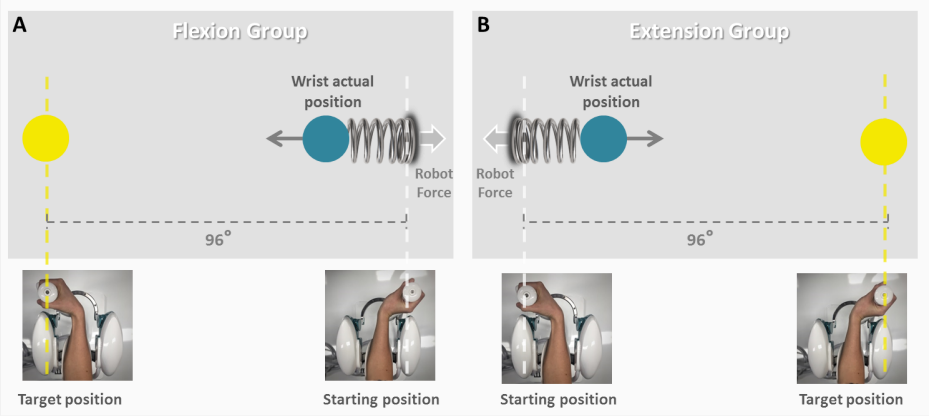

Figure 3.6 Fatigue test. Scheme of the task for the flexion group (FG) during a flexion movement (Panel a) and the extension group (EG) during an extension movement (Panel b). The blue circle represents the end-effector of the subject, the yellow circle is the target to reach

time was not imposed. We allowed subjects to modulate their pace in order to verify if any change in kinematic parameters was induced by muscle fatigue. Subjects were instructed

to perform the target reaching task until they could no longer do the task. In this moment we could consider the level of fatigue experienced by the subject to be maximal (at least by our definition) and this corresponds to the maximum score on the VAS scale (Wolfe et al., 1996). During the execution of the task, the experimenter encouraged participants to perform as many repetitions as possible to assure the maximum level of acceptable fatigue had been reached. Therefore, for each subject the number of repeated 'task-movements' N could be different and the sequence duration for each subject was normalized, 0-100% (rather than 1-N movements) to compare subjects. During task execution, the adduction-abduction and pronation-supination degrees of freedom were haptically blocked in order to constrain movements only to the flexion-extension. Throughout the task, we recorded electromyographic signals of subject's right *extensor* and *flexor carpi radialis* muscles, using a multichannel surface electromyograph (OTBiolab EMG-USB2+). Standard electrode preparation was followed and Ag/AgCl electrodes with an interelectrode distance of 26 mm were used. The sampling frequency was 2048 Hz, with a gain of 1000, and an internal band pass filter with cut-off frequencies of [10-900] Hz. sEMG signals and kinematic data were synchronized through a trigger signal sent from the robot to the sEMG base unit to assure association between each muscle activation and the corresponding movement. The preparation for the test (namely, electrodes placement, grip force recording, adjustment of Wristbot height and oral instructions) required about 180 s; the duration of the test itself varied among subjects, mainly as a function of the total number of movements performed, with an average value of 80s (maximum duration in the overall population of subjects was 180 s). Globally, the assessment protocol could be performed with an average duration of 260 s and never exceeded 360 s.

Data Analysis

Wrist joint rotations, recorded from the robot encoders (data collection frequency set at 100 Hz), were converted to angular displacements and used to compute angular velocities. All kinematic data were processed with a sixth-order Savitzky-Golay low-pass filter (10 Hz cut-off frequency) and re-sampled at the sEMG sample rate (2048 Hz) by linear interpolation while sEMG data were band-pass filtered (5-350 Hz). sEMG and kinematic data were segmented to focus the analysis on the concentric phase for each group. In details, the analysis of the trajectory data recorded by the robot allows the extraction of each single flexion or extension movements as shown in Figure 3.7 (Panel A and B). According to that, we analyzed the signal of *flexor carpi radialis* just during flexion movements and the signal

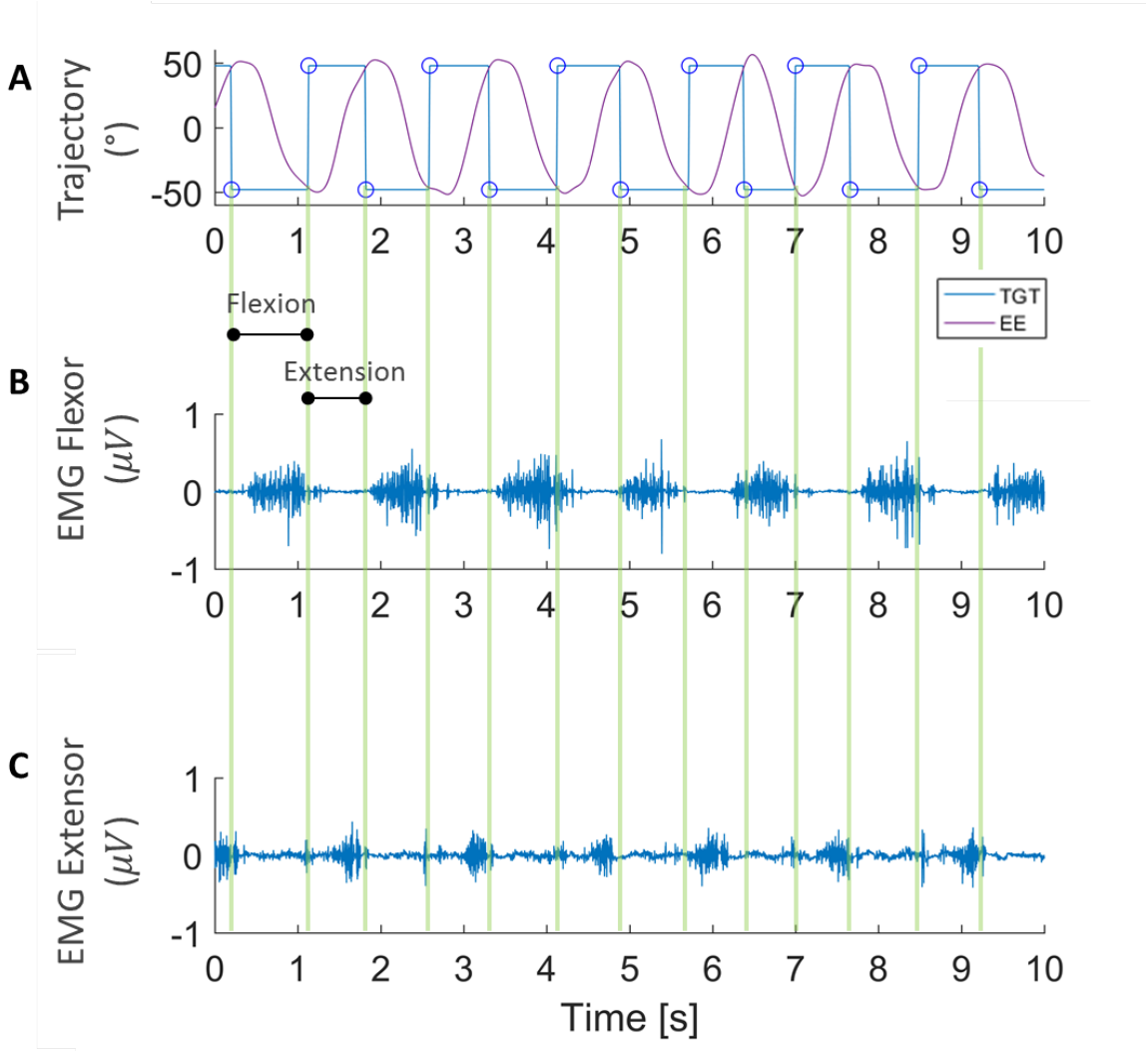

Figure 3.7 Example of data segmentation. a. Red lines represent an example of the end-effector trajectory in the flexion-extension plane to reach the target at $\pm 48°$ (blue lines). b Example of sEMG signal of the *Extensor carpi radialis* during the task. The signal was segmented according to the trajectory shown in Panel a

of the *Extensor carpi radialis*just during the extension ones. Then we computed a single value of the *Mean Frequency* for each of the obtained interval of sEMG signal. Therefore we got N values of *Mean Frequency* ($F_{Mean}(k)$, *k=1...N*) for each subject with N the total number of movements performed by the subject.
In particular the *Mean Frequency* was calculated following equation 2.3.The obtained N values of *Mean Frequency* of each subject, were fitted with a third order polynomial function based on mean least square approximations in order to calculate the *Onset of Fatigue (OF)*. This indicator was defined as follows: *OF* is the k-movement at which the initial F_{Mean} value of the sequence decreases by a given percentage ($P\%$) (i.e. $F_{Mean}(k=1)$). More precisely we used the following equation:

$$OF_{P\%} = k : F_{Mean}(k) \leq F_{Mean}(1) - P\% \cdot (F_{Mean}(1) - min(F_{Mean})) \tag{3.3}$$

In order to choose the most appropriate value of $P\%$, the acquired data were analyzed with three reference values, namely 25%, 50% and 75%, thus yielding $OF_{25\%}$, $OF_{50\%}$ and $OF_{75\%}$ respectively. The decrement $(P\%)$, in equation 3.3, is calculated with respect to the minimum value in the F_{Mean} sequence. This value may not correspond (as will become evident in the results section) with the final element of the sequence ($min(F_{Mean}) \neq F_{Mean}(k = N)$).
To ascertain that muscular behavior was not due or related to changes in motor strategy we calculated for each movement two additional indicators based on movement kinematics: the *Time to velocity peak ratio* (*TPR*) and the *Mean speed* (m/s). The *TPR* is defined as the ratio between the time from the beginning of the movement and the main peak of the speed profile, and the total duration of the main movement (T):

$$TPR = \frac{TP}{T} \tag{3.4}$$

Correlation analysis was performed to investigate the relationship between *Mean Frequency* and *Mean Speed* by evaluating the Correlation index (*CI*) between the two metrics. To constantly monitor the required effort throughout the task we evaluated the mechanical energy consumption in Joules for each subject for each movement, consisting of N samples, from the torque exerted (τ_k) and the angular position (θ_k) recorded by the robot, according to the following equation:

$$E = \sum_{k=1}^{N} \tau_k \cdot (\theta_{k+1} - \theta_k) \tag{3.5}$$

Such energy expenditure was converted into calories as to compare it with the basal metabolic rate. A statistical analysis was performed to investigate the possible significance of differences

on the *OF*. *OF* data for the 40 subjects were z-transformed before the analysis. A post-hoc two-way ANOVA was chosen to investigate any difference in the *OF* between the three percentage levels in the two groups. The group factor (*FG*/*EG*) was set as "between" while, the *OF* percentage level (25/50/75) as "within". Significant main and interaction effects were evaluated using a two tailed t-test with Bonferroni correction for multiple comparisons. Significance was set at $p < 0.05$.

3.3.3 Results

The *Mean Frequency* of both the *Flexion Group (FG)* and the *Extension Group (EG)* decreased during the first half of the task execution, and eventually reached a plateau (Figure 3.8, Panel A and Panel B respectively), although in a few cases the trend was not monotonically decreasing: consider, in particular, subjects S2-S4-S5-S6-S13 of the *FG* and subjects S13-S18-S19 of the *EG*.

The fitting analysis indicated that the third-order polynomial model is a good predictor

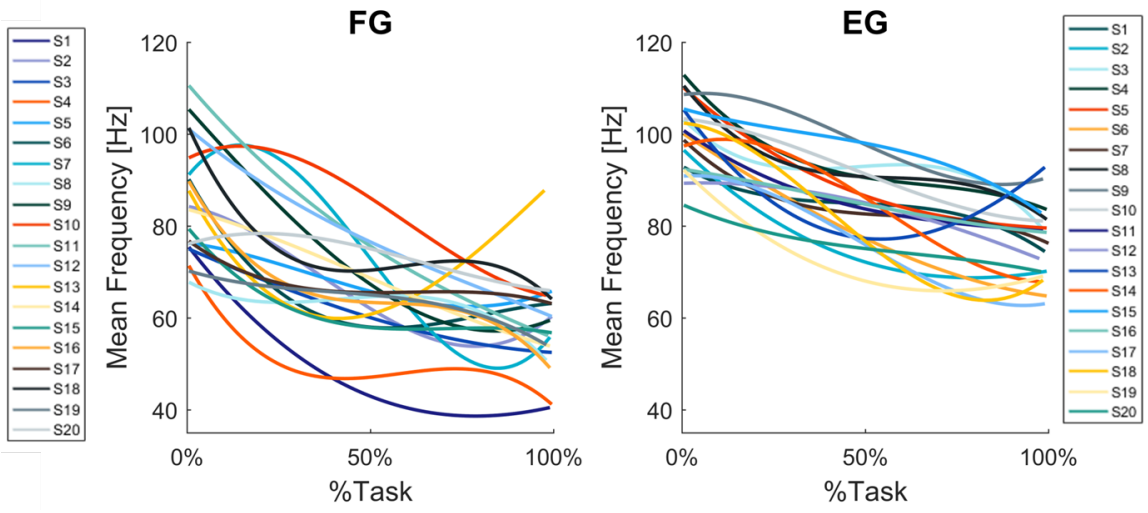

Figure 3.8 Mean Frequency results. Normalized F_{Mean} (Hz), of the FG (Panel a) and EG (Panel b), fitted with a third order polynomial function. Each line and color indicates a different subject

of the *Mean Frequency* trend, especially for the *Extension Group*. Indeed, 12 subjects out of 20 from the *EG* presented a goodness of fit higher than 0.6; such a goodness of fit was reached for 9 out of 20 from the *FG* (See Table 3.3). Additionally, comparing the two groups, we found that the reduction in *Mean Frequency* was greater for the *Flexor Carpi Radialis*, fatigued in the *FG*, than for the *Extensor Carpi Radialis*, fatigued in the *EG*.

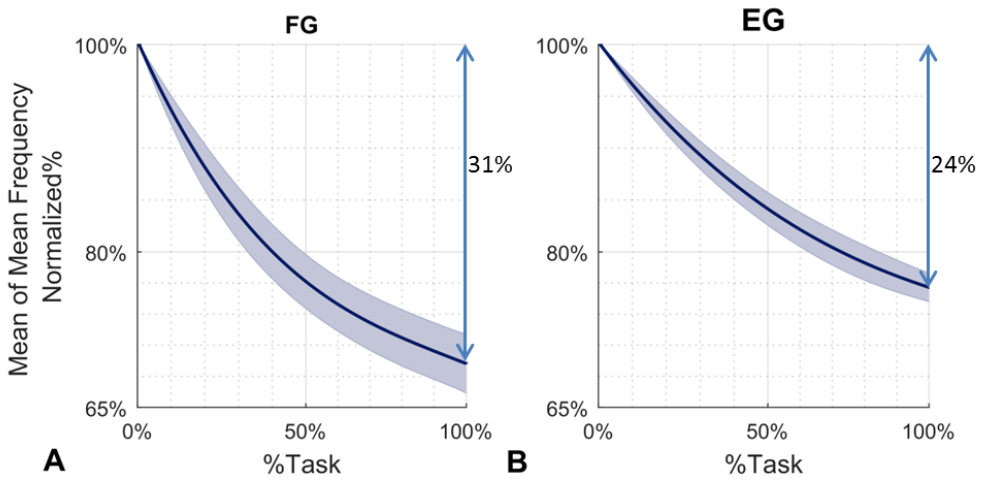

Figure 3.9 Averaged Mean Frequency results. Normalized F_{Mean} (Hz), of the FG (Panel a) and EG (Panel b), fitted with a third order polynomial function. Frequency was normalized to the initial frequency of each sequence and averaged across subjects. Shaded area represents standard error

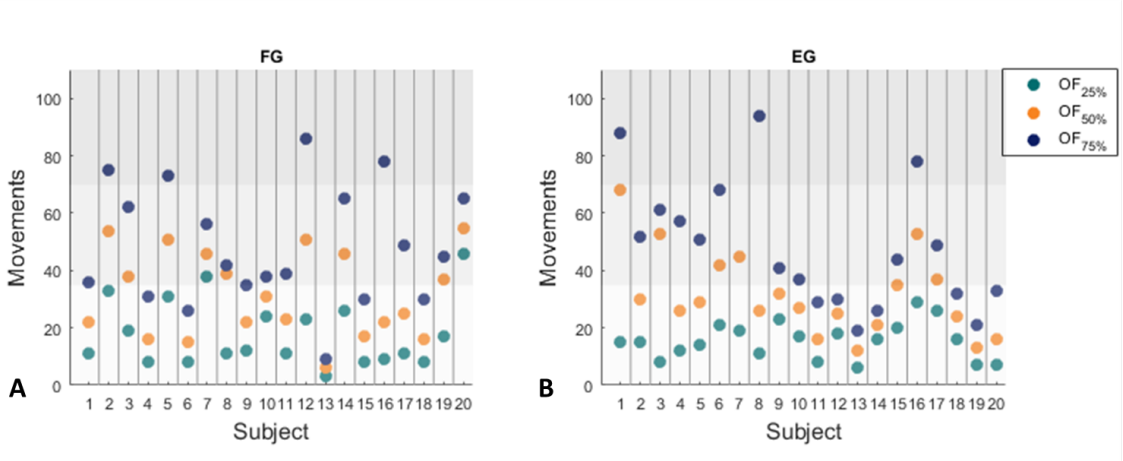

Figure 3.10 *OF* results. Results related to *OF* indicators (Onset of Fatigue). Panels a and b show, for each FG subject (panel a) and EG subject (panel b), the values of the three *OF* indicators: *OF*25%, *OF*50%, *OF*75%, expressed as number of "movements" that satisfy equation 3.3. Grey areas divide the task in three phases.

Specifically, Figure 3.9 represents the evolution of the averaged *Mean Frequency* across *FG* and *EG* subjects (panel A and B respectively), normalized with respect to the initial value. From such a curve, it is possible to evaluate the percentage decrease of the averaged *Mean Frequency* of the fatigued muscles, with respect to the beginning of the task execution: 31% for the *flexor* and 24% for the *extensor*.

Table 3.3 Goodness of fit (R^2) and RMSE of *Mean Frequency* curves for each subject. Goodness higher than 0.6 is underlined.

	FG		*EG*	
	R^2	RMSE	R^2	RMSE
S1	<u>0.89</u>	3.7	0.33	5.37
S2	<u>0.75</u>	5.39	<u>0.66</u>	5.75
S3	<u>0.74</u>	3.94	0.20	8.06
S4	0.34	8.16	0.53	6.65
S5	0.21	8.41	<u>0.76</u>	4.94
S6	<u>0.86</u>	3.25	<u>0.89</u>	3.62
S7	<u>0.73</u>	11	<u>0.66</u>	3.57
S8	0.41	3.97	<u>0.65</u>	4.44
S9	<u>0.91</u>	4.53	<u>0.83</u>	3.32
S10	0.45	11.87	0.49	7.33
S11	<u>0.71</u>	9.78	0.58	5.04
S12	<u>0.84</u>	4.89	0.14	9.44
S13	0.49	8.40	<u>0.79</u>	3.73
S14	<u>0.71</u>	5.63	<u>0.78</u>	5.67
S15	0.37	7.36	0.23	9.78
S16	0.42	9.62	0.50	4.17
S17	0.35	3.94	<u>0.61</u>	8
S18	0.42	8.86	<u>0.82</u>	6.20
S19	0.47	3.94	<u>0.67</u>	5.08
S20	0.22	7.24	<u>0.67</u>	2.56

We also compared the three criteria for the identification of the *Onset of Fatigue* (namely, $OF_{25\%}$, $OF_{50\%}$ and $OF_{75\%}$) in order to identify the most reliable approach. Figure 3.10 shows the results of the three versions of the *OF* of each subjects while Figure 3.11 indicates the distribution of such indicators in the two populations. In details, the Gaussian approximation of the probability density functions of the three versions of the *OF* (shown in Figure 3.11) indicates that the main difference among the three *OF*s lays in their reliability: $OF_{25\%}$ provides a more reliable estimate of onset of fatigue because it is characterized by a much smaller variance than the other two, with $OF_{75\%}$ being the least robust and most variable. It is worth mentioning that, despite a higher variance than $OF_{25\%}$, $OF_{50\%}$ presented the highest consistency between the two groups, as indicated by the two orange Gaussian functions that are almost identical. The mean values of the three *OF* indicators are represented with circular

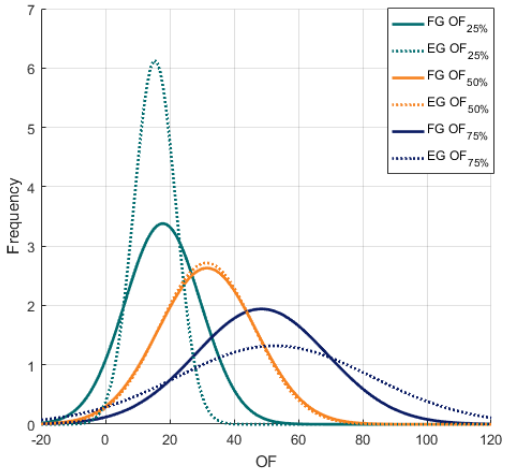

Figure 3.11 Gaussian approximation of the probability density functions of the three *OF* indicators for the FG population (solid lines) and EG population (dashed lines).

markers in Figure 3.12 for both groups. The mean value of $OF_{25\%}$ resulted 17.85 $\pm$ 2.64 (mean $\pm$ standard error) for *FG* group and 15.45 $\pm$ 1.4 for the *EG* group independently of the number of movements performed by each subject (see Table 3.5); $OF_{50\%}$ occurred at 31.71 $\pm$ 3.28 and at 31.72 $\pm$ 3.06 for the *FG* and the *EG* group respectively; the $OF_{75\%}$ occurred at 48.66 $\pm$ 4.75 for the *FG* subjects and 52.65 $\pm$ 6.75 for the *EG* group. The statistical analysis revealed significant differences among the three *OF*s ($F(2, 114)=35.485$, $p<0.001$) independently from the group. There was no interaction between *OF* and the group ($F(2, 114)=0.34286$, $p=0.71046$). There were no significant differences between the two groups for the number of movements to *OF* (shown in Figure 3.10 Panel D) ($F(1, 114)=0.02614$, $p=0.87183$). However, post-hoc analysis demonstrated a significant difference

between $OF_{25\%}$ and $OF_{50\%}$ (p=0.001), between $OF_{25\%}$ and $OF_{75\%}$ (p<0.001), and between $OF_{50\%}$ and $OF_{75\%}$ ($p < 0.001$). The kinematic analysis of the performed experiments should demonstrate any potential relationship between a subject's motor strategy and patterns of muscle activity. In particular, we evaluated the Correlation Index (*CI*) between the *Mean*

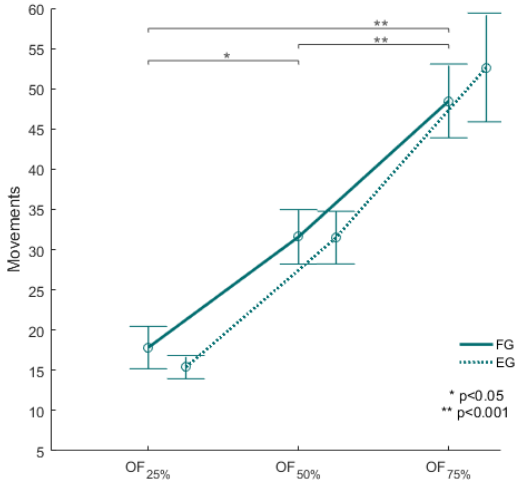

Figure 3.12 Mean values and standard errors of the three *OF* indicators for the FG population (solid line) and the EG population (dashed line).

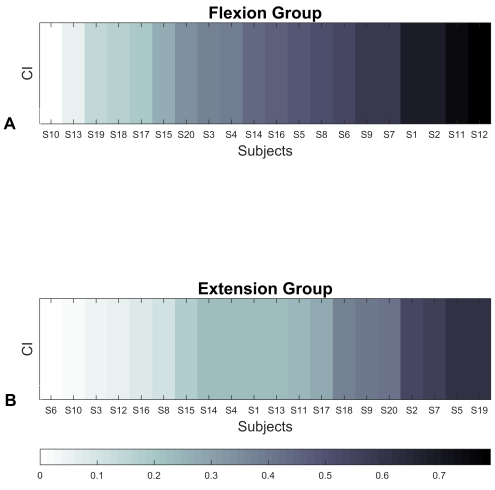

Figure 3.13 CI results. Absolute values of the Mean speed and the Mean Frequency correlation for the FG (Panel a) and the EG (Panel b. Subjects are sorted by correlation, as indicated in the bottom panel legend.

speed and the *Mean Frequency*, and this is reported in Table 3.4 and Figure 3.13 (absolute values). Overall, the correlation is negative, namely higher *Mean speed* implies lower *Mean Frequency*, but, in general, it is a weak relationship: on average, the absolute correlation value was 0.42 for the *FG* population and 0.27 for the *EG* population, and it never exceeded 0.8.

In spite of the low correlation between speed and frequency, the kinematic analysis of the

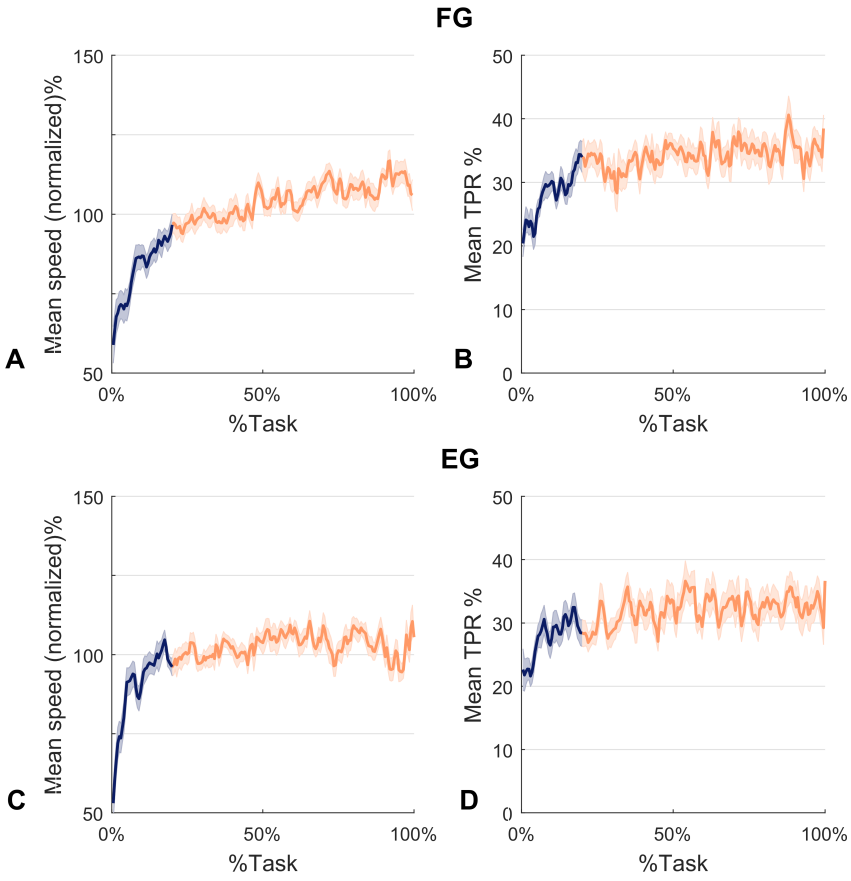

Figure 3.14 Kinematics results. Panel a and c: Mean speed normalized by the mean of each subject and averaged over FG and EG subjects respectively. Panel b and d: Time to peak ratio averaged over FG and EG subjects respectively. %Task identifies the relative ordinal number of the task-movements of all the sequence. In all panels shaded areas indicate the standard error, the blue portions refer to the first 20% of the task while the red corresponds to the remaining 80%.

movement was valuable for demonstrating the consistency of the designed protocol. This is shown in Figure 3.14 which plots the evolution during task execution of the normalized *Mean speed* (panels A and C) and the *Time to velocity peak ratio* (panels B and D). The *Mean*

speed graph is characterized, for both groups of subjects, by a steady increase in the first 20% of the task execution (blue portion of the curve) followed by a plateau in the remaining 80% of the task. The graph of the *Time to velocity peak ratio* (*TPR*) is characterized by a similar trend, with an initial transient related to the first 20% of the task execution, followed by a plateau for the rest of the task. This suggests that there were no changes in wrist kinematic strategies. It is worth noting, there was a difference between the two groups. The *FG* subjects exhibited a speed profile with higher symmetry as indicated by the fact that *TPR* is closer to 50% than for the *EG* subjects.

Finally, the analysis of the energy consumption revealed that the average number of calories consumed to perform the task was 63.80 $\pm$ 4.75 calories (mean and sem). Individual values are shown in Table 3.5.

Table 3.4 Number of movements performed by each subject and total calorie consumption.

	FG		*EG*	
	N° Mov	Cal	N° Mov	Cal
S1	94	70	97	55
S2	145	109	133	113
S3	104	62	66	50
S4	104	81	117	102
S5	146	103	105	64
S6	101	59	110	82
S7	86	73	209	137
S8	44	40	117	80
S9	73	60	66	37
S10	48	51	54	43
S11	61	40	60	22
S12	126	117	34	22
S13	38	18	67	39
S14	89	74	34	28
S15	105	90	49	37
S16	92	70	114	83
S17	150	106	75	51
S18	104	92	56	49
S19	49	31	57	33
S20	78	51	48	28

Table 3.5 *Mean speed* - *Mean Frequency* correlation coefficients.

	FG	*EG*
S1	-0.68	-0.23
S2	-0.68	-0.54
S3	-0.37	0.04
S4	-0.39	-0.22
S5	-0.49	-0.61
S6	-0.54	0.01
S7	-0.58	-0.56
S8	-0.51	0.09
S9	-0.58	-0.56
S10	-0.01	-0.02
S11	-0.74	0.24
S12	-0.79	-0.06
S13	-0.06	-0.23
S14	-0.44	-0.22
S15	-0.26	-0.17
S16	-0.46	0.07
S17	-0.19	-0.28
S18	-0.17	-0.37
S19	0.15	-0.61
S20	0.34	-0.42

3.3.4 Discussion

This work revealed that the proposed test is easy, fast to administer and provides an objective and reliable measure of muscle fatigue. Additionally, the kinematic analysis demonstrated the stability of the *OF* indicators and it appears robust, given different motor control strategies. Regarding the applicability of the method, the experimental setup is minimal, requiring sEMG from two target muscles and the correct alignment between the human wrist and the robotic device. From a clinical perspective, test duration is also important and our test never lasted more than 3 minutes. It is even reasonable to expect a shorter test time in clinical populations compared to our healthy participants. We chose to base our indicator of *Onset of Fatigue* on the *Mean frequency* since its variance is typically lower than that of *Median frequency* (Knaflitz et al., 1990). The shift in *Mean frequency* towards the lower frequency spectrum was noticeable in both the *flexion* and *extension* groups, however the shift was greater in the former. This may be due to different physiological properties of the two muscles: I) from a biomechanical perspective of the human wrist joint, the amplitude of the range of motion in flexion is higher than that achievable in extension (the amplitude of the peak flexion moment is approximately 70% higher than peak extension moment (Gonzalez et al., 1997)); II) the percentage decrement of *Mean Frequency* is proportional to the amount of catabolites produced by muscle fibers during activity (Merletti et al., 1990). In particular, the quantity of catabolites depends on the average number of muscle fibers per square unit of the muscle crossection (Merletti et al., 1990) and consequently the higher the crossection, the higher the amount of catabolites and the greatest the rate of decrease of the *Mean Frequency* ; III) muscle fiber type will influence sEMG parameters, in particular, a greater percentage of type II fibers leads to a greater rate of decrease of the *Mean Frequency* (Gerdle et al., 1991). As reported from other studies, muscles belonging to the *extensor* group fatigue more and faster than flexors (Hägg and Milerad, 1997), therefore, *EG* population was expected to exhibit more fatigue. However, directly comparing the single muscles *extensor* and *flexor Carpi Radialis*, the physiological cross-sectional area (PCSA) of *flexor Carpi Radialis* is about half the size of the one of the *Extensor Carpi Radialis* (Mirakhorlo et al., 2016). Therefore, we can assume that *Flexor Carpi Radialis* has a lower force generating capacity. We can guess that on a whole, using the same force field intensity for both muscles, the extensors would fatigue more than the flexors. However we have measured just one of the muscle involved in the wrist extension. The most important contribution of this method is the evaluation of the *Onset of Fatigue*. The *OF* in the *EG* presented less variability compared to the *FG*, probably because of the different muscle properties mentioned above. As for the optimal method for determining the *Onset of Fatigue*, the comparison among $OF_{25\%}$, $OF_{50\%}$ and $OF_{75\%}$ revealed

that $OF_{25\%}$ is the more consistent and less variable. We can postulate that after an initial decrease, which is very similar in both groups, the *Mean Frequency* curves decreased with different slopes due to different subject training levels and muscle physical and physiological properties. Our $OF_{25\%}$ is also more inline with previous studies that have suggested that a mean frequency decrease of 8% is representative of muscle fatigue onset (Öberg et al., 1990; Szucs et al., 2009). Moreover, our subjects' ability to perform the task correctly from the very beginning and the consequent stability of the kinematic parameters, support the adoption of $OF_{25\%}$ as an indicator of fatigue. *Mean speed* stabilized in the first 20% of the task, suggesting that *Mean Frequency* and $OF_{25\%}$ are not related to kinematic changes. It is worth noting that, in some cases, during the last part of the task, the trend was inverted. From a physiological perspective, this may be related to a de-recruitment of fatigued motor units, in favor of the recruitment of new motor units (Vøllestad, 1997). This finding is in line with our previous experiment (shown in Section 3.2). Moreover other studies showed that during submaximal contractions motor units recruitment can still increase when motor units start to be fatigued, while during maximal contractions such a rise is limited (Croce and Miller, 2003; Marbini et al., 2002). On the other hand, we are aware that the frequency recovery could be due to the effect of cross-talk between adjacent muscles. However, since we collected signal just from the *flexor* and the *Extensor Carpi Radialis*, further investigations recording additional muscles are needed to examine the potential effect of cross-talk during our task. Regarding kinematic measurements, we found that the *Mean Speed* stabilized and remained constant after an initial phase, corresponding to the first 20% of the task, in which it increased up to a plateau level. This suggests that *Mean Speed* was not affected by muscle fatigue (and vice-versa), which is in line with previous finding (Gates and Dingwell, 2008; Lucidi and Lehman, 1992; Selen et al., 2007). Conversely from what was expected, we did not find changes in kinematic strategies that correlated with increasing fatigue level. Specifically, the *TPR* did not show a shift in the peak of the bell-shaped speed profile (Abend et al., 1982) from early trials to the late trials in which fatigue appeared. A final aspect to consider was task duration. In the proposed protocol, the number of repetitions performed was decided by the subjects and not superimposed by the experimenter. Subjects were instructed to stop when they felt tired, which is crucial in a clinical scenario. The number of repetitions, therefore, could also be considered as an additional measure of performance (Octavia et al., 2015), especially for populations with neuromuscular impairments, where kinematics and sEMG might have to be cautiously interpreted. Our results in healthy participants demonstrate that Onset of fatigue was independent from the amount of repetitions of the reaching movements performed. This may be a consequence of the population studied, who could tolerate a

high level of resistance and may not stop the test even if they felt fatigue. To conclude, the developed algorithm could be improved in the future by measuring individual wrist strength and grip force throughout the task (Hägg and Milerad, 1997). Our approach uses two levels of force, according to subjects' gender, but customizing the force level to each subject capabilities and therefore normalizing to individual strength, could yield to improve *OF* results. Lastly, this study suggested that a fatigue assessment coupling a robotic task and EMG recordings is highly feasible and practical. The wrist robotic device guarantees the repeatability of the task, providing the same force and trajectory. This approach also allows for the exact calculation of mechanical work spent by the subject, which demonstrated that the task required little effort and will not impact daily energy expenditure which is about 2500-3000 kcal (Tooze et al., 2007).

3.4 Pilot study on subjects with Duchenne and Becker Muscular Dystrophy

3.4.1 Introduction

A reliable method for fatigue assessment in subjects with Duchenne and Becker Muscular Dystrophy may be crucial for understanding how specific disease features evolve over time or for monitoring the efficacy of a therapy. In the previous sections (3.2 and 3.3), we proposed a fast and easy test to measure muscle fatigue and we validated it with healthy adult population. In the present paragraph, we tested the method on subjects with two different muscular dystrophies, to investigate the feasibility of its implementation in clinical practice. Our goal was to prove the ease of execution of the task and its acceptance by subjects with different ages and level of disabilities. If the test would result to be well accepted and correctly executed by neuromuscular subjects, this work would encourage its systematic use and inclusion in the clinical routine. Accordingly, clinicians could periodically administer the proposed test to the subjects and potential differences in the objective results of different testing session could reflect the progression of the disease.

3.4.2 Methods

Participants

5 male subjects with DMD and 5 male subjects with BMD were enrolled in the study. Their disabilities were assessed by clinicians with the North Star Ambulatory Assessment (NSAA) scale on the same day of the robotic test. The NSAA evaluates 17 items, ranging from standing to running, with a 3 point rating scales where 2 indicates the ability to perform the test normally, 1 the need of assistance and 0 if subject was unable to execute it. Total score can range from 0 (non-ambulant subject) to 34 (able to fully complete all activities) (Mazzone et al., 2009). The outcome of the scale for each subject is reported in are reported in Table 3.6 together with their age. 15 healthy age-matched controls were additionally tested to provide reference values from the healthy population and to further understand muscular behavior during a fatiguing task. In details they were equally divided in 3 ranges of age: 6/8 – 9/11 – 12/16 as shown in Table 3.7. The study, approved by the Ethics Committee of the regional health authority, Azienda Sanitaria Locale Genovese (ASL) N.3 (Protocol number 378REG2014), was carried out at joint lab for Robotic Pediatric Rehabilitation between Istituto Italiano di Tecnologia and the G. Gaslini Institute (Genoa). All subjects were not

Table 3.6 Details of subjects with DMD and BMD

Subject	Age	NSAA (0-34)	Subject	Age	NSAA (0-34)
DMD1	7	30	BMD1	7	34
DMD2	8	17	BMD2	7	34
DMD3	10	0	BMD3	15	34
DMD4	10	19	BMD4	16	34
DMD5	15	0	BMD5	16	34

Table 3.7 Demographics of healthy controls.

Subject	Age (6/8)	Age (9/11)	Age (12/16)
S1	7	9	12
S2	7	10	12
S3	8	10	14
S4	8	11	15
S5	8	11	16

enrolled in any other concomitant treatment or observational study as indicated by the good clinical practices.

Experimental Setup

As for the previous studies, the experiment involved the use of Wristbot (see section 2.4 for further details). During the experiment we recorded muscle activity of right *flexor carpi radialis* using a multichannel surface electromyograph (OTBiolab EMG-USB2+) with a 2048 Hz sampling rate, a gain of 1000 and a hardware bandpass filter [10-900 Hz]. Standard electrode placement was followed according to SENIAMs recommendation [34] and Ag/AgCl electrodes with an interelectrode distance of 26 mm were used. sEMG signals and kinematic data were synchronized through a trigger signal sent from the robot to the sEMG base unit as to assure a correct segmentation and analysis of the signals.

Experimental protocol

We adapted the protocol used in Section 3.3 in order to make it suitable for pathological populations.
Indeed, prior to the fatigue assessment test, subjects were requested to perform a simple preliminary task. Holding the handle of the robot, they had to flex three times their wrist as strong as they could against a resistive force field given by the robot in order to come

as close as possible to a target presented in the flexion direction (Figure 3.15, Panel A). Through this preliminary test we evaluated the maximum force subjects were able to sustain allowing therefore to tailor the fatigue test on their residual muscular function. Moreover the test gives the possibility to patients to familiarize with the robot, to its haptic and visual feedbacks. After a period of rest, patients performed the test for the assessment of fatigue. The task consisted of a series of target reaching movements while immersed in a visco-elastic force-field, as represented in Figure 3.15 Panel B. In details, the targets were presented at an angular flexion-extension rotation of 42° with respect to the neutral wrist position (Flexion and Extension targets were presented alternately). The range of motion of the wrist was previously tested to ascertain that all subjects could reach the target correctly without additionally forearm movements. In order to avoid a possible fatigue recovery between one movement subjects have to reach the target within 1.5 seconds, a visual feedback (i.e. a change in the color of the target) was given in case they were moving too slow. As for the visco-elastic force-field, it assisted the extension movements and counteracted the flexion ones. According to equation 3.6, it was implemented as a virtual spring whose equilibrium angle was θ_{eq}= 42°, with the addition of a small viscous force in order to compensate the inertia of the hand.

$$F = -k(\theta - \theta_{eq}) - b\dot{\theta} \tag{3.6}$$

The stiffness parameter k was set so that the experienced force F was equal to 10% of the maximum force of the patient, measured with the previous test. Since our aim was to detect early sign of muscle fatigue, patients were instructed to repeat the target reaching movements until the level of fatigue was tolerable thus preventing any muscle damage.

Data Analysis

Robot encoders provided data at a 100 Hz sample rate which were used to extract angular displacements and angular velocities. Kinematic data were processed with a sixth-order Savitzky-Golay lowpass filter (10 Hz cut-off frequency) and re-sampled at the sEMG sample rate (2048 Hz) by linear interpolation. The sEMG signals recorded during the fatigue test were band-pass filtered (5-350 Hz) and then segmented according to kinematic data in order to focus the analysis on the concentric phase of the movements. As an example, thanks to the trajectory data, we segmented the sEMG signal of the *Flexor Carpi Radialis* obtaining the window relative to a single flexion movement. Then we computed a single value of the Mean Frequency on that portion of signal. Therefore we obtained N values of Mean Frequency for each subject, with N the total number of movements performed by the subject. The same

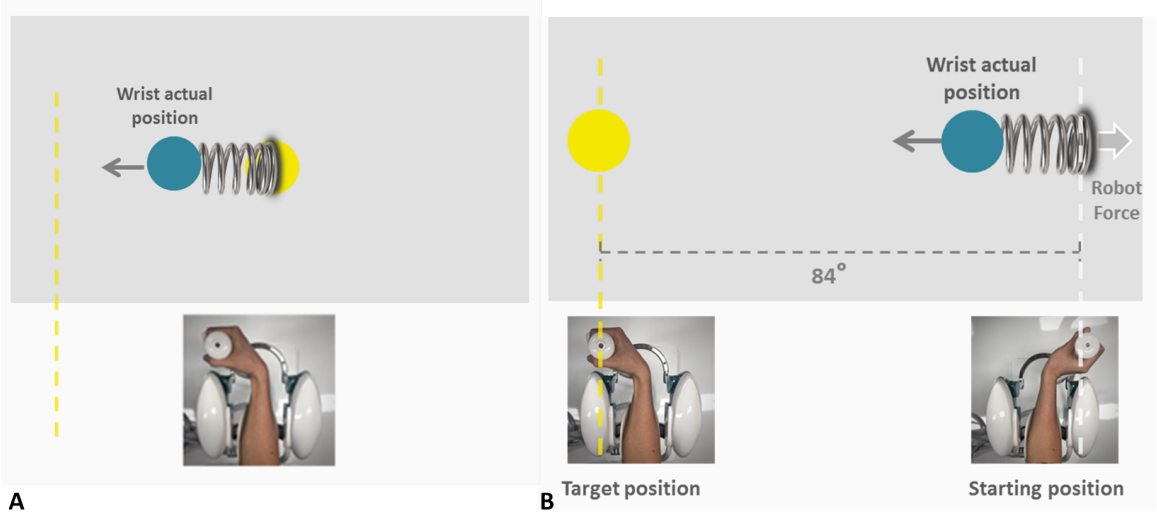

Figure 3.15 Schemes of the tasks: Panel A shows the preliminary task to evaluate the maximum force, Panel B shows the fatigue assessment test. The blue circle represents the end-effector of the subject, the yellow circle is the target to reach.

intervals of sEMG signal were also analyzed in the time domain to extract the Root Mean Square (RMS) values.

The obtained N values of Mean Frequency were then fitted using a third order polynomial function based on mean least square approximations. From these fitted curves, we calculated the Onset of Fatigue (*OF*) of each subject, following the already presented equation (equation 3.3). In particular we aimed to detect the earliest sign of fatigability and we used a value of P% of 25%, thus leading to $OF25\%$.

3.4.3 Results

All subjects correctly performed the test and, as expected, showed a decreasing trend of the Mean frequency revealing the occurrence of muscle fatigue during the execution of the task. Figure 3.16 and Figure 3.17 reports the mean frequency curves relative to subjects with DMD and with BMD respectively, their goodness of fit is reported in Table 3.8, while the percentages of decrease of these curves, as well as the ones of the healthy subjects, are reported on Table 3.9. This information demonstrates substantial level of decrement, higher than 10% for both controls and neuromuscular subjects. Moreover as shown by the x-axis of the Mean Frequency curves, and in the table, it is worth noticing how the number of movements performed highly differed among subjects. Indeed, among the three groups, the

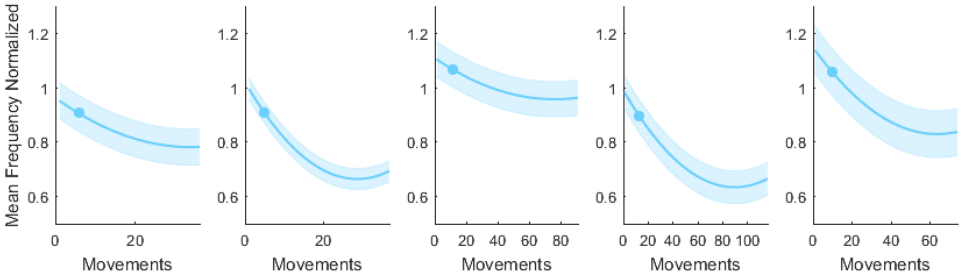

Figure 3.16 Mean Frequency curves relative DMD subjects normalized on the initial value for each subject. The dashed area indicates the RMSE while the circle marker shows the *OF*.

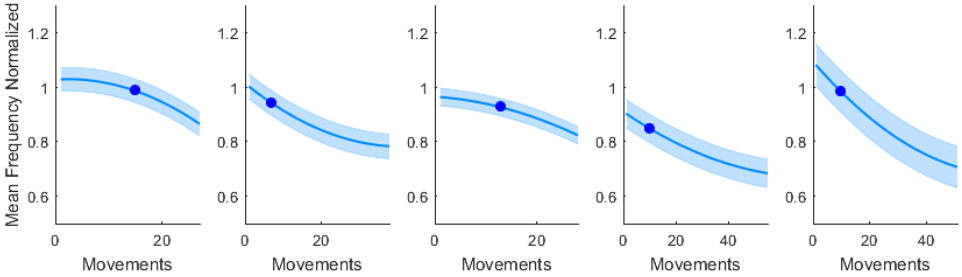

Figure 3.17 Mean Frequency curves relative to BMD subjects normalized on the initial value for each subject. The dashed area indicates the RMSE while the circle marker shows the *OF*.

Table 3.8 Goodness of fit relative to subjects with dystrophyes

Subject	R^2	RMSE	Subject	R^2	RMSE
DMD1	0.54	2.66	BMD1	0.36	7.39
DMD2	0.61	4.09	BMD2	0.87	3.13
DMD3	0.59	2.2	BMD3	0.31	4.94
DMD4	0.55	4.6	BMD4	0.74	5.75
DMD5	0.71	5.72	BMD5	0.53	7.35

Table 3.9 Total number of movements, Onset of Fatigue values, Percentage of Mean Frequency Decrement and Percentage of RMS Increment relative to each Duchenne and Becker subjects, and average values ± standard error of control subjects divided by group of age

Subject	#Movements	*OF*	Decrement Mean Frequency %	Increment RMS %
DMD1	27	15	15.94	47.34
DMD2	38	7	21.83	86.4
DMD3	28	13	14.58	20.63
DMD4	55	10	24.22	188
DMD5	51	10	34.6	20.46
BMD1	36	6	3.54	17.9
BMD2	37	5	33.3	119.6
BMD3	91	12	13.33	49.5
BMD4	116	13	35.53	77.73
BMD5	74	10	27.13	64.13
Mean Controls ±std err (6/8)	69±18	11±2	24.3±3.93	55.38±17.45
Mean Controls ±std err(9/11)	74±15	17±4	21.27±2.36	43.14± 9.28
Mean Controls ±std err (12/16)	109±10	19±4	29.98±6.62	126.62±43.2

highest number of movements was, as expected, performed by the healthy controls, and in the other two groups it ranged from 27 of subject DMD1 to 116 of BMD4.

Generally, BMD subjects showed longer resistance to fatigue than the ones with DMD, as proven by the lower number of movements performed by DMD subjects. Vice versa, the Onset of Fatigue, represented by a circular marker on the Mean Frequency curves (Figure 3.16 and 3.17) and reported in Table 3.9, resulted to be comparable between the two neuromuscular populations.

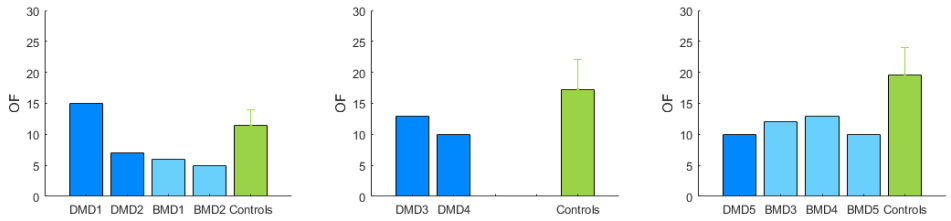

Figure 3.18 The bars indicate the number of movement defined as the Onset of Fatigue

In addition figure 3.18 compares the *OF* of the three populations divided in age groups. With the exception of DMD1, all subjects with neuromuscular disorders presented an earlier

OF with respect to the one of healthy subject in the same range of age. Further, considering just healthy controls, it is interesting to note that the *OF* occurred progressively later in time among the three age groups. In addition, the number of movements performed by control subjects followed the same increasing trend: from an amount of 69 ± 18 of the youngest group to a total of 109 ± 10 of the group aged (12/16). All subjects presented an higher final RMS value with respect to the initial one as indicated by the percentage of rms increase in Table 3.9.

3.4.4 Discussion

Although muscle fatigue is a widely experienced symptom in subjects with neuromuscular disorders, its effect is often overlooked or only qualitatively evaluated in clinical assessment. In this work we investigated the feasibility of a novel robot-based test to assess muscle fatigue in boys with Duchenne and Becker Muscular dystrophy and compared their results with age matched healthy subjects. Our results proved the feasibility of our method with subjects with different age and level of disability. In this respect, the test was well tolerated by all the participants and it was able to provide clear and objective evidence of muscle fatigue. In fact, all subjects showed the typical decline in the value of the Mean Frequency, that reflects the reduction in muscle fiber conduction velocity due to muscle fatigue, and it was greater than 8%, which is considered as the minimal value representative of muscle fatigue onset (Szucs et al., 2009). The occurrence of muscle fatigue suggested by the decline of Mean Frequency was further confirmed by the increase in the RMS values. In fact, amplitude parameters, such as RMS, are often presented in combination with the spectral analysis to reinforce the outcome obtained (Luttmann et al., 2000). As expected, the number of movements performed by the controls was higher than the subjects with dystrophy. However, the test did not reveal just the differences in the subjective tolerance of muscle fatigue, but through the Onset of Fatigue values, it confirmed the earlier fatigability of the subjects with neuromuscular disorders compared to the controls in an objective and reliable way. Concerning the execution of the task by the healthy subjects, all healthy subjects presented the Onset of Fatigue in the first 25 movements despite the amount of repetitions executed. This could be explained by the fact that controls had a high level of physical endurance and may not stop the test even if they felt fatigue. Moreover, the increase in total amount of movements performed by controls with the increase of age suggests that fatigability of healthy subjects decrease with the growth. However, unfortunately, in contrast to adults, the physiological and metabolic responses during medium/high-intensity exercises are poorly documented in children and

adolescents (Ratel et al., 2006). We can speculate that the increase in number of movements with age could be due to a higher level of participation. As a conclusion, the proposed test provided valuable information about muscle behavior of the participating subjects in terms of Mean Frequency, RMS values, number of movements performed and Onset of Fatigue that highlighted the fatigability of the subjects with neuromuscular disorders.

Chapter 4

Implication of muscle fatigue on wrist proprioception and performance

4.1 Introduction

Over the last half-century researchers have convincingly demonstrated the importance of proprioceptive acuity in the control and regulation of coordinated movements, motor learning, and error correction (Jeannerod and Marc 1988; Schmidt and Lee 2005). Consequently, a large body of literature has been dedicated to investigate any changes in proprioception due to physical injury (Hertel 2008) or ageing (Hughes et al. 2015). Similarly, finding out the effect of muscle fatigue on proprioception acuity is an interesting research goal that has been addressed by many studies (Givoni et al. 2007; Kazutomo et al. 2004). However, the extent to which proprioceptive acuity is influenced by local muscle fatigue is obscured by methodological differences in proprioceptive and fatigue protocols.
The following paragraphs are focused on this topic considering different aspects: in section 4.2 the effect of forearm muscle fatigue on wrist proprioception has been investigated; the work presented in section 4.3 examines potential changes in wrist proprioception as consequence of neck muscle fatigue; finally in section 4.4 we evaluated the effect of isometric forearm muscle fatigue in terms of changes in tracking performance.

4.2 The effects of Muscle Fatigue on Wrist Position Sense in the Flexion-Extension Plane

4.2.1 Introduction

Previous research has examined the effects of exercise induced local muscle fatigue on joint position sense (JPS) in different body parts (Givoni et al. 2007; Ju et al. 2010; Karagiannopoulos et al. 2019; Kazutomo et al. 2004; Sadler and Cressman 2019). However, the findings were not consistent between studies with research which claimed an influence of muscle fatigue on JPS (e.g. Ribeiro and Oliveira 2010). and other which demonstrated no effect of fatigue on proprioception (e.g. Sterner et al. 1998). Indeed, Ribeiro and Oliveira investigated the changes in knee JPS due to exercise-induced muscle fatigue (i.e. 30 consecutive maximal concentric contractions of the knee extensors and flexors) and reported an increase in both absolute and relative angular error in the extension direction after fatigue. In contrast, the group of Sterner failed to find differences in internal and external shoulder proprioception after a fatigue protocol in which participants performed two bouts of maximal reciprocal concentric isokinetic contractions until force output decreased below 50% of the participant's maximum voluntary contraction (MVC). One possible explanation for the divergent results lies in the different JPS protocols used in prior studies (Ager et al. 2017). For example, in the study of Sterner and in other previous protocols (Kazutomo et al. 2004; Sharpe and Miles 1993) an experimenter passively moved the patient's limb to a target position and then back to the starting position, after which the participant actively moved the same limb to the remembered position. Given that it is nearly impossible for the experimenter to maintain movement velocity across trials and participants, and that JPS is influenced by the speed of movement (Goble et al. 2009), this approach is considered to be a coarse measure of proprioceptive acuity. With respect to measurements of end-point error, researchers have used techniques such as 2D motion capture based on video analysis (Ribeiro and Oliveira 2010) which have been found to be less reliable than isokinetic dynamometer and continuous passive motion devices (Ager et al. 2017). Moreover, the conflicting findings in prior studies may arise from the specific fatiguing protocol used to induce local muscle fatigue, as well as the way that fatigue is quantified. For example, many researchers have defined local muscle fatigue as the exercise-induced decline of the peak torque (Ribeiro and Oliveira 2010; Sharpe and Miles 1993; Sterner et al. 1998). However, these studies did not use surface electromyography (sEMG) to confirm whether their fatigue protocols resulted in a decrease in the frequency of motor unit discharge and muscle conduction velocity (Enoka 2008). The benefit of using

sEMG to quantify the physiological responses accompanying local muscle fatigue is that frequency domain measurements (e.g. Fast Fourier Transform (FFT)) are capable of reliably measuring the spectrum shift to lower frequencies while temporal parameters (e.g. Root Mean Square (RMS)) measure the typical increase in signal amplitude (Cifrek et al. 2009; González-Izal et al. 2010; Merletti and Parker 2004). A second benefit of using sEMG - rather than peak torque - to measure fatigue is its possible application to clinical rehabilitation settings. Post-stroke upper limb hemiplegia alters the neural strategies underlying force regulation, resulting in decreased voluntary muscle activation (Bowden et al. 2014), altered motor unit (MU) firing rates (McNulty et al. 2014), a reduced ability to modulate MU firing (Mottram et al. 2014) and abnormal MU recruitment patterns (Hu et al. 2013). As such, fatigue protocols in which participants are required to generate muscle force levels during the performance of maximal voluntary torque movements are not appropriate for stroke patients. However, in order to understand sensorimotor functions in these populations, it is important that we have a clear understanding of normative function in neurologically and physically healthy individuals. Such data can enable the comparison of measurement values during initial clinical assessment and at later periods in the rehabilitation life cycle. As such, the aim of this study was to examine the effects of local muscle fatigue on wrist proprioceptive acuity using a robotic device specifically designed for human neuromotor control and rehabilitation (see Section 2.4) and ensuring the rise of muscle fatigue through frequency domain analyses captured via sEMG. To this end, sixteen participants first performed an ipsilateral wrist flexion-extension joint position matching (JPM) test, then a series of planar wrist flexion and extension movements while immersed in a visco-elastic force field that induced local muscle fatigue in the *flexor carpi radialis* (FCR) muscle, followed immediately by a second block of the JPM test. It is hypothesized that the fatigue protocol would lead to a decrease in JPS performance in the flexion direction. However, because the fatigue protocol targets the FCR, but not the *extensor carpi radialis* (ECR) muscles, it is hypothesized that there would be no change in proprioceptive acuity in the extension direction.

4.2.2 Methods

Participants

Sixteen neurologically and physically healthy right-handed individuals (seven males and nine females, mean age 27.6$\pm$2.9 years) participated in the current study. The study was carried out at the Motor Learning, Assistive and Rehabilitation Robotics Laboratory of the

Istituto Italiano di Tecnologia (Genoa, Italy) in accordance with the Declaration of Helsinki and the local ethical committee (Liguria Region: n. 222REG2015).

Experimental Apparatus

The experiment involved the use of Wristbot (see 2.4 for further details). A multichannel surface electromyography (sEMG) system (OTBiolab EMG-USB2C) was used to quantify activity of right *extensor carpi radialis* and *flexor carpi radialis* muscles (ECR and FCR, respectively) during the experiment. The sEMG system was set to collect data at 2048 Hz, with a gain of 1000, and a hardware bandpass filter (10–900 Hz). Following standard electrode preparation (Hermens et al. 1999), Ag/AgCl electrodes were placed on the ECR and FCR with an interelectrode distance of 26 mm. At the beginning of the fatigue task, a trigger signal was sent from the Wristbot to the sEMG base unit to ensure that the sEMG and Wristbot kinematic signals were correctly segmented and analyzed.

Experimental Protocol

Prior to the experiment, participant provided written informed consent, after which his/her handedness was evaluated using the EdinburghHandedness Inventory (Oldfield 1971). Subsequently, the participant sat in front of the experimental setup, so that the participant's body midline was vertically arranged with the computer monitor, and grasped the Wristbot handle with his/her right hand. Then the experimenter ensured that the participant's wrist axes were in correct alignment with the Wristbot, and used soft bands to strap the forearm to the mechanical support to ensure that the alignment would be maintained across the experimental protocol. Participants first performed an ipsilateral Joint Position Matching (JPM) test (Figure 4.1, Panel A). Test instructions were explained to the participants, after which they performed 10 practice trials to familiarize themselves with the task and with the robot. Once the experimenter answered any of the participants' questions, the participants' vision was blocked with a pair of opaque glasses and the alignment of their wrist was rechecked. At the start of each trial, a high-frequency auditory cue sounded and the Wristbot moved the wrist from the start position (0°, neutral) to a determined angular position (passive reaching phase), and after 3 s brought the Wristbot handle back to the start position (passive return phase). A low-frequency auditory cue then sounded, and the participant moved actively the robot handle to the remembered target position and pressed the handheld response button when they believed they were in the correct position (active matching phase). The Wristbot then returned the robot handle to the start position (return phase). The targets were randomly

presented at $\pm 48^\circ$ of ROM in the FE DoF (with a random shift of $\pm 0.5^\circ$ to prevent learning effects). Participants performed 18 trials in the flexion DoF and 18 in the extension DoF, yielding a total of 36 initial JPM test trials.Participants subsequently performed a series of planar wrist flexion and extension movements while immersed in a visco-elastic force field that induced local muscle fatigue in the FCR muscles. The targets were presented at $\pm 48^\circ$ of FE ROM in an alternating fashion, and participants moved the cursor to the target position using the visual feedback of the hand position provided on the computer screen (Figure 4.1, Panel B). A speed constraint prevented subjects resting between trials, and in the event that the participant did not reach the target within 1.5 s, the color of the cursor changed from green to yellow. The applied visco-elastic force field provided assistive forces to wrist extension movements and resistive forces during wrist flexion movements (see Eq. 4.1):

$$F = -k(\theta - \theta_e) - b\dot{\theta} \tag{4.1}$$

where $\theta = \theta_f = 48^\circ$ is the virtual spring equilibrium angle, θ is the actual wrist position that moves at speed $\dot{\theta}$, k (k =22.2 N/rad for female and k=27.7 N/rad for male subjects, respectively) and b (b= 1.77 Ns/rad) are the stiffness of the elastic force and the damping coefficient of the viscous contribution. The difference in the stiffness value between genders was based on the empirical literature demonstrating that female grip force values are 30% lower than male grip force values (Bäckman et al. 1995; Phillips et al. 2000), and enabled us to obtain comparable results for all participants. Participants were instructed to perform the fatigue task until the experienced forearm fatigue prevented them from flexing or extending the wrist. During the fatigue task, the experimenter verbally encouraged participants to sustain the task as long as possible to ensure the maximum level of subjective fatigue was reached (i.e. “completely fatigued” on the Borg CR-10 scale of perceived fatigue (Borg 1990). After the fatigue task, participants immediately completed a second block of the JPM test. The mean inter-task interval between the fatiguing protocol and the second JPM task was 45 ± 12 s.

Data and statistical Analysis

Robot encoders provided data at a 100Hz sample rate which were used to extract angular displacements and angular velocities. The acquired data were processed with a sixth-order Savitzky–Golay low-pass filter (10 Hz cut-off frequency). Wrist proprioceptive acuity was evaluated using the metrics Error Bias and Variability (Dukelow et al. 2010; Marini et al. 2018, 2016b; Schmidt and Lee 2005). Error Bias is defined as the average over the N trials,

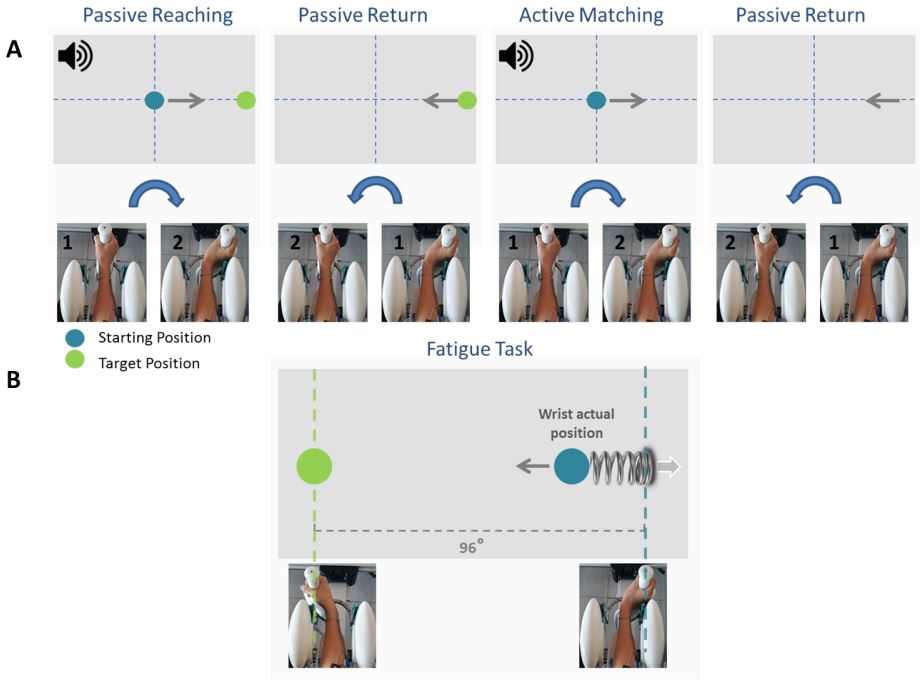

Figure 4.1 The temporal sequence of the Joint Position Matching task and the Fatigue task. During the Joint Position Matching task (A), the robot moved the participant's hand to a target location, held it there for 3 s, then brought the hand back to the start position. The participant then moved the robot handle to the remembered target position. During the fatigue task (B), participants performed alternating flexion-extension movements, and the robotic device applied a visco-elastic force field that provided assistive forces to wrist extension movements and resistive forces during wrist flexion movements.

in each of the two directions (flexion and extension), of the difference between the reference joint angle (θ_T) and the participants matching position (θ_i) in the i-trial.

$$ErrorBias = \frac{\sum_{i=1}^{N} \theta_i - \theta_T}{N} \tag{4.2}$$

Error Bias provides information about participants' response bias: it is the directional distance evaluated as algebraic summation between the ideal proprioceptive target and the actual wrist position, indicating the subjects' tendency in undershooting (negative Error Bias) or overshooting (positive Error Bias) the target.
Variability is defined as the standard deviation of matching position ((θ_i)) across the N repetitions in each of the two directions (flexion and extension).

$$Variability = StD(\theta_{1:N}) \tag{4.3}$$

While the Error Bias indicates error amplitude and is a direct measure of proprioceptive acuity and accuracy, the Variability measures the consistency across the 18 repetitions of the same target, thus providing information about precision. To ascertain the occurrence of muscular fatigue, we first filtered the sEMG signals, recorded during the fatigue task, with a band-pass filter (5–350 Hz). The trajectory data was then extracted from the robot, and allowed us to determine the concentric phase of each movement. The sEMG signal of the FCR was analyzed during flexion movements, while ECR muscle activity was analyzed during extension movements. Indeed, the wrist kinematics recorded by the robot enabled us to segment the sEMG signal of the *flexor*and *extensor carpi radialis* during flexion and extension movements, separately. For each movement, we then computed a single value of the Mean Frequency of the sEMG spectrum (Cifrek et al. 2009). Therefore, N Mean Frequency values were obtained for each subject,with N reflecting the total number of movements performed by the subjects. The obtained Mean Frequency values were then fitted using a second order polynomial function based on mean least square approximation. To compare data among participants, Mean Frequency curves were interpolated separately for each participant, were normalized respect to the value of the first trial, and then averaged among subjects. In addition to spectral analysis, we ensured the occurrence of muscle fatigue by examining the sEMG signal amplitude. Following the same segmentation and fitting procedures as above, we calculated the Root Mean Square parameter (RMS) on the filtered and rectified sEMG signal using the formula. Potential differences effects of muscular fatigue on wrist proprioceptive acuity were examined using Repeated Measures Analysis of Variance

(RM ANOVA) with Fatigue (pre, post) and Direction (flexion, extension) as the within subjects factors, separately for the variables Error Bias and Variability.

4.2.3 Results

Participants performed an average of 146± 19 movements, during which the Mean Frequency of the sEMG signals decreased (Figure 4.2 depicts the normalized Mean Frequency curves for the *flexor*and *extensor* muscles (averaged across participants), with the corresponding goodness of the fit (r2) and rmse).

Overall, the Mean Frequency of the *flexor* muscles exhibited a consistent decrease than that of

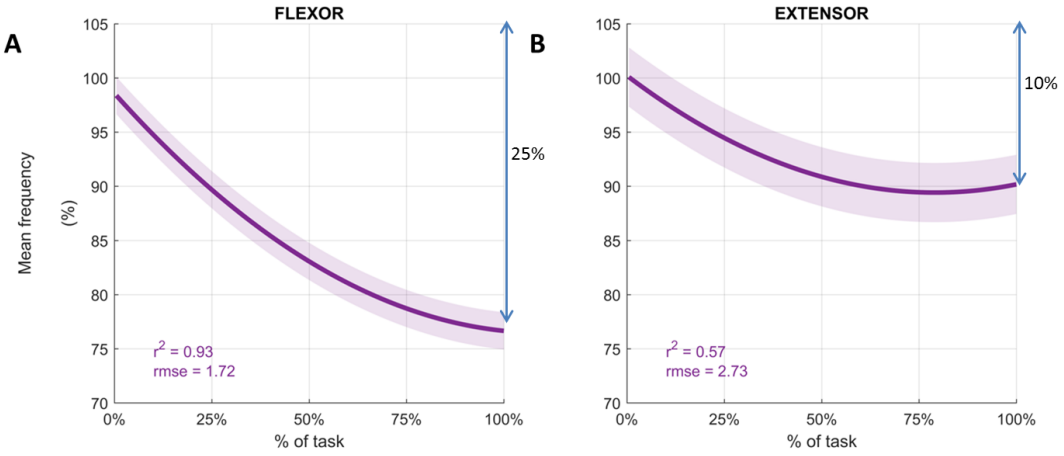

Figure 4.2 Average mean frequency values (%) for the *flexor carpi radialis* (A) and *extensor carpi radialis* muscles (B) during the fatigue protocol. Mean frequency (Hz) was normalized to the initial frequency of each sequence and averaged across participants to obtain the percentage. Depicted data was fitted with a second order polynomial function (dark purple) and standard error (light purple).

the *extensor* muscles. Indeed, the average decrease in *flexor* muscle Mean Frequency was 25% of the original value (average r^2 = 0.93), while *extensor* muscle Mean Frequency decreased by only 10% (average r^2 = 0.57). The shift toward lower frequencies was accompanied by an increase in the signal amplitude, as shown by the RMS curves in Figure 4.3. Similarly, the rise of the RMS values was greater for the *flexor* than in the *extensor* muscles. Indeed, RMS reached 154% of the initial value in the *flexor*muscle (average r^2 = 0.52), while RMS reached 98% in the *extensor* muscle (average r^2 = 0.17).

Individual results of the difference between the Error Bias before and after the fatigue task showed that 13 subjects out of 16 had a negative difference in the flexion direction (see Figure 4.4, Panel A) resulting from a greater overestimation of the reference position after

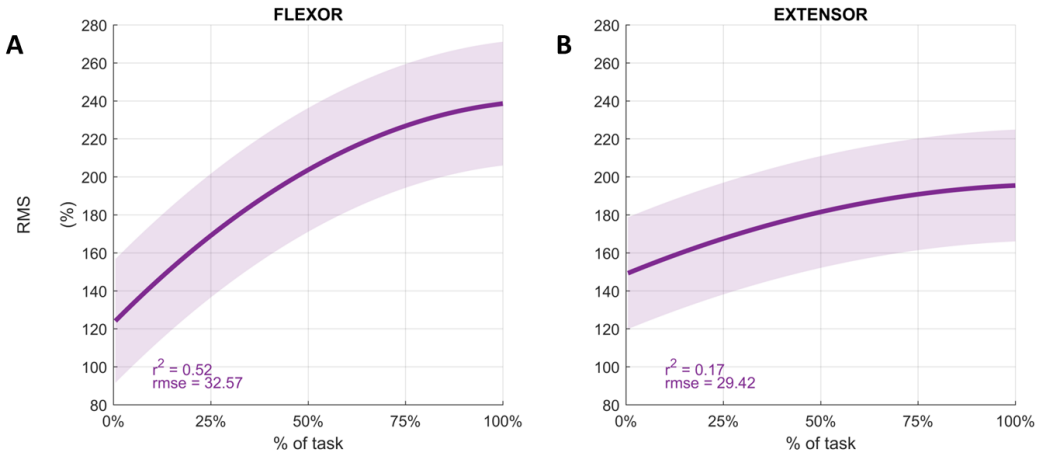

Figure 4.3 Average Root Mean Square values (%) for the *flexor carpi radialis* (A) and *extensor carpi radialis* muscles (B) during the fatigue protocol. RMS was normalized to the initial value of each sequence and averaged across participants to obtain the percentage. Depicted data was fitted with a second order polynomial function (dark purple) and standard error (light purple).

the fatigue task. However, this trend was not present for targets located in the extension direction (Figure 4.4, Panel B). Results of the mean Error Bias values prior to and after the fatigue protocol are displayed in Figure 4.5 Panel A.

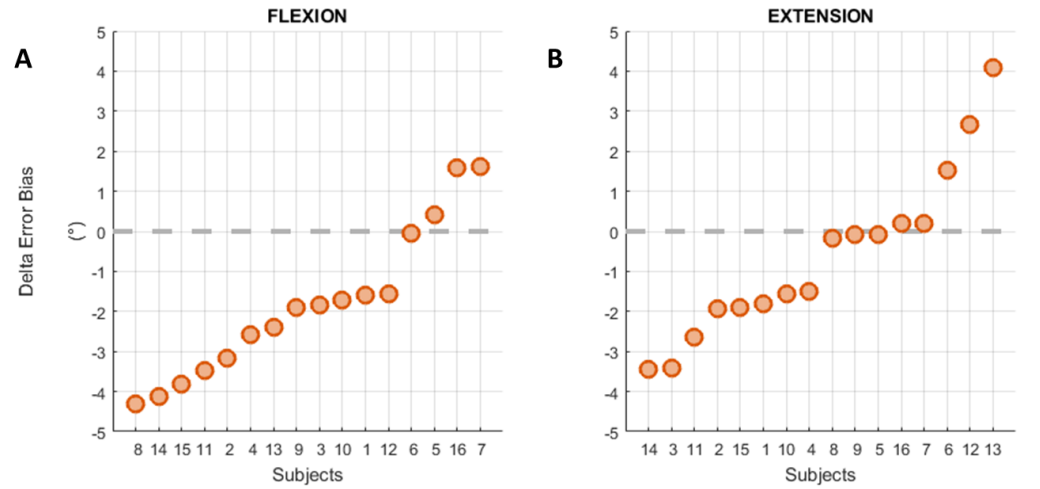

Figure 4.4 Individual differences between the Error Bias before and after the fatigue task in flexion (A) and extension (B) movements. The delta is computed as the Error Bias values pre fatigue minus the Error Bias values after the fatigue task.

Analysis indicated that there was a significant main effect of Fatigue, with participants exhibiting a greater tendency to undershoot the target prior to the fatigue protocol (-1.535°)

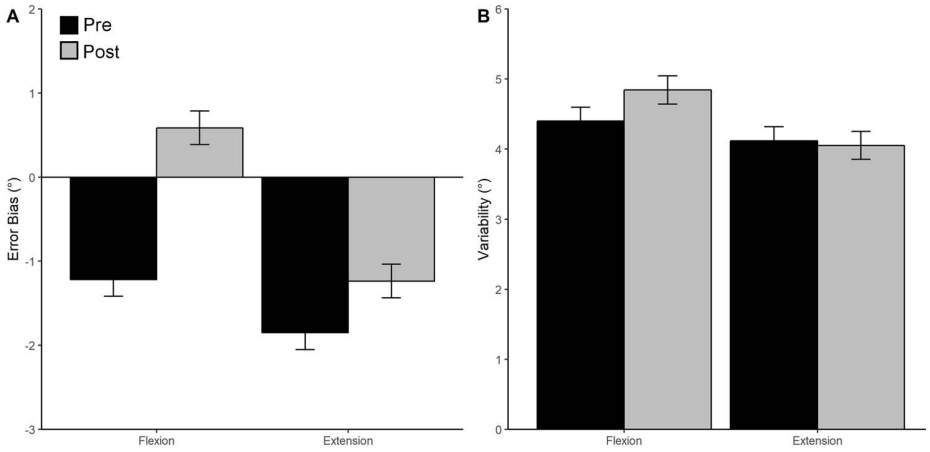

Figure 4.5 Mean and standard error values of Error Bias (A) and Variability (B) for movements performed in the flexion and extension directions before (black bars) and after (gray bars) the fatigue task.

compared to after the fatigue protocol (- 0.325°) regardless from the direction, F(1,15) = 8.607, p = 0.010, η_p^2= 0.365. There was also a significant Fatigue x Direction interaction, F(1,15) = 4.574, p = 0.049, η_p^2 = 0.234. Post hoc analysis indicated that Error Bias values were similar before and after (pre = -1.852° post = -1.237°) the fatigue protocol for the extension direction and reflected a tendency to undershoot the target. In contrast, the fatigue protocol had a significant effect on movements performed in flexion direction, with participants exhibiting a tendency to undershoot the target before the fatigue protocol (-1.218°, but overshooting after the fatigue protocol (0.587°). Mean wrist proprioceptive acuity Variability is shown in 4.5 Panel B. RM ANOVA revealed that mean Variability was similar regardless of direction [F(1,15) = 2.942, p = 0.107, η_p^2 = 0.164] and Fatigue [F(1,15) = 1.221, p = 0.287, η_p^2 = 0.075]. In addition, the interaction between Direction and Fatigue was nonsignificant [F(1,15) = 0.945, p = 0.347, η_p^2 = 0.059], indicating that movement Variability was not influenced by the fatigue protocol or movement direction.

4.2.4 Discussion

This study utilized a high resolution robotic device and sEMG to examine the effects of local muscle fatigue on wrist proprioceptive acuity in healthy young adults. Congruent with prior research on the shoulder (Carpenter et al. 1998; Voight et al. 1996) and knee joints (Lattanzio et al. 1997; Skinner et al. 1986) we found that local muscle fatigue induces impairments in proprioceptive acuity. Prior research into this line of work used high-intensity isometric or isokinetic exercise protocols to elicit local muscle fatigue (Forestier et al. 2002; Lee et al.

2003; Walsh et al. 2004). However, we designed and implemented a fatigue task that involved concentric contractions restricted to the *flexor* muscles so that the impact of the fatigue task on the forearm *extensor* muscles could be minimized, and any potential damage to all forearm muscles could be avoided (Proske and Morgan 2001). Utilizing this protocol, we were able to demonstrate that a high resistive visco-elastic force field that targets only the FCR muscles is capable of eliciting a significant change in JPS response bias for the FCR, but not the ECR, muscle. Additionally, examining proprioceptive acuity in both flexion and extension muscles provided data regarding the repeatability of the measures. The lack of significant differences in proprioceptive acuity for the extension direction indicates that participants were equally focused on the task during the two repetitions of the test, thus ensuring that the changes in repositioning bias in flexion targets were entirely due to the fatigued FCR. Indeed, we attribute the changes in proprioceptive accuracy and precision to the impact that muscle fatigue exerts on muscle spindle discharge according to literature. In fact, when the muscle is fatigued, the high concentration of metabolites and inflammatory products of muscular contraction (e.g., bradykinin, arachidonic acid, prostaglandin E2, potassium, and lactic acid) causes an increase in the muscle spindle discharge rate (Pedersen et al. 1998). However, we hypothesize that muscle spindle discharge rate although affected did not vary throughout the execution of the test. Consequently, the altered muscle spindle discharge rate did not prevent subjects from repeating similar errors in repositioning during the whole session as indicated by the absence of significant differences in Variability values between Pre and Post fatigue condition. Therefore, the precise methods used in the present study not only clarifies conflicting findings from previous studies (Givoni et al. 2007; Kazutomo et al. 2004; Sterner et al. 1998), but also confirms that muscle fatigue decreases proprioception acuity by affecting the muscle spindles, but that muscle spindle discharge rate may not vary as long as the muscle is in a fatigued condition. The small but significant post-fatigue increase in Error Bias is congruent with prior studies that have reported a 1° difference in proprioceptive acuity, regardless of the examined joint (knee (Lattanzio et al. 1997), ankle (Forestier et al. 2002) , elbow (Walsh et al. 2004)) and modality used to induce muscle fatigue (MVC or isokinetic movements). However, whether the magnitude of decrease in proprioceptive acuity is clinically relevant is still an open question (Refshaug 2002), and the relationship between JPS acuity decline and alterations in motion or joint instability cannot be determined from the present work.

The efficacy of the fatiguing protocol used in the present study is supported by both the frequency and time domain analyses of the muscular signals captured via sEMG, in which a concurrent decrease in mean frequency and an increase in signal amplitude was observed.

Time domain analysis indicated that a greater increase in RMS for the FCR muscle compared to the ECR muscle. Supporting this work, the frequency domain analysis revealed a 25% decrease in Mean Frequency for the FCR muscle, and 10% decrease in Mean Frequency for the ECR muscle, both of which are greater than the 8% decrease in Mean Frequency indicative of fatigue onset forwarded by prior research (Öberg et al. 1990). While at first glance (and according to the threshold proposed) it may appear that the fatigue protocol elicited local muscle fatigue to both the wrist extensors and flexors, it is more likely that the muscle activation observed for the ECR is due to the co-activation of the FCR and ECR required to provide global stability to the wrist joint (Myers et al. 1999) and maintain smooth and even motions. Another noteworthy point regards the locus of fatigue. It is well recognized that muscle fatigue can originate from central (e.g., insufficient drive from supraspinal sites, reflex inhibition, and disfacilitation) and/or peripheral mechanisms (e.g. decreased muscle fiber conduction velocity) (cf. Taylor et al. 2016). The observed decrease in EMG mean frequency, reflective of a decline in muscle fiber conduction velocity, indicates that the fatigue protocol resulted in peripheral muscle fatigue. However, we cannot conclusively state whether central muscle fatigue occurred in our study, as we did not employ the twitch interpolation technique or calculate the fractal dimension of the sEMG interference pattern (Beretta-Piccoli et al. 2015). In evaluating the effects of local muscle fatigue on proprioceptive acuity, it is essential that the time interval between the execution of the fatiguing protocol and the following JPM test is minimized. Prior works used one device to test proprioceptive acuity and another one to implement the fatiguing protocol (Allen et al. 2007; Lattanzio et al. 1997; Walsh et al. 2004). For example proprioception of the knee joint has been measured using a JPM task where the participant sat on the end of a table with the knee at 90°, and the experimenter passively moved the participant's limb to a target position and then back to the start position (Kazutomo et al. 2004). However, the local muscle fatiguing protocol required the participant sit on a Cybex isokinetic dynamometer and perform 60 consecutive maximum concentric knee flexion and extension contractions. We postulate that the lack of significant results found in different studies (Kazutomo et al. 2004; Sharpe and Miles 1993; Sterner et al. 1998) may result from the amount of time that elapsed between the fatigue protocol and second proprioceptive acuity test. As such, a further novelty of the present work is the use of a robotic device that can both evaluate proprioceptive acuity and deliver the fatiguing protocol. In contrast to prior studies that had reported large intervals between the fatiguing protocol and the second JPM task (e.g. 15 min in Allen et al. 2007, 3 min in Lee et al. 2003, 5 min in Lattanzio et al. 1997), we were able to minimize the time between the execution of the fatigue task and the following JPM test to 45 ± 12 s, and as such avoided any potential muscle fatigue

recovery between the two tests which could jeopardize the reliability of the JPM results. Furthermore, the use of the robotic device ensures the repeatability of the test and its high-resolution encoders guarantee the precision of the measures. Such advantages have already been exploited in previous works allowing to investigate the codification of proprioceptive information both in terms of kinesthesia (Marini et al. 2018) and joint position sense (Marini et al. 2017a, 2016b). Our interest lies in understanding the neuromotor control mechanisms surrounding proprioceptive function, especially given that sensorimotor impairment in older adults is associated with recurrence of falls (Rossat et al. 2010) and a decline in the ability to perform functional activities (Shaffer and Harrison 2007). It is likely that these deficits occur, in large part, due to the numerous anatomical and physiological changes that happen in the muscle spindle apparatus as people age (e.g. an increase in muscle spindle thickness (Swash and Fox 1972), a decrease in intrafusal fibers and nuclear chain fibers (Liu et al. 2005), and an increased proportion of type I extrafusal muscle fibers (Jennekens et al. 1972; Lexell and Downham 1992). Furthermore, changes in motor unit size, number, properties, and morphology due to ageing make older adults more prone to muscular fatigability compared to their younger counterparts (Hepple and Rice 2016; Kent-Braun et al. 2014). Future research will aim to examine how local muscle fatigue impacts JPS acuity in aging populations, as well as determining factors (e.g., physical activity) that influence proprioceptive acuity in the aging population.

4.3 Investigating the Effects of Subclinical Neck Pain and Neck Muscle Fatigue on Wrist Joint Position Sense

4.3.1 Introduction

Neck muscles are rich in sensory receptors and as such are known to play a very important role in sensory input to the central nervous system (CNS) (Zabihhosseinian et al. 2015). It has been shown that the CNS uses the position of the head and neck to interpret the position of the upper limb (Knox and Hodges 2005). As such, any altered input from neck muscles may affect the sensory inputs to the CNS and therefore affect upper limb proprioception. Given the high prevalence of neck pain, defined as pain in the anatomical region of the neck without any specific pathological cause, in the population (60-70% of the general population (Abichandani and Parkar 2015)) many authors have examined the effects of neck pain on cervical kinesthetic sensibility (Feipel et al. 2005; Heikkilä and Wenngren 1998; Lee et al. 2008). For example, in 1991, Revel and colleagues investigated the effects of neck pain on cervicocephalic kinesthetic sensibility using a head repositioning task finding out that neck pain participants had less performance accuracy as compared to the healthy controls (Revel et al. 1991). More recently, researchers have shown interest in the influence that neck pain might have on structures further down the kinematic chain. Abichandani and Parkar 2015 measured repositioning error in the shoulder, elbow and wrist joints in women with chronic mechanical neck pain. Their results showed a statistically significant difference in wrist and shoulder proprioception when compared to the healthy control group. Furthermore, similar study has been conducted to investigate the effect of neck fatigue on proprioception ability. Zabihhosseinian et al. 2015 were among the first to look at the effect of neck fatigue further down the kinematic chain and investigate the effects of cervical *extensor* muscle (CEM) fatigue on elbow joint position sense. They found that an isometric cervical *extensor* muscle (CEM) fatigue protocol could reduce elbow JPS due to an altered internal body schema . Despite the growing amount of research focusing on neck pain and neck fatigue, little to no research exists on the effects that neck pain or fatigue may have on wrist proprioception. The hand and wrist provide the last degree of freedom for adjustments or corrections in reaching movements along the kinematic chain. Thus, if wrist proprioception is affected by altered sensory processes due to neck pain, this can have significant consequences for upper extremity task performance for work, leisure and sport. In the present work we examine the effect of sub-clinical neck pain (SCNP) and of CEM fatigue on wrist proprioception. Individuals with SCNP have mild to moderate neck pain, and may be disposed to fatigue

related injuries. Therefore, this group can provide an intuitive understanding into pain and upper- limb motor control.

4.3.2 Methods

Participants

All experimental procedures were approved by the research ethics board at Brock University (REB:18-113) and written consent was obtained from all participants. Twenty-four right-handed participants were recruited; 12 participants with chronic subclinical neck pain (25.8±5.0 years) and 12 healthy controls (24.7±5.1 years). There were seven males and five females in each group. Participants completed a neck pain disability index (NDI) and chronic pain grading scale and were placed into either the control group or the pain group based on their scores. Neck pain was graded between Grade I and Grade IV on the chronic pain grading scale18. To be included in the pain group, participants were required to have a history of reoccurring neck pain or stiffness and be pain free at the time of the experiment. The exclusion criteria were: specific diagnosis of cervical spine dysfunction; traumatic spinal cord injury; any medical condition affecting the sensory system; cervical treatment (at least three months prior to data collection); and any wrist injury within the last 12 months.

Experimental Protocol

Before beginning the protocol, participants were familiarized with the wrist robotic device that was used during the experiment (Wristbot, Genoa, Italy)(see Section 2.4 for further details). Participants completed two proprioception sessions separated by an isometric CEM fatigue protocol. Specifically, they performed the second session of proprioception test immediately after the CEM fatigue protocol without any rest period.
Each proprioception session consisted of 12 randomized JPS trials. Participants grasped the handle of the robotic device, starting in a neutral anatomical wrist position (0° of flexion-extension, no deviation, mid-prone). The robot passively moved the participants' hand to a randomized position and held the position for three seconds. After three seconds, the robot passively moved the participant back to the neutral position and provided an auditory cue which signaled the participant to actively move their wrist back to the previously presented target with no assistance from the robot. Participants' vision was occluded to eliminate visual feedback from the target and their wrist. Participants also wore noise cancelling headphones to eliminate background noise as well as to cue each active movement with an audible signal provided by the robot. Only flexion-extension DoF was tested during the experiment and

targets were set at a distance no greater than 80% of the wrist's total functional ROM in order to ensure all participants could actively match the targets. Proprioceptive targets were presented 6 times for each direction for a total of 12 trials. During each trial, the robot allowed movement into the DoF being tested (i.e. radial/ulnar deviation and pronation/supination were locked).

As for the fatigue protocol, participants in both the control and SCNP group completed an isometric neck *extensor* task to fatigue the CEM (Figure 4.6). The test-retest reliability of the fatigue protocol has been previously demonstrated (Edmondston et al. 2008). Participants lay prone on a plinth, with their arms at their side, with head and neck over the edge of the table. Their head was supported by the examiner for the duration of the setup. A Velcro strap was fixed around the head with an inclinometer (AUTOUTLET Digital Inclinometer) attached to a headband over the occiput. A 2-kg weight was suspended from the headband and hung just above the floor. The participants head was positioned in neutral in the sagittal plane. The test began once the examiner removed support from the participants head and the participant was required to hold the cervical spine in the neutral position for as long as possible. The test was terminated if the participant could no longer hold the head horizontal due to CEM fatigue, if the weight returned to the floor, or if the neck position changed more than five degrees. The holding time was measured in seconds and encouragement was provided by the researcher.

Figure 4.6 Cervical extensor fatigue protocol

Data Analysis

Wrist JPS was evaluated by comparing the actual (participant's re-creation of the target), and the desired (actual target position) wrist positions. Three variables were calculated to provide

detailed information about participants' performance: matching error (ME), variability of error, and error bias (EB).

ME represented the absolute angular deviation from the target. ME was calculated by averaging the number of trials (N=6) across the same direction and quantified performance accuracy during the active movement and defined error amplitude as follows:

$$MatchingError = \frac{\sum_{i=1}^{6} |\theta_i - \theta_T|}{6} \tag{4.4}$$

Variability assessed the consistency between the trials and was calculated following equation 4.3 with N = 6.

EB provided information about each participants response bias. It represented the directional distance between the wrist (desired) target and the reproduced (actual) target. It indicates the participants tendency to undershoot (negative error bias) or overshoot (positive error bias) the target. EB was calculated following equation 4.2 with N = 6.

Statistical Analysis

To evaluate the effect of CEM fatigue on wrist proprioception between groups (control and SCNP), a 3-way repeated measures mixed analysis of variances (ANOVAs) [2 groups (control, SCNP) x 2 direction (wrist extension, wrist flexion) x 2 conditions (pre-fatigue, post-fatigue)] evaluated ME, EB, and Variability.

4.3.3 Results

Neck Pain Demographics

Participants in the SCNP group scored between I and IV on the chronic neck pain grading scale. The average time to fatigue for the SCNP group was 10:00$\pm$0.13 minutes (mean value $\pm$ standard error) and 12:42$\pm$0.11 minutes for the control group.

Group differences for wrist proprioception

There was a main effect of group ($p<0.05$) for matching error. ME was significantly greater for the SCNP group than the control group (SCNP = 4.42$\pm$1.32°; control = 3.13$\pm$0.42°). Similarly, EB was significantly different for the SCNP group when compared to the control group (SCNP = -0.863$\pm$1.06°; control = 0.773$\pm$1.62°, $p<0.05$). Interestingly, an opposite effect was found in directionality of error between the groups as shown in Figure 4.7. A

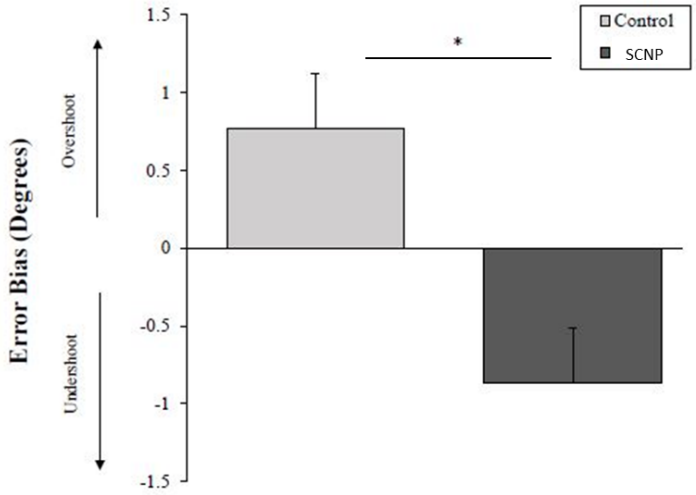

Figure 4.7 Changes in EB (degrees±SE) from baseline to post fatigue. Data represents both control and SCNP group.

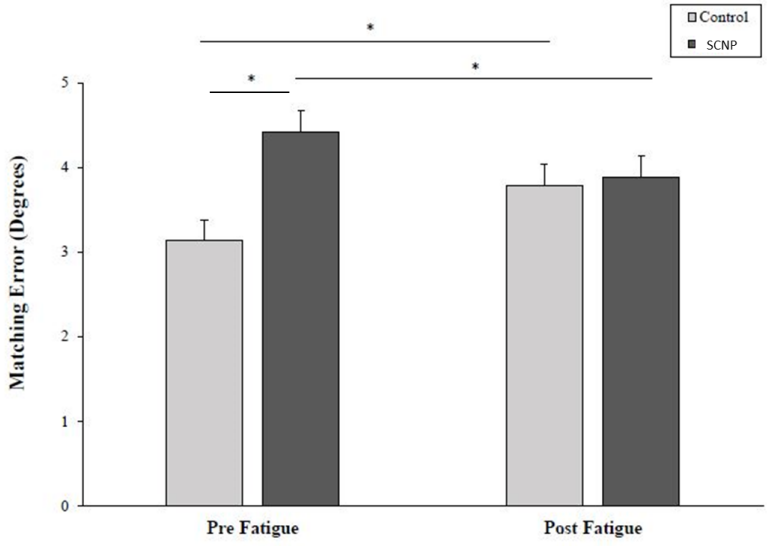

Figure 4.8 Changes in ME (degrees ±SE) from baseline (pre-fatigue) to post-fatigue for both control and SCNP groups.* indicates significant main effect between the groups or post-hoc comparisons.

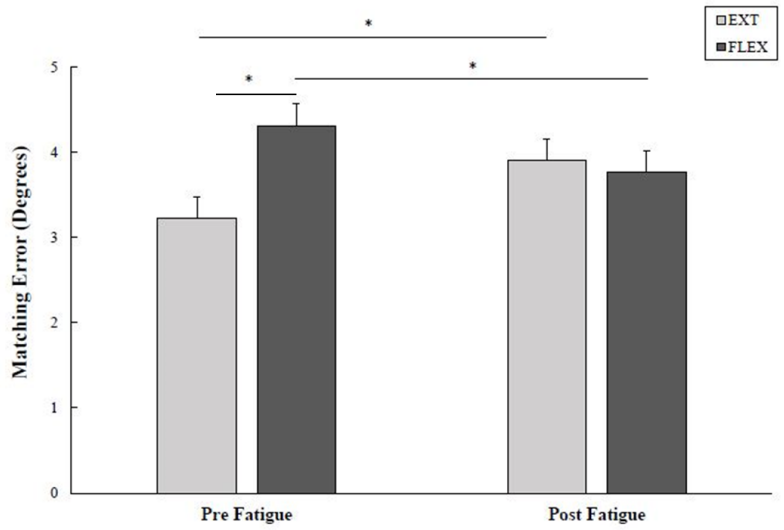

Figure 4.9 Changes in ME (degrees±SE) from baseline to post-fatigue for both directions (Extension and Flexion). Data of control and SCNP group are considered together.

negative error bias indicates an undershooting of the target in the SCNP group, and a positive error bias indicates an overshoot of the target in the control group.

Neck Muscle Fatigue and Wrist Proprioception

There was a significant group by Fatigue interaction ($p<0.05$) for matching error (Figure 4.8). Following fatigue, the ME decreased from baseline in the SCNP group, and it increased in control group (SCNP = 3.88±0.64°, control = 3.78±1.12°). There was also a significant Fatigue by direction interaction ($p<0.05$) for ME (Figure 4.9). ME for wrist extension was lower pre fatigue than ME for wrist flexion (ext = 3.23±0.79°, flex = 4.31±1.34°).
Following the CEM fatigue protocol, ME for wrist extension increased from baseline, and ME for wrist flexion decreased (ext = 3.90±1.08°, flex = 3.76±0.74°). There was also a main effect of Fatigue ($p<0.05$). EB was significantly different at baseline from post-fatigue (baseline = -0.552±1.40°, post-fatigue = 0.463±1.35°). Overall, participants tended to undershoot the target at baseline, and overshoot the target after the CEM fatigue protocol. There was no significant Fatigue by group interaction, however, the SCNP group consistently undershot the target and the control group consistently overshot the target. There were no significant differences found for variability of error.

4.3.4 Discussion

Neck Pain and Wrist proprioception

In the present study, ME for the control group was significantly lower at baseline than the SCNP group. This suggests that the control group had a better ability to match the target than the SCNP group. This is consistent with previous research demonstrating that neck pain affects JPS at the neck and shoulder (Lindner 2008; Revel et al. 1991). There is evidence to suggest that muscle impairment occurs early in the onset of neck complaints and that this muscle impairment does not automatically resolve when neck pain symptoms disappear (Sterling et al. 2003). Moreover, it has been postulated that pain or dysfunctional spinal joints may create a state of altered afferent input resulting in ongoing central plastic changes (Wall et al. 2002). As such, altered sensory inputs cause an altered processing in the cerebellum which plays a crucial role in the creation of an internal model of the body (Popa et al. 2013). The concept of an altered body schema in individuals with chronic pain has become a new area of interest and recent neurophysiologic studies specifically addressed the impact of neck pain on cerebellar processing (Baarbé et al. 2016; Daligadu et al. 2013). The differences in JPS accuracy of the wrist between SCNP subjects and healthy controls at baseline support the hypothesis of an altered body schema due to neck pain. Interestingly, previous work showed less error at the shoulder (pain = 2.03°, control = 1.51°) than our wrist error scores (ME in SCNP = 4.42±1.3°; ME in control = 3.13±0.4°) (Lindner 2008). These differences could suggest that differences in the error between the SCNP and healthy control groups are larger more distally (at the wrist) than proximally (at the shoulder). However, differences in angular displacement during the proprioception tests at the shoulder and wrist could have contributed to these across joint differences. When examining the direction of error, our SCNP group consistently undershot the target while the control group consistently overshot the target. To our knowledge, there is no previous literature to support or refute differences in the tendency to overshoot and undershoot the target in a control vs. SCNP population. Previous research focusing on wrist proprioception found mixed results in flexion and extension, with no consistent patterns of undershooting and overshooting the target in a healthy population (Marini et al. 2016a). However, when compared to other DoF at the wrist (abduction/adduction, pronation/supination), flexion and extension scores yielded undershooting of the target.

Neck Muscle Fatigue and Wrist proprioception

This study is the first to demonstrate that neck muscle fatigue impacts wrist JPS. After completing the CEM fatigue protocol, ME for the control group increased and ME for the SCNP group decreased, indicating a decrease in performance for the control group. It should be noted that the wrist muscles were not fatigued in our work. Our results agree with Zabihhosseinian whose findings demonstrated reduced elbow JPS after a CEM fatigue protocol in healthy participants (Zabihhosseinian et al. 2015). Our work confirms that these effects are also apparent more distally at the wrist. The decreased performance as a result of the CEM fatigue protocol is likely due to altered afferent input from the neck that subsequently impacted body schema. JPS is mediated largely by muscle spindles and Golgi tendon organs, and it has been hypothesized that the decline in JPS of one joint, following fatigue of another, may be due to decreased muscle spindle performance (of the neck) (Gear 2011). As a result, the sense of movement is disturbed and a position matching task can be altered (Letafakatar et al. 2009). These findings support our hypothesis that neck muscle fatigue affects wrist JPS in healthy controls. Although participants attempted to recreate the target as accurately as possible, altered afferent feedback to the CNS due to the CEM fatigue protocol impacted the ability to accurately reproduce the target.

4.4 The influence of isometric wrist flexor-extensor fatigue on tracking performance

4.4.1 Introduction

As discussed in the sections above, muscle fatigue and muscle pain may lead to a decrease in the proprioceptive acuity. This reduced accuracy in the perception of movement or positions of body parts is likely to affect the accuracy in performance. Some studies have reported a significant decrease in shooting performance (Evans et al. 2003; Hoffman et al. 1992), hammering performance (Hammarskjöld and Harms-Ringdahl 1992) due to fatigue, whereas others found no significant effect of fatigue in similar tasks (Côté et al. 2005; Huffenus et al. 2006). Whether muscle fatigue also leads to a decreased task performance in tasks which required lower level of force and more precision than the ones listed above, has to our knowledge been investigated by few studies. Huysmans and colleagues in particular focused on wrist extensor muscle and demonstrate that muscle fatigue leads to higher error during a tracking task with a computer mouse (Huysmans et al. 2006). Similarly, in another study muscle fatigue was induced in the extensor digitorum communis and the flexor digitorum superficialis, which are responsible for the final wrist work during the throw, to investigate the effect of muscle fatigue in a throwing task (Forestier and Nougier 1998). The purpose of the following work was to examine how isometric fatigue of the wrist extensors and flexors influences strength and performance during a robot-based tracking task.

4.4.2 Methods

Experimental protocol

The study involved twelve right-handed healthy male participants (Age: 23.9 ± 2.7 years) and it was carried out at the Neuromechanics and Ergonomics Lab of Brock University (St. Catharines, Canada). The experimental protocol consisted of an isometric fatigue task and a tracking task. In details, subjects were requested to perform as accurate as possible a tracking grasping the handle of Wristbot (see 2.4 for further details). The tracking pattern was implemented as a 3:2 Lissajous curve (see Figure 4.10) sized to $\pm 45^{\circ}$ of wrist flexion-extension and $\pm 25^{\circ}$ of radial/ulnar deviation following the equations:

$$\begin{aligned} x_{Tg}(t) &= Asin(2 \cdot \tfrac{2\pi t}{T})) \\ y_{Tg}(t) &= Bsin(3 \cdot \tfrac{2\pi t}{T})) \end{aligned} \tag{4.5}$$

where A and B are the amplitude of the curve in the flexion-extension and radial-ulnar deviation respectively. T is the period of the Lissajous curve (i.e. the time necessary for the target to complete a lap) and it was equal to 20 seconds. 5 baseline traces were performed

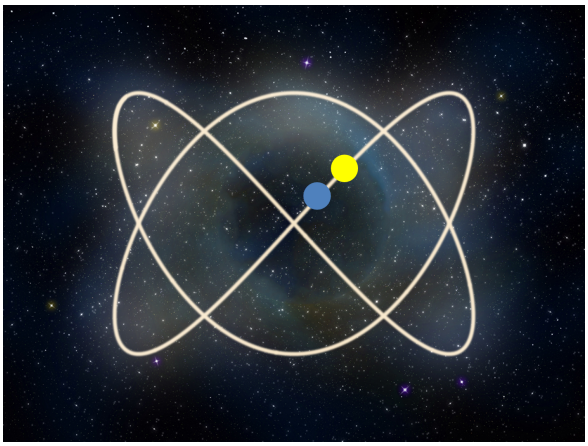

Figure 4.10 Tracking Task. Subjects were requested to move the handle of the Wristbot (displayed by a blue marker) in order to track the target (yellow marker following a Lissajous curve.

prior to fatigue separated by 1 minute of rest each.
For the fatigue trial, participants moved forward in their seat to a table-mounted force transducer and exerted maximal wrist extension or flexion force against the transducer until they were unable to maintain 25% of their pre-fatigue maximal voluntary contraction (MVC). Participants then returned to the robotic device and performed 7 traces in the following timing: immediately post-fatigue, at minute 1-2-4-6-8 and 10 from the end of the fatigue test. To assess the alteration in strength due to fatigue, MVCs were executed at 2, 6, and 10 minutes post-fatigue, between traces.
Participants performed the experiment into two different days: during one session the *flexor* muscles were fatigued while during the other they fatigued the *extensor* ones. The order of the two session was randomly assigned.

Data Analysis

Robot encoders provided data at a 100Hz sample rate which were used to extract angular displacements and angular velocities. The acquired data were processed with a sixth-order Savitzky–Golay low-pass filter (10 Hz cut-off frequency). The filtered data were thus used to estimate the performance of the subjects during the tracking task through the following metrics:

- δ *Tracking Error*: it is the mean value of the distance between the target and the hand over a turn (Squeri et al. 2010). It is decomposed into two components: the longitudinal component (δ_l) and the normal component (δ_n) δ is always positive while (δ_l) and (δ_n) are signed quantities. In details, δ_l is positive if the hand is ahead of the target and δ_n is positive if it is on the right. The two components are computed as follows:

$$\begin{cases} \vec{u_l} = \frac{1}{\sqrt{\dot{x}^2+\dot{y}^2}} \begin{bmatrix} \dot{x_T} \\ \dot{y_T} \end{bmatrix} = \begin{bmatrix} u_{xl} \\ u_{yl} \end{bmatrix} \\ \vec{u_n} = \begin{bmatrix} u_{yl} \\ -u_{xl} \end{bmatrix} \\ \vec{e} = \vec{P_H} - \vec{P_T} \\ \delta = ||\vec{e}|| \\ \delta_l = \vec{e} \cdot \vec{u_l} \\ \delta_n = \vec{e} \cdot \vec{u_n} \end{cases} \tag{4.6}$$

  where $\vec{u}_l$ and $\vec{u}_n$ are the longitudinal and normal unit-vectors respectively.

- *Figural error (FE)*: It is defined as a distance measurement between the ideal trajectory generated by the target and the trajectory of the participant. It is a measure of how accurately the participant recreates the target path and it is insensitive to differences in speed between the target and the end-effector. The measure is given by the following equations:

$$\begin{gathered} dist_{AB}(i) = min_j||A_i - B_j|| \;\; i = 1,2..n \\ dist_{BA}(j) = min_i||A_i - B_j|| \;\; j = 1,2..m \\ FE_{AB} = \frac{\sum_{i=1}^{n} dist_{AB}(i)) + \sum_{j=1}^{m} dist_{BA}(j)}{n+m} \end{gathered} \tag{4.7}$$

  Where "A" and "m" are the time series and total samples of the target trajectory and "B" and "n" are the time series and total samples of the end-effector trajectory.

- *Jerk Ratio*: it is the ratio between the integrated squared jerk (ISJ) of the handle and the ideal ISJ of the target. The ISJ was computed as follow:

$$ISJ = \int \dddot{P}_x^2 + \dddot{P}_y^2 \tag{4.8}$$

where P is the vector of coordinates of the target or of the end-effector and it is integrated over the entire tracking trial (Salmond et al. 2017). A Jerk Ratio value equal to 1 means that the participant is as smooth as possible.

A two-way repeated measures ANOVA (fatigue condition x measurement time) was conducted for all metrics and MVC data to identify differences between both the two fatigue sessions as well as between pre and post fatigue. In cases where a main effect of measurement time was found, post-hoc pairwise comparisons were conducted with a bonferroni correction. Effect sizes (ES) were evaluated using partial ETA squared calculated as the division of the sum of squares of the effects (SSEffect) by both the SSEffect and the sum of squares of the error (SSError). Significance level was set at $P < .05$. Statistical analyses were performed on kinematic data in degrees (°) and on force data in Newtons (N). However, to more clearly communicate experimental findings, data has been shown in some figures as normalized to baseline measures. Group data is reported as mean ± SD in text and illustrated in figures as SE.

4.4.3 Results

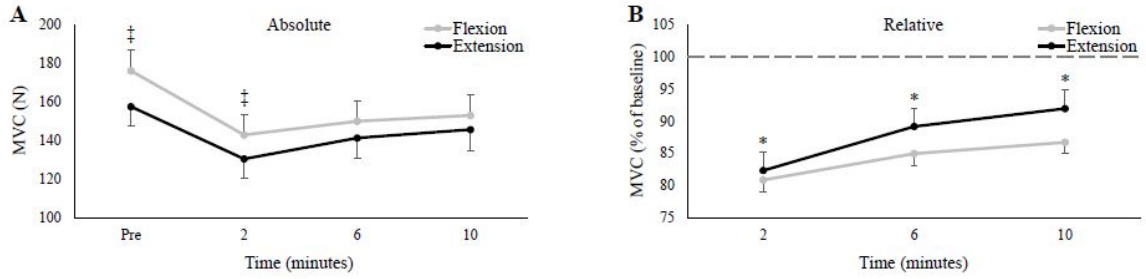

Figure 4.11 Group averages of A) absolute (N) and B) relative (% of baseline) MVC force between the wrist flexion and wrist extension sessions. In both graphs, grey lines depict wrist flexion MVC force collected on the wrist flexion fatigue day, while black lines represent wrist extension MVC force collected on the wrist extension fatigue day. The x-axis denotes the time of collection, with "pre" being pre-fatigue measures; the remaining numbers refer to time of collection after fatigue. The dotted-line in B) represents pre-fatigue (or baseline) MVC force. ‡ denotes a significant difference between flexion and extension force. * denotes a significant difference of both relative flexion and extension force from baseline.

Regarding the strength, prior to fatigue, wrist flexion MVCs were significantly greater than wrist extension (flexion: 176.1 ± 38.2N, extension: 157.6 ± 34.6N, $p < 0.05$). Figure 4.11 A and B show absolute and relative MVC force, respectively, across all time points.

There was a two-way interaction (time x fatigue condition) on MVC force ($F(3,33) = 3.55$, $P < 0.05$, ES = 0.24). Secondary analyses showed that flexion force remained greater than extension force at 2 minutes following fatigue (Flexion: 142.9 $\pm$ 36.7, Extension: 130.5 $\pm$ 34.6, $P < 0.05$) but was not significantly different at 6 or 10 minutes. This seems to be due to the faster relative force recovery of wrist extension (seen Figure 3B). Separate one-way repeated measures ANOVAs demonstrated main effects of time for both flexion MVCs ($F(3,33) = 45.22$, $P < 0.05$, ES = 0.8) and extension MVCs ($F(3,33) = 40.41$, $P < 0.05$, ED = 0.79). Also for both testing sessions, MVC force was significantly reduced from baseline at minutes 2, 6, and 10 ($P < 0.05$ for all three).

As for the fatigue protocol, subjects reached their 25% of pre-MVC force cut-off in similar time between the two muscles (Flexion: 76.1 $\pm$ 26.8 seconds, Extension: 73.1 $\pm$ 19.3 seconds, $P = 0.65$). Figure 4.12 shows group data for mean tracking error calculated over

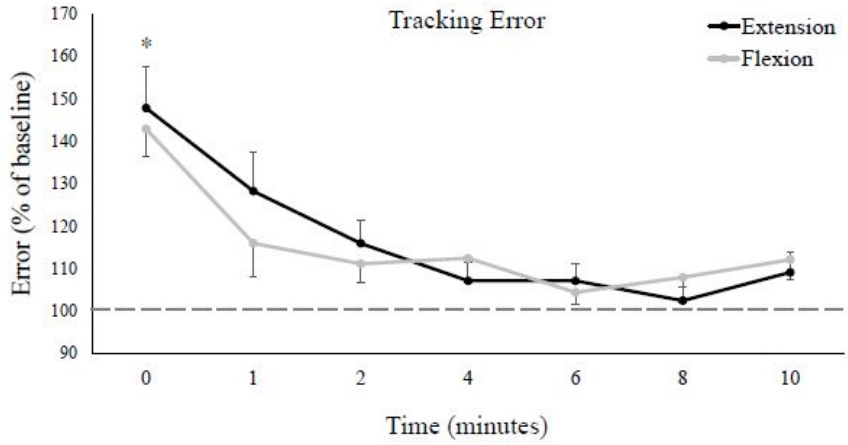

Figure 4.12 Group averages of mean tracking error calculated over the entire Lissajous curve (excluding the dotted-line portion). Tracking error is normalized to baseline (shown by the dashed horizontal line), and data points are shown in minutes after fatigue (0-10). Black lines represent tracking error from the wrist extension fatigue session, while grey lines represent tracking error from the wrist flexion fatigue session. * denotes a significant difference of both extension and flexion compared to baseline.

the full trajectory. While statistical analyses found no difference between the extension and flexion sessions ($F(7,77) = 0.06$, $P = 0.81$, ES = 0.01), there was a main effect of time on tracking error ($F(7,77) = 12.35$, $P < 0.05$, ES = 0.53), with error significantly worse from baseline immediately post fatigue (Baseline: 1.40 $\pm$ 0.54°, 0: 2.02 $\pm$ 0.51°, $P < 0.05$). Although group means never returned (or fell below) baseline error (even up to 10 minutes post-fatigue), tracking error recovered rapidly and was not significantly different

from baseline at, or following, 1 minute post-fatigue.

Figures 4.13 A and B depict group data of the longitudinal (ahead or behind) and normal

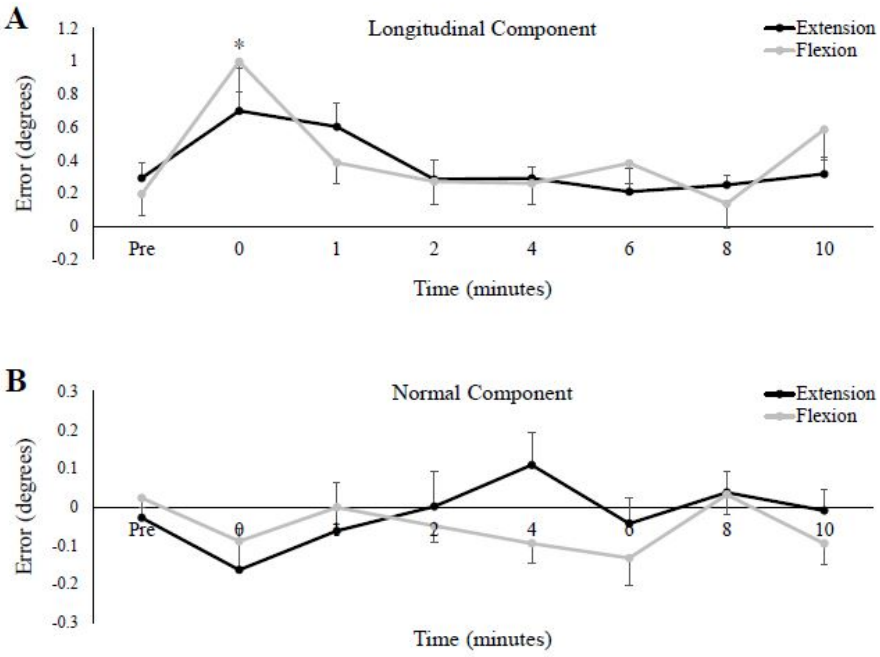

Figure 4.13 Group averages of the mean A) longitudinal component of the tracking error, and B) the normal component of the tracking error. For both metrics, error is shown in degrees (°) and data points are shown from pre-fatigue to 10 minutes-post. Black lines represent tracking error from the wrist extension fatigue session, while grey lines represent tracking error from the wrist flexion fatigue session. * denotes a significant difference of both extension and flexion compared to baseline.

(right or left) components, respectively, of the tracking error. As a group, participants tended to rush ahead of the target as it moved around the Lissajous curve. Even at baseline, the longitudinal component averaged $0.24 \pm 0.61^{\circ}$ between the two testing sessions. This tendency increased immediately post-fatigue, with participants significantly farther ahead than at baseline (Baseline: $0.24 \pm 0.61^{\circ}$, 0: $0.85 \pm 0.70^{\circ}$, $P < 0.05$). However, there was no difference in the longitudinal component between testing sessions, and the error across both sessions was not significantly different from baseline at, or following, 1-minute post-fatigue. Regarding the normal component of error, data seemed to hover around 0 for all conditions, meaning that as a group, participants missed the target to the right and to left to a nearly equal extent. The normal component of error was not significantly different between the two testing sessions ($F(7,77) = 0.52$, $P = 0.50$, $ES = 0.05$), nor did it significantly change over time ($F(7,77) = 1.61$, $P = 0.21$, $ES = 0.13$).

Group data on figural error is shown in Figure 4.14, and much like tracking error, demonstrated a main effect of time ($F(7,77) = 7.10$, $P < 0.05$, $ES = 0.392$), with no difference between the flexion and extension sessions ($F(7,77) = 1.55$, $P = 0.24$, $ES = 0.12$). Figural error significantly increased immediately post-fatigue (Baseline: $0.74 \pm 0.19°$, 0: $0.94 \pm 0.22°$, $P < 0.05$), but was not significantly different from baseline at, or following, 1-minute. Jerk ratios (representing movement smoothness) also demonstrated a main effect of time ($F(7,77) = 3.37$, $P < 0.05$, $ES = 0.23$), although interestingly, pairwise comparisons revealed no differences between any two time points. There was also no difference between the flexion and extension test sessions on jerk ratios ($F(7,77) = 0.07$, $P = 0.79$, $ES = 0.01$).

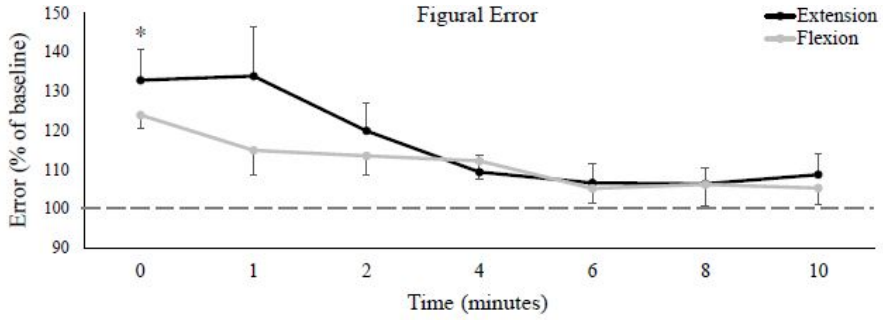

Figure 4.14 Group averages of figural error. Error is relative to baseline (shown by the dashed horizontal lines in each graph), and data points are shown in minutes after fatigue (0-10). Black lines represent tracking error from the wrist extension fatigue session, while grey lines represent tracking error from the wrist flexion fatigue session. * denotes a significant difference of both extension and flexion compared to baseline.

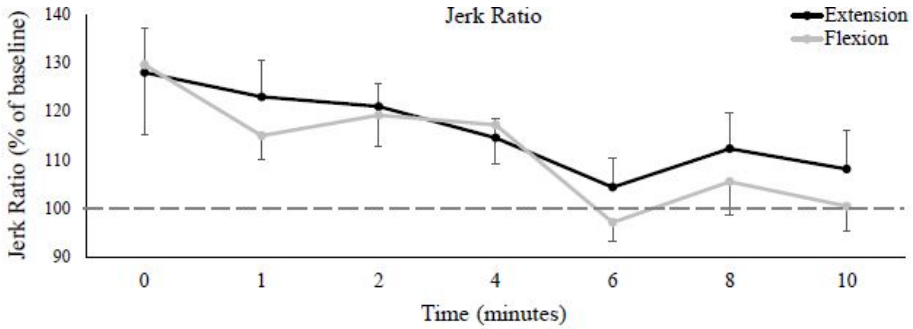

Figure 4.15 Group averages of the jerk ratio. Black lines represent jerk ratio from the wrist extension fatigue session, while grey lines represent jerk ratio from the wrist flexion fatigue session. * denotes a significant difference of both extension and flexion compared to baseline.

4.4.4 Discussion

The present study examined the effect of isometric fatigue on hand tracking performance considering two opposing forearm muscles. To compare muscle fatigue-induced changes in accuracy due to fatigue between flexion and extension muscles, the isometric fatigue protocol used a relative cut-off frequency (25% of MVC for each fatigue condition). The average fatigue duration was not different between flexion and extension fatigue.

Results showed that isometric fatigue significantly impaired hand-tracking performance immediately after the fatigue trial both in terms of *tracking error* and *figural error*. In details, a shift in error tendencies was also observed: the longitudinal component of *tracking error* immediately after the cessation of the fatigue task was significantly higher compared to the baseline. The positive sign of this component indicated that participants were more inclined to be ahead of the target following fatigue. On the contrary, the greater amplitude of the normal component of the *tracking error* (in absolute value) was not associated with a changes in left/right error tendencies. Therefore, participants altered their tracking strategy in terms of timing but not in left/right preferences.

The deficits in hand-tracking performance may reflect impairments in motor control due to fatigue thus supporting the hypothesis that fatigue alters proprioception sense as documented in the previous sections (4.2 and 4.3) and in literature (Jaric et al. 1999; Missenard et al. 2008). Moreover, our results of error metrics showed that the performance mostly recovered within 1-minute post-fatigue according to previous study (Huysmans et al. 2006).

To the best of our knowledge, the present study is the first to have examined isometric fatigue between opposing forearm muscles. Despite unique functional roles between the flexors and extensors of the wrist (Holmes et al. 2015), there were no differences between conditions. The findings of the present study seem to indicate that fatigue of either muscle group results in similar accuracy losses. This may be due to the tendency of extensors to exhibit high muscle activity even when extensors are not the prime mover (Forman et al. 2019; Mogk and Keir 2003).

Chapter 5

Implication of forearm posture on muscular strategies

5.1 Introduction

Forearm muscles, detailed in section 1.2, fulfill different role and functions during wrist movements. Indeed, wrist flexor muscles of the forearm are highly task-dependent and function chiefly as the prime movers in most hand-related tasks (Duque et al. 1995; Kattel et al. 1996). The forces produced by the wrist flexors are balanced by the wrist extensor muscles, which thus function mainly as wrist stabilizers (Hägg et al. 1997; Holmes et al. 2015; Snijders et al. 1987).

However, despite this general differentiation between muscles of the flexor or extensor group, the specific contribute of each muscles in performing wrist movements and their co-activation may change depending on the force required for the execution of task or on the posture (Finneran and O'Sullivan 2013).

The effects of posture should be thus considered in the prevention of injuries, in particular in workplace where workers have to repetitively perform tasks at low intensities for long duration with short breaks.

Given that musculoskeletal disorders, especially those of the upper limb are a common concern in modern industry, and physical risk factors such as force and posture are linked to their causation, the studies presented in the next paragraphs addressed this issue.

The study in section 5.2 provides a first overview about the characterization of forearm muscle activity in three different forearm postures and it has been conducted with a significant contribution of the researchers of the Neuromechanics and Ergonomics Lab of Brock

University (St. Catharines, Canada). In addition, we carried out an extension of the study considering seven different forearm postures.

5.2 Characterizing forearm muscle activity during dynamic wrist flexion-extension movement.

5.2.1 Introduction

The wrist extensor muscles exhibit higher levels of muscle activity than the flexors in most distal upper-limb tasks (Forman et al. 2019; Mogk and Keir 2003). While these differences are due in part to anatomical factors (the wrist extensors possess smaller cross-sectional areas and moment arms than the wrist flexors (Gonzalez et al. 1997), it has also been proposed that high wrist extensor activity results from their primary function as wrist joint stabilizers.
The effect of forearm posture on muscle activity has been evaluated by Mogk and Keir (2003) while producing various handgrip workloads. Muscle activity, evaluated in terms of amplitude of the EMG signal, resulted generally highest in pronation and lowest in supination. Additionally, wrist extensor muscle activity was significantly greater than the wrist flexors, at least during low handgrip forces. Considering that continuous sustained activity contribute in the development of chronic overuse injuries (Aarås and Westgaard 1987), the study suggested that the extensors were at a greater injury risk.
However, conclusions regarding flexor/extensor muscle roles have arisen mostly from isometric experiments (Forman et al. 2019; Mogk and Keir 2003). Literature as a whole concerning this topic is almost exclusively centered on isometric paradigms, with a scarcity of dynamic investigations. As such, it is currently unclear if patterns of forearm muscle recruitment obtained from isometric studies can be generalized to other forms of muscle contraction.
Considering the added biomechanical complexities associated with dynamic muscle mechanics, variable moment arms and changing muscle-tendon lengths (Holzbaur et al. 2005), increased muscle spindle activity (Eccles and Lundberg 1958), and greater cycling of cross-bridge formation (Huxley 2000), it is possible that the activity of wrist flexors/extensors might deviate from isometric work. Thus, the purpose of the present study was to examine forearm muscle activity during dynamic wrist flexion and extension. Muscle activity was assessed during robot-mediated wrist movements across 3 different forearm postures.

5.2.2 Methods

Participants

Experimental procedures were approved by the research ethics boards (REB) of Brock University (REB number 16-263) and the University of Ontario Institute of Technology (RE number 15044).
Written consent was obtained from all participants prior to the experiment. Twelve males (Age: 23.8±3.1 years, 11 right-handed, 1 left-handed) were recruited for this study. Participants were excluded if they presented with any upper-body, neuromuscular injuries.

Experimental setup

Participants were seated with their dominant forearm supported in a three-degrees-of freedom wrist manipulandum (Wristbot, Genoa, Italy; see 2.4 for further details) with their hand firmly gripping the device's handle.
Participants were requested to track a target moving from 40° of wrist flexion to 40° of wrist extension in three separate forearm positions: 1)30° of supination; 2) neutral posture; 3) 30° of pronation. For all experimental conditions, the manipulandum exerted a force of 15% of the individual's maximum wrist extension torque. This force was applied in either the flexion or extension direction, resulting in a total of 6 experimental conditions (3 forearm positions x 2 force directions). For each experimental condition, participants performed six repetitions of either wrist flexion or wrist extension (consisting of both a concentric and eccentric component). To control for angular velocity, the position of the handle was displayed to participants on a monitor. A circular target moved in the flexion-extension direction following a minimum jerk trajectory. Each complete repetition lasted 4 seconds and participants were required to match that target with the handle of the robot. The manipulandum compensated for the weight and inertia of the device throughout movement taking into account the different gravity components of the three rotations. Angular position of the handle was synchronized with measures of muscle activity.

Electromyography

Muscle activity was recorded using pairs of surface electrodes (Blue Sensor, Ambu A/S, Denmark) from eight muscles of the dominant arm: flexor carpi radialis (FCR), flexor carpi ulnaris (FCU), flexor digitorum superficialis (FDS), extensor carpi radialis (ECR), extensor carpi ulnaris (ECU), extensor digitorum (ED), biceps brachii (BB), and the triceps

Table 5.1 Summary of all 6 experimental conditions.

Forearm Position	Supination 30°	Neutral	Pronation 30°
Concentric Wrist Action	Flexion	Flexion	Flexion
	Extension	Extension	Extension

brachii (TB). Electrodes were placed over the muscle belly, in-line with fiber orientation, and procedures followed previous placement guidelines (Forman et al. 2019; Holmes et al. 2015; Mogk and Keir 2003). A ground electrode was placed on the lateral epicondyle of the dominant arm. EMG was band-pass filtered (10-1000 Hz) and differentially amplified (Bortec Biomedical Ltd, Calgary, AB, Canada). EMG data was sampled at 2000 Hz (USB-6229 BNC, National Instruments).

Experimental Protocol

Participants were first familiarized with the manipulandum using minimal resistance. Then maximal wrist extension force was evaluated using a force transducer (Model: BG 500, Mark-10 Corporation, New York, USA) mounted in parallel with the surface of a table. Participants sat near the table and laid both the arms on the table. The dominant arm was used to exert the maximal wrist extension against the transducer, in detail the transducer made contact with the posterior surface of the distal phalanges (back of the knuckles; closed hand) while participants exerted maximal wrist extension force for a single trial. The distance between the participants' wrist and the center of the transducer were measured to calculate maximum extension moment. EMG procedures were then conducted and muscle-specific MVCs were performed against the manual resistance of the experimenters.
Participants returned to the manipulandum and performed one of the 6 experimental conditions (summarized in Table 5.1) of the robotic task. The forearm was rotated into one of 3 positions (supination/neutral/pronation) and force was applied in one of two directions (flexion-extension). Example: for the supinated-flexion condition, the manipulandum's handle rotated into 30° of supination. An external load of 15% of maximum wrist extension was applied, which acted to move the subject's hand towards wrist extension. In order to overcome this end effector force, the participant would exert a concentric wrist flexion force as they matched the computer-displayed target. All force directions therefore refer to the agonist concentric muscle action in each condition. The order of the 3 forearm positions was randomized, as well as the 2 force directions within each posture. Two minutes of rest were provided between conditions to minimize the effects of muscle fatigue.

Data Analysis

EMG and kinematic data of the manipulandum's handle were analyzed off-line. EMG was full-wave rectified, digitally low pass filtered (Butterworth, dual pass, 2nd order, 3 Hz cut-off) and normalized to muscle-specific MVCs. For all conditions, EMG data was separated into concentric/eccentric phases determined according to the kinematic data of the manipulandum. Phases were separated based on when participants reached end-range of wrist flexion and extension. Mean EMG was then measured within the concentric and eccentric phases for 3 of the 6 repetitions (first 2 repetitions excluded so participants could catch up with the computer-displayed target). These measures were averaged into a single concentric and eccentric value for each condition. Co-contraction was calculated as a ratio of antagonist/agonist for all anatomical pairs of flexors and extensors (i.e. FCR-ECR, FCU-ECU, FDS-ED, and BB-TB) (Damiano et al. 2000; Forman et al. 2019). In addition, a temporal curve of co-contraction (antagonist/agonist) was calculated for each time point during the entire range of motion of the dynamic task. Three-way, repeated measures ANOVAs (forearm position x force direction x phase of movement) were conducted within each muscle for both mean EMG and cocontraction ratios (SPSS, V24, IBM Corporation, Armonk, NY, USA). In cases where interactions were observed, post-hoc simple main effects were performed with a Bonferroni correction. Effect sizes were evaluated using partial ETA Squared calculated as the division of the sum of squares of the effects (SSEffect) by both the SSEffect and the sum of squares of the error (SSError). Significance level was set at $P < .05$. Data is reported as mean$\pm$SD and illustrated in figures as SE.

5.2.3 Results

Figure 5.1 depicts the mean EMG data split across concentric and eccentric phases. FCR,ECR, FDS, ED and FCU all demonstrated a 2-way interaction of force direction and phase with no influence of forearm posture. Secondary analyses revealed a significant difference between phases in the flexion force direction (Table 5.2), with greater EMG during concentric for the three wrist flexors (FCR, FDS, and FCU) while greater in eccentric for the two wrist extensors (ECR and ED). In extension, EMG was higher in the eccentric phase for FCR and FDS, while higher in the concentric phase for ECR and ED. EMG during the concentric phase was also significantly different across force directions, with greater EMG in flexion for the three wrist flexors and greater EMG in extension for the two extensors. There were no differences in eccentric EMG between force directions. ECU, BB and TB demonstrated a 3-way interaction of posture, force direction, and movement. Subsequent analysis revealed a

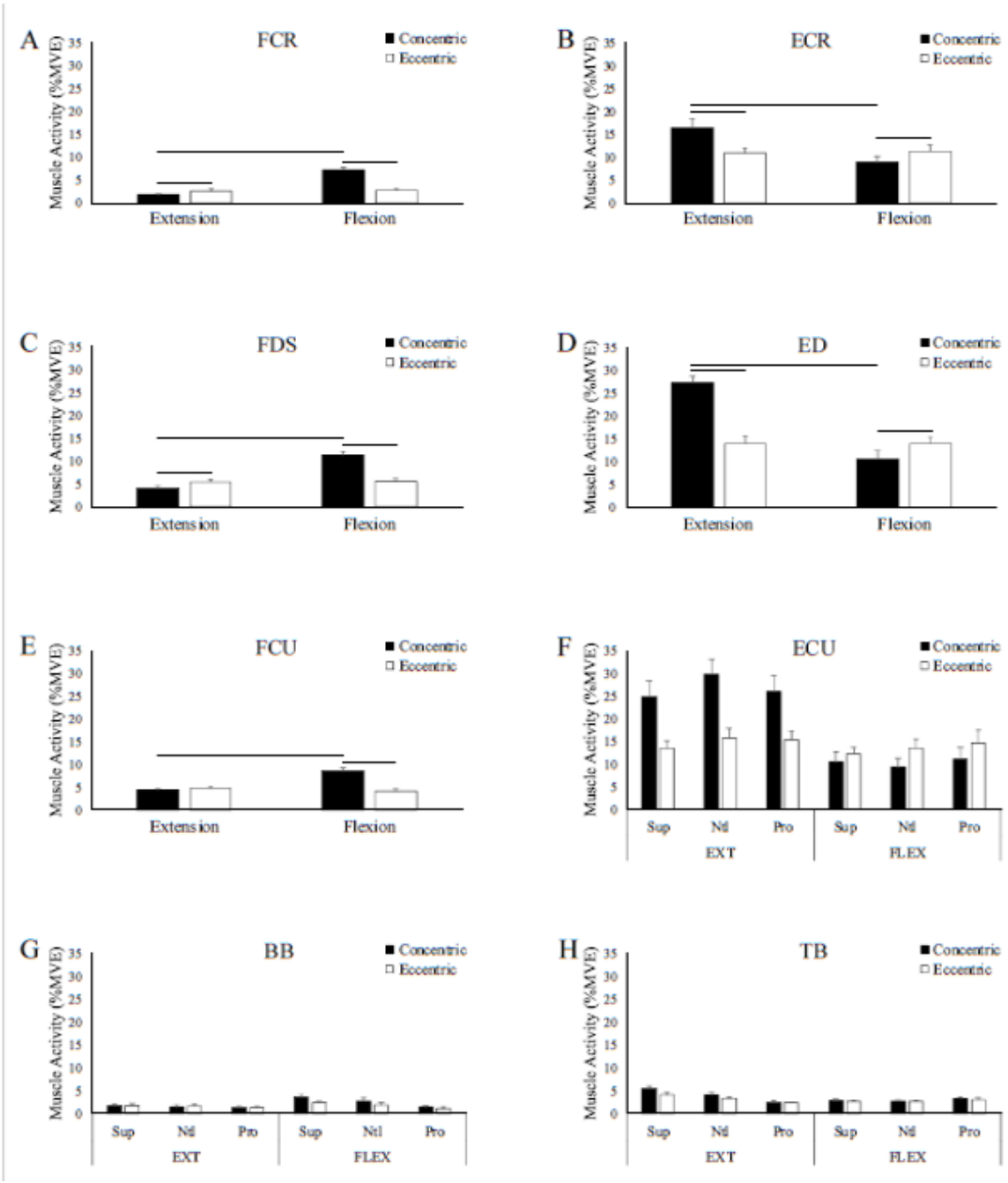

Figure 5.1 Group averages of mean muscle activity (displayed as a % of maximum) in the concentric (black) and eccentric (white) phases. A – E depict 2-way interactions of force direction and movement phase. F – H depict 3-way interactions. Horizontal lines denote a significant difference ($P < 0.05$) between either concentric and eccentric phases within a force direction or between flexion and extension within a movement phase.

Table 5.2 Post-hoc analyses of mean EMG for all muscles that demonstrated a 2-way interaction of force direction and movement phase. Data was collapsed across forearm postures and main effects were conducted with a Bonferroni correction. Results are listed as P-Values, F-statistics, and effect sizes (represented by Partial ETA Squared (η_p^2).

		Flexion (Con vs. Ecc)	Extension (Con vs. Ecc)	Concentric (Flex vs Ext)	Eccentric (Flex vs Ext)
	P-value	<.001*	0.005	<.001*	0.661
FCR	F-Stat	$F_{(1,29)} = 68.89$	$F_{(1,29)} = 9.28$	$F_{(1,29)} = 85.37$	$F_{(1,29)} = 0.196$
	Effect Size	0.703	0.242	0.746	0.007
	P-value	<.001*	0.029	<.001*	0.803
FDS	F-Stat	$F_{(1,29)} = 31.25$	$F_{(1,29)} = 5.29$	$F_{(1,29)} = 38.11$	$F_{(1,29)} = 0.064$
	Effect Size	0.519	0.159	0.576	0.002
	P-value	<.001*	0.279	<.001*	0.093
FCU	F-Stat	$F_{(1,32)} = 97.33$	$F_{(1,32)} = 1.215$	$F_{(1,32)} = 58.35$	$F_{(1,32)} = 3.0$
	Effect Size	0.753	0.037	0.646	0.086
	P-value	0.021	<.001*	<0.001	0.689
ECR	F-Stat	$F_{(1,32)} = 5.93$	$F_{(1,32)} = 16.38$	$F_{(1,32)} = 16.48$	$F_{(1,32)} = 0.164$
	Effect Size	0.156	0.339	0.34	0.005
	P-value	0.047	<.001*	<.001	0.992
ED	F-Stat	$F_{(1,35)} = 4.23$	$F_{(1,35)} = 38.74$	$F_{(1,35)} = 47.54$	$F_{(1,35)} < .001$*
	Effect Size	0.108	0.525	0.576	<.001*

main effect of posture in ECU during extension, with EMG (averaged across phases) greater in neutral than supination (P = 0.043) and pronation (P = 0.032). Concentric EMG was significantly higher than eccentric during extension (F(1,10) = 13.42, P = 0.004) but was not different between phases during flexion. For the BB, EMG was greater in flexion than extension, but only during concentric (F(1,35) = 17.56, P < .001). Also, BB EMG was greater during concentric than eccentric, but only in flexion (F(1,35) = 22.75, P < 0.001). For the TB, EMG was greater in extension than flexion for both phases (F(1,11) = 18.75, P = 0.001) and greater during concentric than eccentric for both force directions (F(1,11) = 22.51, P = 0.001). Posture significantly influenced EMG in the flexion direction for BB (F(2,10) = 9.89, P = 0.001) and in the extension direction for TB (F(2,10) = 26.83, P < 0.001).

Co-contraction ratios

Figure 5.2 depicts heat maps of the co-contraction ratios for all muscle-pairings averaged across the full sample. Data is reported over the entire wrist flexion-extension range ($\pm$ 40°). In Figure 5.3, the FCR-ECR, FDS-ED, and BB-TB pairings demonstrated 2-way interactions, with statistical results displayed in Table 5.3. With the exception of the BB-TB ratio, all

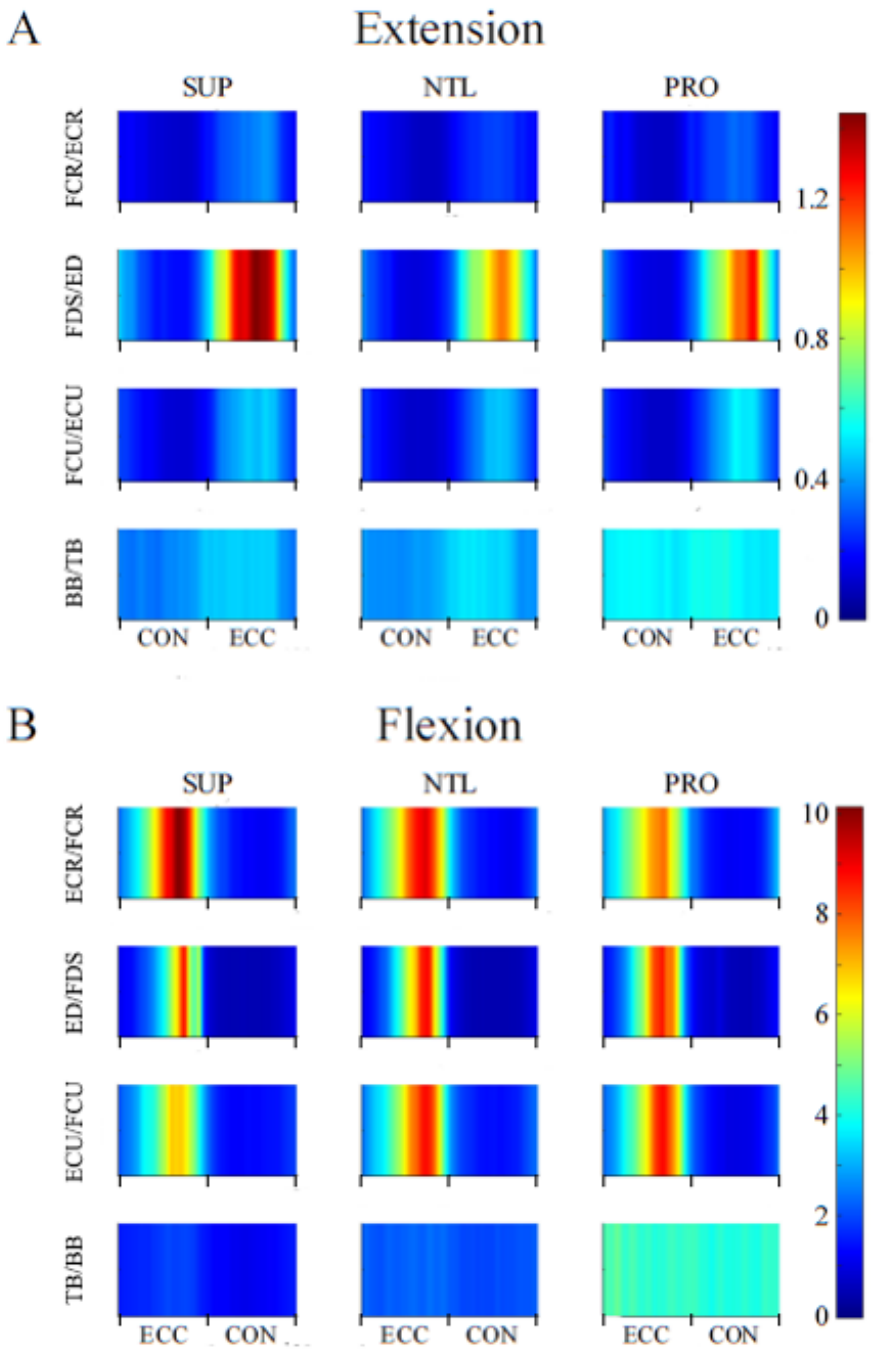

Figure 5.2 Heat maps of the group averages of co-contraction ratios (antagonist/agonist muscle pairs) throughout the entire wrist extension-flexion repetition range. A) represents the heat maps during the wrist extension trials (whereby participants overcame an external load pushing them into wrist flexion), whereas B) represents heat maps during the wrist flexion trials. For all heat maps, the left most data represents the wrist beginning to extend and finishes on the right of the graphs at maximum wrist flexion. Red and blue colours denote high and low co-contraction values, respectively, however, A) and B) heat maps utilize separate scaling of the colour bar.

Table 5.3 Post-hoc analyses of co-contractions (anatomical antagonist/agonist muscle pairings) that demonstrated a 2-way interaction of A) force direction and movement phase, and B) posture and force direction. Results are listed as P-Values, F-statistics and effect sizes (represented by Partial ETA Squared (η_p^2).

		Flexion (Conc vs. Ecc)	Extension (Conc vs. Ecc)	Concentric (Flex vs. Ext)	Eccentric (Flex vs. Ext)
	P-value	<.001*	<.001*	<.001*	<.001*
FCR-ECR	F-Stat	$F_{(1,26)} = 49.878$	$F_{(1,26)} = 49.796$	$F_{(1,26)} = 60.774$	$F_{(1,26)} = 55.202$
	Effect Size	0.657	0.643	0.7	0.68
	P-value	0.004*	0.011	0.002*	<.001*
FDS-ED	F-Stat	$F_{(1,29)} = 9.606$	$F_{(1,29)} = 7.482$	$F_{(1,29)} = 11.56$	$F_{(1,29)} = 63.332$
	Effect Size	0.519	0.205	0.285	0.686

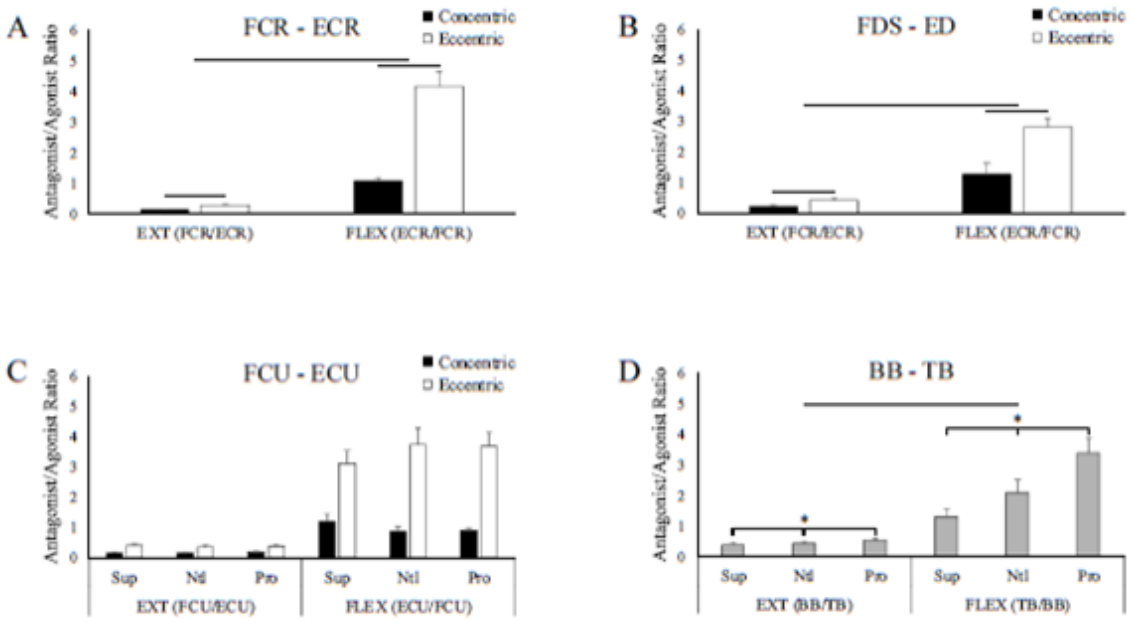

Figure 5.3 Group averages of co-contraction ratios (antagonist/agonist muscle pairs). A and B depict 2-way interactions of force direction and movement phase (black: concentric, white: eccentric). C depicts a 3-way interaction while D depicts a 2-way interaction of posture and force direction. Horizontal lines denote a significant difference ($P < 0.05$) between either concentric and eccentric phases within a force direction or a difference between force directions (flexion vs extension). * denotes a significant main effect of forearm posture.

muscle pairings showed significantly greater co-contraction in the eccentric than concentric phases (FCU-ECU: $F(1,9) = 70.17$, $P < 0.001$). There was also greater co-contraction in the flexion than extension force direction for all four muscle pairings (FCU-ECU: $F(1,9) = 36.96$, $P < 0.001$). The BB-TB pairing revealed a main effect of posture during flexion, with greater

co-contraction occurring towards pronation. The FCU-ECU was the only muscle-pairing to demonstrate a 3-way interaction of posture, phase, and direction ($F(2,9) = 4.85$, $P = 0.021$). However, secondary analyses revealed no effect of posture on co-contraction in either force direction (flexion: $F(2,19) = 0.515$, $P = 0.61$, extension: $F(2,19) = 0.941$, $P = 0.41$) or either movement phase (concentric: $F(2,19) = 2.83$, $P = 0.086$, eccentric: $F(2,19) = 2.29$, $P = 0.13$).

5.2.4 Discussion

This work offered a comprehensive examinations of the interactions between forearm posture, force direction, and movement phase on forearm muscle recruitment during dynamic wrist exertions. The findings indicated that forearm posture had minimal influence on forearm muscle activity, but significantly altered the activity of the biceps and triceps brachii. Force direction influenced muscle activity in nearly every muscle, with EMG levels higher in the concentric phase when muscles acted as agonists. Interestingly, muscle activity in the eccentric phase was equal across force directions, regardless of whether the muscle acted as the agonist or antagonist. Movement phase also dictated muscle activity in every muscle and was dependent upon force direction. Lastly, co-contraction ratios were higher in the flexion conditions, suggesting significantly greater wrist extensor antagonist activity. This highlights the vulnerability of the wrist extensors to overuse injuries in settings requiring repeated or prolonged dynamic wrist exertions.

Posture

In the present study, forearm posture significantly influenced muscle activity and cocontraction of the muscles acting upon the elbow joint. In flexion trials for the biceps brachii, and extension trials for the triceps brachii, EMG increased towards supination. However, forearm posture had almost no effect on forearm muscle activity, with only ECU influenced during extension trials. This was somewhat unexpected given literature on forearm rotation and wrist forces. Both La Delfa et al. (2015) and Yoshii et al. (2015) examined wrist force in three forearm postures and found that wrist extension generated greater force in pronation. While the wrist flexion results differed between the studies (likely due to variations in protocol: open hand (La Delfa et al. 2015) vs gripping hand (Yoshii et al. 2015), forearm rotation influenced flexion force in both. Considering that forearm posture seems to modulate wrist forces, it was expected that forearm muscle activity in the present study would have been lower in stronger postures (pronation) and higher in weaker postures (supination). However, the aforementioned studies conducted their investigations under maximal force conditions;

the present study used a submaximal external load. It's possible that the interaction of posture and force might have influenced muscle activity to a larger extent had a greater load been used. Reflecting upon handgrip literature, Mogk and Keir (2003) demonstrated that forearm rotation influenced muscle activity, with lower activity in supination than pronation for most muscles and in most handgrip loads. Muscle activity was likely lower in supination than pronation as maximal handgrip forces tend to be greater in supination (Claudon 1998. However, the postures used in Mogk and Keir 2003 were full pronation/supination, compared to the $\pm 30^{\circ}$ used in the present study. Additionally, the dynamic nature of the current wrist flexion-extension task makes comparisons to isometric handgrip protocols difficult.

Force Direction and Movement Phase

Forearm muscles produced more EMG when functioning as agonists versus antagonists (Figure 5.1), at least in the concentric phase (i.e. flexors more active in flexion; extensors more active in extension). Muscle activity was also higher in concentric than eccentric phases (only for agonists) and this finding is well supported by literature (Duchateau and Baudry 2013; Kellis and Baltzopoulos 1998. Evidence suggests that motor pathways employ unique control strategies for lengthening and shortening contractions (Enoka 1996), which may stem in part from changes in muscle properties. In lengthening contractions, fewer motor units are required to reach equivalent torque as shortening contractions, given the increased intrinsic force production of muscle fibers (Edman et al. 1978; Herzog 2013; Katz 1939). A progressive derecruitment of motor units (Pasquet et al. 2006) in combination with decreased discharge rate of active motor units (Del Valle and Thomas 2005; Tax et al. 1989) is likely responsible for the reduction of eccentric EMG. Interestingly, muscle activity in the eccentric phases was not different between force directions in any forearm muscle. For instance, FCR (Figure 5.1A) demonstrated $2.6 \pm 2.1\%$ and $2.7 \pm 1.5\%$ of maximum in the eccentric phases of wrist extension and wrist flexion, respectively. This could suggest that during dynamic contractions, forearm muscles exhibit equal activity whether they function as lengthening agonists or shortening antagonists. Therefore the summation of motor unit recruitment and discharge rates are likely equal during an eccentric contraction both if the muscle is assisting or resisting the movements. Further, it is important to consider that equal muscle activity does not imply equal muscle load. Less muscle activity in eccentric contraction is required to maintain the same level of force as concentric contraction (Edman et al. 1978). Predictive applications can be developed considering all these aspects. If eccentric EMG between flexion and extension force directions is consistent across postures (shown in the present study), loads, and movement velocity, it might be possible to make large inferences

on forearm recruitment patterns with limited EMG data. This could also help simplify control systems for prosthetic/robotic work aimed at the distal upper extremity.

Finally, co-contraction ratios were significantly influenced by force direction. Across all agonist-antagonist muscle pairings (Figure 5.2), there was greater co-contraction during wrist flexion than extension trials. Summed across all forearm muscles (Figures 5.2A-5.2C), postures, and phases, wrist extension exhibited a co-contraction value of 0.32 ± 0.27 versus 2.28 ± 2.04 in wrist flexion. This finding is noteworthy for two reasons: 1) at only 32% the activity of the wrist extensors, the wrist flexors provided minimal co-contraction during wrist extension trials, and 2) as the antagonists during wrist flexion, the wrist extensors provided more than twice the activity (228%) of the wrist flexors. Despite the dynamic novelty of the present work, these results are in-line with findings taken from isometric research (Mogk and Keir 2003; Snijders et al. 1987). As the wrist extensors possess both a smaller cumulative cross-sectional area and moment arm than the wrist flexors (Gonzalez et al. 1997), their force generating capacity is significantly less. Consequently, the wrist extensors must function at a higher percent of maximal activation to counteract the stronger flexors, which pose injury risks. One factor in the development of chronic overuse injuries is insufficient rest intervals between periods of muscle loading. These results suggest that manipulating factors (i.e. posture or force direction) may be insufficient in reducing muscle activity as the wrist extensors were never active to less than 9% of maximum in our work (an amount of activity that exceeds recommendations for continuous work (Jonsson 1978).

5.2.5 Extension study

The little influence of forearm posture on forearm muscle activity may be related to the small range of motion adopted in the study. The evaluation of forearm postures involving larger rotation might modify mechanical properties, and subsequently muscle activity, to a greater extent. Therefore, we evaluated further forearm postures as an extension of the previous study.

Eleven right-handed males (Age: 23.7 ± 3.7 years, 11 right-handed) were recruited for this study. The experimental setup, electromyography procedures as well as the muscles recorded were the same as in the previous study. Similarly, participants were requested to perform the same tracking task as above during two experimental sessions (flexion fatigue day and extension fatigue day). Seven separate forearm positions were used: 1) 45° of supination; 2)30° of supination; 3) 15° of supination; 4) neutral posture; 5) 15° of pronation; 6) 30° of pronation; 7) 45° of pronation.

Preliminary results seem to confirm the little influence of forearm posture on forearm muscle activity even considering larger range of motion. Figure 5.4 depicts the mean muscle activity, of all muscles recorded, during concentric phases of movements while interacting with the resistive force in the flexion direction.
It is worth noting that, even if in this case the concentric phase of movement was actually during wrist flexions, the extensor muscles presented comparable level of activation as the muscles of the flexor group. Similarly, Figure 5.5 shows the mean muscle activity relative to concentric phases of movements in the extension direction condition (i.e. the resistive force opposed to the wrist extension movements). Muscle activity was not influenced by forearm postures with the exception of ECU that exhibited higher activation when rotated of 30° and 45° of supination. As for the influence of force direction, as expected, EMG levels of every muscle were higher in the concentric phase when muscles acted as prime mover, i.e. comparing FCR during flexion force direction (Figure 5.4 top left panel) with the same muscle in the extension force direction (Figure 5.5 top left panel) it is possible to note that the muscle activity was higher in the first situation. Future studies involving task with higher level of force may add useful insight in the fatigability of muscles when adopting different postures.

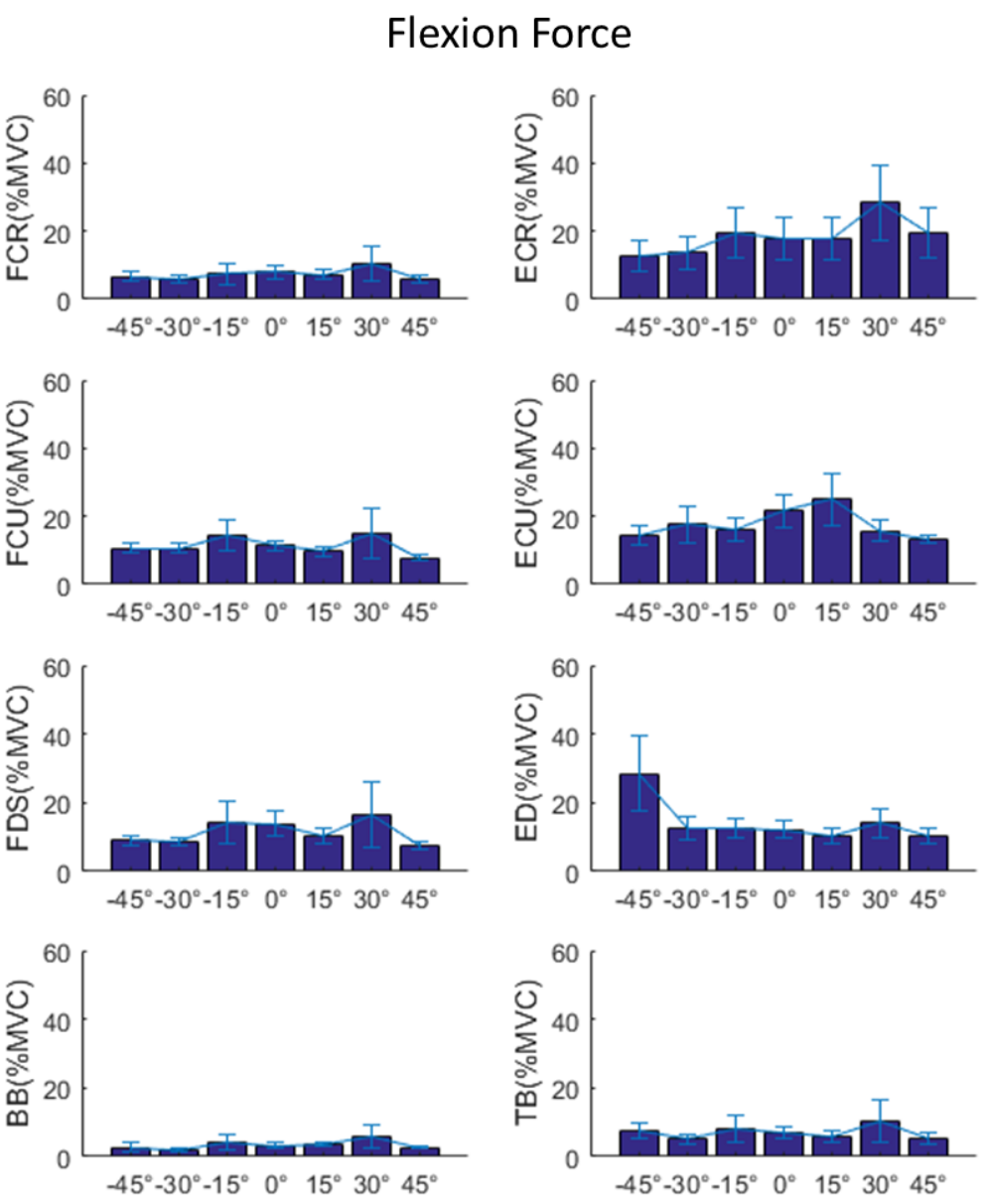

Figure 5.4 Group averages of mean muscle activity (displayed as a % of maximum) of all muscles during concentric phase of movements while interacting with a resistive force in the flexion direction. x-axis shows different rotation in the pronation-supination direction: 15° 30° 45° are relative to supination, while negative angles are relative to pronation.

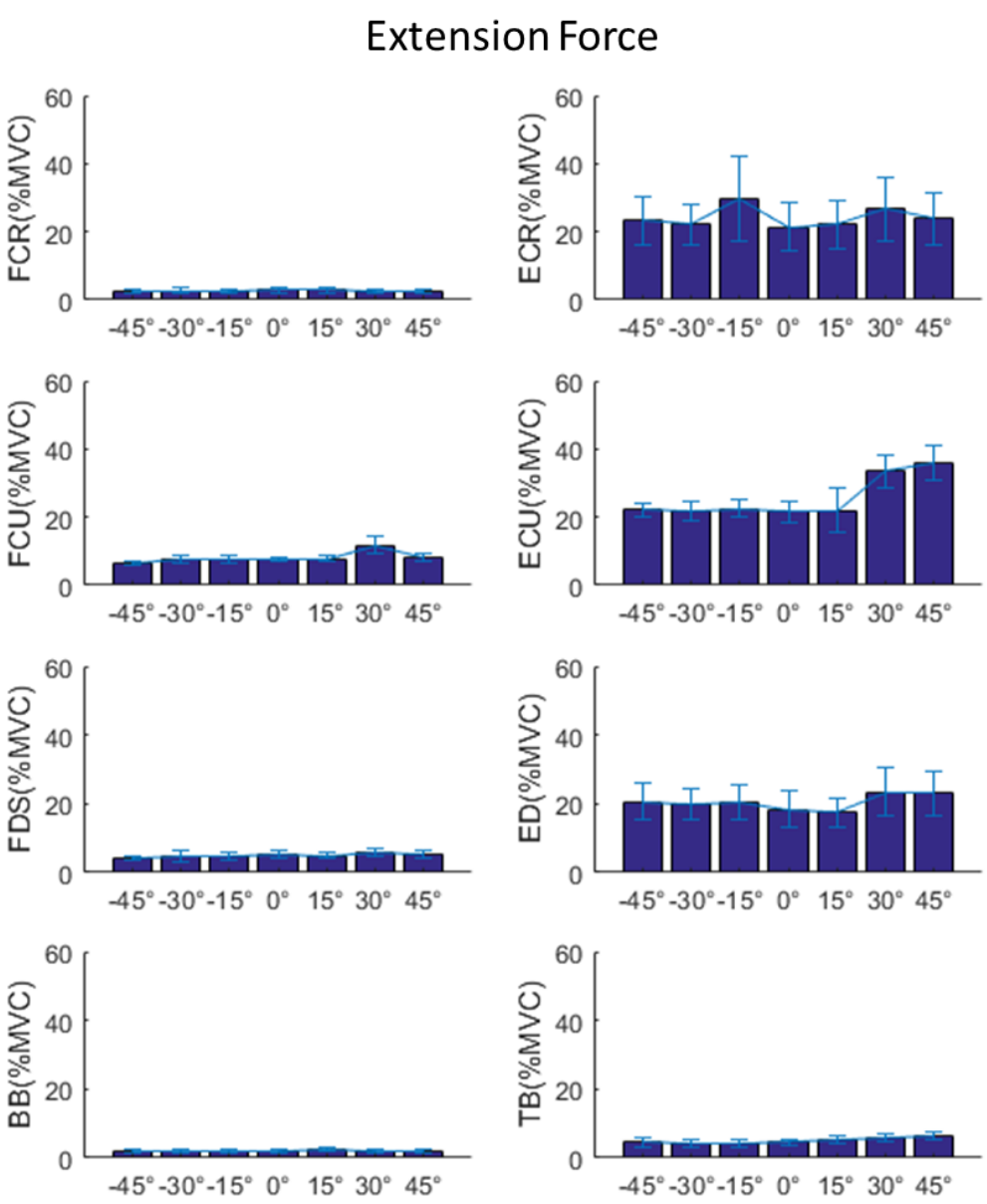

Figure 5.5 Group averages of mean muscle activity (displayed as a % of maximum) of all muscles during concentric phase of movements while interacting with a resistive force in the extension direction. x-axis shows different rotation in the pronation-supination direction: 15° 30° 45° are relative to supination, while negative angles are relative to pronation.

Chapter 6

Conclusions

The studies presented in this thesis exploited novel and objective approaches to provide insights about forearm muscle activity with a focus on muscle fatigue and on its effect on position sense. We carried out all the experiments coupling a robotic device for wrist rehabilitation with surface electromyography. This procedure allowed to analyze muscle activity in different experimental conditions and to extract quantitative parameters. From a clinical perspective, we also proposed a method that could be included in the standard assessment routine. Indeed, the test we developed can meet the needs of clinicians in the assessment of muscle fatigue. The method is simple, easy to administer and provides easy readable information about muscle fatigue. It is suitable for patients or healthy participants who are not able to generate high levels of muscle contractions. This overcomes the problem of administering maximal contraction tests in neurological or injured populations. We applied the method on healthy adults population to test its validity and repeatability. Then we carried out a pilot study on children with Duchenne and Becker Muscular Dystrophy. The results proved the feasibility of our method with subjects with different age and level of disability. Therefore, the future perspective is to retest patients to correlate fatigue measure with the progress of the disease and/or the efficacy of an eventual therapy. Moreover, the robotic task can be easily modified in terms of force, velocity and range of motion according to the ability of each patient. The test is thus a valuable tool that could help clinicians in the assessment of muscle fatigue in different pathological populations.

Taking into account muscle fatigue is not only important in the management and assessment of pathological populations but also in the prevention of injuries in workers or athletes. In fact, muscle fatigue may have a great impact in healthy subjects affecting their sensorimotor control mechanisms. The consequently altered coordination of movements and muscle activity may in turn lead to a higher risk of injuries.

In this thesis, the three studies related to the impact of muscle fatigue on sensorimotor control confirmed the decrease of proprioceptive acuity due to muscle fatigue. In details, the first experiment proved that muscle fatigue of flexor carpi radialis muscle affect individual's estimation of wrist joint displacement but not precision. The possible explanation is that muscle spindle discharge was affected by muscle fatigue, which resulted in the significant reduction in proprioceptive accuracy. However, although affected, the muscle spindle discharge rate did not vary throughout the execution of the test as indicated by the absence of significant differences in precision.

The experiment carried out together with the team of Brock University provided further insights about proprioceptive decline due to muscle fatigue. Indeed, changes in wrist proprioception sense was found as a consequence of pain or muscle fatigue in the neck muscle (in particular Cervical Extensor Muscle). Similarly to the previous experiment, and using the same robotic test of joint position sense, there was a significant reduction in the estimation of wrist joint displacement in the flexion-extension direction due to neck muscle fatigue in healthy subjects. Moreover, we tested participants with sub-clinical neck pain and we found a significant decline in joint position sense of this population compared to control subjects. This study suggested that neck pain and neck muscle fatigue may result in altered sensory processing ultimately leading to decreased proprioception of the wrist. Due to the prevalence of neck pain and neck muscle fatigue as well as the demands of many occupational tasks, these findings should be considered in order to promote safety and productivity in the workplace.

In accordance to these experiments, the third study indicated that muscle fatigue impair also hand tracking performance. It showed a significant decline in subjects' performance after an isometric flexion or extension fatigue protocol compared with baseline. This study, which was conducted in collaboration with Brock University, also allowed to compare the role of flexor and extensor muscles, showing that despite unique functional roles between the flexors and extensors of the wrist, isometric extension/flexion fatigue impairs tracing performance of the hand similarly.

Finally, we investigated the effect of different forearm postures on muscle activity with the purpose of improving the knowledge of forearm muscle activity and ultimately supporting the prevention of injuries in workplaces. This work (carried out in collaboration with Brock University) reported little influence of posture on forearm muscle activity and greater extensor muscles activity rather than flexor highlighting the high risk of extensor injuries.

Summarizing, this thesis highlighted the impact that muscle fatigue can have on everyday life in both healthy and subjects with neuromuscular disorders. A quantitative assessment

of muscle fatigue is thus fundamental in the management of pathological subjects. We developed a simple and objective method to assess muscle fatigue. Our preliminary studies lay down the basis for the implementation of the test in clinical practice.
Furthermore, we suggested that muscle fatigue has to be taken into account also in healthy subjects especially in case of workers. Delayed identification of workplace fatigue could indeed contribute to the development of chronic overuse injuries. Moreover, muscle fatigue can be also associated with a decline in proprioceptive acuity. Consequently, the alterations in the control of movements could lead to a decrease in the performance of a specific task and to a high risk of injuries in workers or athletes.

References

Aarås, A. and Westgaard, R. (1987). Further studies of postural load and musculo-skeletal injuries of workers at an electro-mechanical assembly plant. *Applied Ergonomics*, 18(3):211–219.

Abend, W., Bizzi, E., and Morasso, P. (1982). Human arm trajectory formation. *Brain : a journal of neurology*, 105(Pt 2):331–48.

Abichandani, D. and Parkar, B. (2015). Comparison of Upper Limb Proprioception in Chronic Mechanical Neck Pain Patients with Age-Sex Matched Healthy Normals. *International Journal of Science and Research*, 6:2319–7064.

Ager, A., Roy, J., Roos, M., Belley, A. F., Cools, A., and Hébert, L. J. (2017). Shoulder proprioception: How is it measured and is it reliable? A systematic review. *Journal of hand therapy : official journal of the American Society of Hand Therapists*, 30(2):221–231.

Allen, D., Lamb, G., and Westerblad, H. (2008). Skeletal muscle fatigue: cellular mechanisms. *Physiological reviews*, 88(1):287–332.

Allen, D. and Trajanovska, S. (2012). The multiple roles of phosphate in muscle fatigue. *Frontiers in physiology*, 3:463.

Allen, D., Westerblad, H., Lee, J., and Lännergren, J. (1992). Role of Excitation-Contraction Coupling in Muscle Fatigue. *Sports Medicine: An International Journal of Applied Medicine and Science in Sport and Exercise*, 13(2):116–126.

Allen, T., Ansems, G. E., and Proske, U. (2007). Effects of muscle conditioning on position sense at the human forearm during loading or fatigue of elbow flexors and the role of the sense of effort. *The Journal of Physiology*, 580(2):423–434.

Amini, D. (2011). Occupational therapy interventions for work-related injuries and conditions of the forearm, wrist, and hand: A systematic review. *American Journal of Occupational Therapy*, 65(1):29–36.

Angelini, C. and Tasca, E. (2012). Fatigue in muscular dystrophies. *Neuromuscular Disorders*, 22:S214–S220.

Arabadzhiev, T., Dimitrov, G., and Dimitrova, N. (2005). Simulation analysis of the performance of a novel high sensitive spectral index for quantifying M-wave changes during fatigue. *Journal of Electromyography*.

Arbogast, S., Vassilakopoulos, T., Darques, J. L., Duvauchelle, J. B., and Jammes, Y. (2000). Influence of oxygen supply on activation of group IV muscle afferents after low-frequency muscle stimulation. *Muscle & nerve*, 23(8):1187–93.

Arendt-Nielsen, L. and Mills, K. (1985). The relationship between mean power frequency of the emg spectrum and muscle fibre conduction velocity. *Electroencephalography and clinical Neurophysiology*, 60(2):130–134.

Arendt-Nielsen, L., Mills, K., and Forster, A. (1989). Changes in muscle fiber conduction velocity, mean power frequency, and mean EMG voltage during prolonged submaximal contractions. *Muscle & Nerve*, 12(6):493–497.

Arnould, C., Penta, M., Renders, A., and Thonnard, J.-L. (2004). ABILHAND-Kids: a measure of manual ability in children with cerebral palsy. *Neurology*, 63(6):1045–52.

Baarbé, J. K., Holmes, M. W., Murphy, H. E., Haavik, H., and Murphy, B. A. (2016). Influence of subclinical neck pain on the ability to perform a mental rotation task: a 4-week longitudinal study with a healthy control group comparison. *Journal of manipulative and physiological therapeutics*, 39(1):23–30.

Bäckman, E., Johansson, V., Häger, B., Sjöblom, P., and Henriksson, K. G. (1995). Isometric muscle strength and muscular endurance in normal persons aged between 17 and 70 years. *Scandinavian journal of rehabilitation medicine*, 27(2):109–17.

Balasubramanian, S., Colombo, R., Sterpi, I., Sanguineti, V., and Burdet, E. (2012). Robotic Assessment of Upper Limb Motor Function After Stroke. *American Journal of Physical Medicine & Rehabilitation*, 91:S255–S269.

Bawa, P., Chalmers, G., Jones, K. E., Søgaard, K., and Walsh, M. L. (2000). Control of the wrist joint in humans. *European Journal of Applied Physiology*, 83(2-3):116–127.

Beretta-Piccoli, M., D'Antona, G., Barbero, M., Fisher, B., Dieli-Conwright, C. M., Clijsen, R., and Cescon, C. (2015). Evaluation of Central and Peripheral Fatigue in the Quadriceps Using Fractal Dimension and Conduction Velocity in Young Females. *PLOS ONE*, 10(4):e0123921.

Bigland-Ritchie, B. and Woods, J. J. (1984). Changes in muscle contractile properties and neural control during human muscular fatigue. *Muscle & Nerve*, 7(9):691–699.

Blanche, E., Bodison, S., Chang, M. C., and Reinoso, G. (2012). Development of the comprehensive observations of proprioception (cop): Validity, reliability, and factor analysis. *American Journal of Occupational Therapy*, 66(6):691–698.

Bongiovanni, L. and Hagbarth, K. E. (1990). Tonic vibration reflexes elicited during fatigue from maximal voluntary contractions in man. *The Journal of Physiology*, 423(1):1–14.

Borg, G. (1990). Psychophysical scaling with applications in physical work and the perception of exertion. *Scand J Work Environ Health*, 16(Suppl 1):55–58.

Bowden, J. L., Taylor, J. L., and McNulty, P. A. (2014). Voluntary Activation is Reduced in Both the More- and Less-Affected Upper Limbs after Unilateral Stroke. *Frontiers in Neurology*, 5:239.

Boyas, S. and Guével, A. (2011). Neuromuscular fatigue in healthy muscle: underlying factors and adaptation mechanisms. *Annals of physical and rehabilitation medicine*, 54(2):88–108.

Burke, R. (2011). Motor Units: Anatomy, Physiology, and Functional Organization. In *Comprehensive Physiology*. John Wiley & Sons, Inc.

Bushby, K., Finkel, R., Birnkrant, D. J., Case, L. E., Clemens, P. R., Cripe, L., Kaul, A., Kinnett, K., McDonald, C., Pandya, S., Poysky, J., Shapiro, F., Tomezsko, J., and Constantin, C. (2010). Diagnosis and management of Duchenne muscular dystrophy, part 2: implementation of multidisciplinary care. *The Lancet Neurology*, 9(2):177–189.

Bushby, K., Hill, A., and Steele, J. G. (1999). Failure of early diagnosis in symptomatic Duchenne muscular dystrophy. *Lancet (London, England)*, 353(9152):557–8.

Carpenter, J., Blasier, R. B., and Pellizzon, G. G. (1998). The Effects of Muscle Fatigue on Shoulder Joint Position Sense. *The American Journal of Sports Medicine*, 26(2):262–265.

Carr, J., Beck, T. W., Ye, X., and Wages, N. P. (2016). Intensity-dependent EMG response for the biceps brachii during sustained maximal and submaximal isometric contractions. *European Journal of Applied Physiology*, 116(9):1747–1755.

Cè, E., Longo, S., Limonta, E., Coratella, G., Rampichini, S., and Esposito, F. (2019). Peripheral fatigue: new mechanistic insights from recent technologies. *European journal of applied physiology*, pages 1–23.

Chaudhuri, A. and Behan, P. O. (2004). Fatigue in neurological disorders. *The lancet*, 363(9413):978–988.

Cifrek, M., Medved, V., Tonković, S., and Ostojić, S. (2009). Surface EMG based muscle fatigue evaluation in biomechanics. *Clinical Biomechanics*, 24(4):327–340.

Claudon, L. (1998). Evaluation of Grip Force Using Electromyograms in Isometric Isotonic Conditions. *Internation Journal of Occupational safety and ergonomics*, 4(2):169–184.

Côté, J., Raymond, D., Mathieu, P. A., Feldman, A. G., and Levin, M. F. (2005). Differences in multi-joint kinematic patterns of repetitive hammering in healthy, fatigued and shoulder-injured individuals. *Clinical Biomechanics*, 20(6):581–590.

Croce, R. and Miller, J. (2003). The effect of movement velocity and movement pattern on the reciprocal co-activation of the hamstrings. *Electromyography and clinical neurophysiology*, 43(8):451–8.

Daligadu, J., Haavik, H., Yielder, P. C., Baarbe, J., and Murphy, B. (2013). Alterations in cortical and cerebellar motor processing in subclinical neck pain patients following spinal manipulation. *Journal of manipulative and physiological therapeutics*, 36(8):527–537.

Damiano, D., Martellotta, T. L., Sullivan, D. J., Granata, K. P., and Abel, M. F. (2000). Muscle force production and functional performance in spastic cerebral palsy: Relationship of cocontraction. *Archives of Physical Medicine and Rehabilitation*, 81(7):895–900.

De Luca, C. J. (1997). The use of surface electromyography in biomechanics. In *Journal of Applied Biomechanics*, volume 13, pages 135–163. Human Kinetics Publishers Inc.

De Santis, D., Zenzeri, J., Casadio, M., Masia, L., Riva, A., Morasso, P., and Squeri, V. (2015). Robot-Assisted Training of the Kinesthetic Sense: Enhancing Proprioception after Stroke. *Frontiers in Human Neuroscience*, 8.

Del Valle, A. and Thomas, C. K. (2005). Firing rates of motor units during strong dynamic contractions. *Muscle & Nerve*, 32(3):316–325.

Dimitrov, G., Arabadzhiev, T., and Mileva, K. (2006). Muscle fatigue during dynamic contractions assessed by new spectral indices. *Medicine and science*.

Dimitrova, N., Arabadzhiev, T., Hogrel, J.-Y., and Dimitrov, G. (2009). Fatigue analysis of interference emg signals obtained from biceps brachii during isometric voluntary contraction at various force levels. *Journal of Electromyography and Kinesiology*, 19(2):252–258.

Duchateau, J. and Baudry, S. (2013). Insights into the neural control of eccentric contractions. *Journal of Applied Physiology*, 116(11):1418–1425.

Dukelow, S., Herter, T., Moore, K., Demers, M., Glasgow, J., Bagg, S., Norman, K., and Scott, S. (2010). Quantitative Assessment of Limb Position Sense Following Stroke. *Neurorehabilitation and Neural Repair*, 24(2):178–187.

Duque, J., Masset, D., and Malchaire, J. (1995). Evaluation of handgrip force from EMG measurements. *Applied Ergonomics*, 26(1):61–66.

Eberstein, A. and Beattie, B. (1985). Simultaneous measurement of muscle conduction velocity and emg power spectrum changes during fatigue. *Muscle & Nerve*, 8(9):768–773.

Eccles, R. and Lundberg, A. (1958). Integrative pattern of Ia synaptic actions on motoneurones of hip and knee muscles. *The Journal of Physiology*, 144(2):271–298.

Edman, K., Elzinga, G., and Noble, M. I. (1978). Enhancement of mechanical performance by stretch during tetanic contractions of vertebrate skeletal muscle fibres. *The Journal of Physiology*, 281(1):139–155.

Edmondston, S., Wallumrød, M., MacLéid, F., Kvamme, L. S., Joebges, S., and Brabham, G. C. (2008). Reliability of isometric muscle endurance tests in subjects with postural neck pain. *Journal of manipulative and physiological therapeutics*, 31(5):348–354.

Enoka, R. (1996). Eccentric contractions require unique activation strategies by the nervous system. *Journal of applied physiology*, 81(6):2339–2346.

Enoka, R. (2008). *Neuromechanics of human movement*. Human kinetics.

Enoka, R. and Duchateau, J. (2008). Muscle fatigue: what, why and how it influences muscle function. *The Journal of physiology*, 586(1):11–23.

Erwin, J. and Varacallo, M. (2018). *Anatomy, Shoulder and Upper Limb, Wrist Joint*. StatPearls Publishing.

Evans, R., Scoville, C., Ito, M., and Mello, R. P. (2003). Upper Body Fatiguing Exercise and Shooting Performance. *Military Medicine*, 168(6):451–456.

Feipel, V., Salvia, P., Klein, H., and Rooze, M. (2005). Head repositioning accuracy in patients with whiplash-associated disorders. *Computer Methods in Biomechanics and Biomedical Engineering*, 8(sup1):97–98.

Finneran, A. and O'Sullivan, L. (2013). Effects of grip type and wrist posture on forearm EMG activity, endurance time and movement accuracy. *International Journal of Industrial Ergonomics*, 43(1):91–99.

Fitts, R. (2008). The cross-bridge cycle and skeletal muscle fatigue. *Journal of applied physiology*, 104(2):551–558.

Forestier, N. and Nougier, V. (1998). The effects of muscular fatigue on the coordination of a multijoint movement in human. *Neuroscience Letters*, 252(3):187–190.

Forestier, N., Teasdale, N., and Nougier, V. (2002). Alteration of the position sense at the ankle induced by muscular fatigue in humans. *Medicine and science in sports and exercise*, 34(1):117.

Forman, D., Forman, G., Robathan, J., and Holmes, M. (2019). The influence of simultaneous handgrip and wrist force on forearm muscle activity. *Journal of Electromyography and Kinesiology*, 45:53–60.

Frontera, W. and Ochala, J. (2015). Skeletal Muscle: A Brief Review of Structure and Function. *Behavior Genetics*, 45(2):183–195.

Gandevia, S. (1998). Neural control in human muscle fatigue: Changes in muscle afferents, moto neurones and moto cortical drive. In *Acta Physiologica Scandinavica*, volume 162, pages 275–283.

Gandevia, S. C. (2001). Spinal and supraspinal factors in human muscle fatigue. *Physiological Reviews*, 81(4):1725–1789.

Gates, D. and Dingwell, J. (2008). The effects of neuromuscular fatigue on task performance during repetitive goal-directed movements. *Experimental Brain Research*, 187(4):573–585.

Gear, W. G. (2011). Effect of different levels of localized muscle fatigue on knee position sense. *journal of sports science medicine*, 10.4: 725.

Gerdle, B., Henriksson-Larsén, K., Lorenzton, R., and Wretling, M.-L. (1991). Dependence of the mean power frequency of the electromyogram on muscle force and fibre type. *Acta Physiologica Scandinavica*, 142(4):457–465.

Givoni, N., Pham, T., Allen, T., and Proske, U. (2007). The effect of quadriceps muscle fatigue on position matching at the knee. *The Journal of Physiology*, 584(1):111–119.

Goble, D., Coxon, J., Wenderoth, N., Van Impe, A., and Swinnen, S. (2009). Proprioceptive sensibility in the elderly: Degeneration, functional consequences and plastic-adaptive processes. *Neuroscience & Biobehavioral Reviews*, 33(3):271–278.

Gonzalez, R., Buchananf, T., and Delp, S. (1997). How muscle architecture and moment arms affect wrist flexion-extension moment. *J. Biomechanics*, 30(7):705–712.

González-Izal, M., Malanda, A., Navarro-Amézqueta, I., Gorostiaga, E., Mallor, F., Ibañez, J., and Izquierdo, M. (2010). EMG spectral indices and muscle power fatigue during dynamic contractions. *Journal of Electromyography and Kinesiology*, 20(2):233–240.

Gowitzke, B. and Milner, M. (1988). *Scientific bases of human movement*. Williams & Wilkins.

Gregory, C. and Bickel, C. S. (2005). Recruitment Patterns in Human Skeletal Muscle During Electrical Stimulation. *Physical Therapy*, 85(4):358–364.

Grigg, P. and Hoffman, A. (1996). Stretch-sensitive afferent neurons in cat knee joint capsule: Sensitivity to axial and compression stresses and strains. *Journal of Neurophysiology*, 75(5):1871–1877.

Gupta, A., O'Malley, M., Patoglu, V., and Burgar, C. (2008). Design, Control and Performance of RiceWrist: A Force Feedback Wrist Exoskeleton for Rehabilitation and Training. *The International Journal of Robotics Research*, 27(2):233–251.

Hagert, E. (2010). Proprioception of the Wrist Joint: A Review of Current Concepts and Possible Implications on the Rehabilitation of the Wrist. *Journal of Hand Therapy*, 23(1):2–17.

Hagert, E., Forsgren, S., and Ljung, B.-O. (2005). Differences in the presence of mechanoreceptors and nerve structures between wrist ligaments may imply differential roles in wrist stabilization. *Journal of Orthopaedic Research*, 23(4):757–763.

Hagert, E., Persson, J., Werner, M., and Ljung, B. O. (2009). Evidence of Wrist Proprioceptive Reflexes Elicited After Stimulation of the Scapholunate Interosseous Ligament. *Journal of Hand Surgery*, 34(4):642–651.

Hägg, G. and Milerad, E. (1997). Forearm extensor and flexor muscle exertion during simulated gripping work—an electromyographic study. *Clinical biomechanics*, 12(1):39–43.

Hägg, G. M., Öster, J., and Byström, S. (1997). Forearm muscular load and wrist angle among automobile assembly line workers in relation to symptoms. *Applied Ergonomics*, 28(1):41–47.

Halin, R., Germain, P., Bercier, S., Kapitaniak, B., and Buttelli, O. (2003). Neuromuscular response of young boys versus men during sustained maximal contraction. *Medicine and science in sports and exercise*, 35(6):1042–8.

Hammarskjöld, E. and Harms-Ringdahl, K. (1992). Effect of arm-shoulder fatigue on carpenters at work. *European Journal of Applied Physiology and Occupational Physiology*, 64(5):402–409.

Heikkilä, H. and Wenngren, B.-I. (1998). Cervicocephalic kinesthetic sensibility, active range of cervical motion, and oculomotor function in patients with whiplash injury. *Archives of physical medicine and rehabilitation*, 79(9):1089–1094.

Henneman, E. and Desmedt, J. (1981). Motor unit types, recruitment and plasticity in health and disease. *Progress in clinical neurophysiology*, 9.

Hepple, R. and Rice, C. L. (2016). Innervation and neuromuscular control in ageing skeletal muscle. *The Journal of Physiology*, 594(8):1965–1978.

Hermens, H., Freriks, B., Merletti, R., Stegeman, D., Blok, J., Rau, G., Disselhorst-Klug, C., and Hägg, G. (1999). *SENIAM - Deliverable 8 - European Recommendations for Surface ElectroMyoGraphy Chapter*.

Hertel, J. (2008). Sensorimotor Deficits with Ankle Sprains and Chronic Ankle Instability. *Clinics in Sports Medicine*, 27(3):353–370.

Herzog, W. (2013). Mechanisms of enhanced force production in lengthening (eccentric) muscle contractions. *Journal of Applied Physiology*, 116(11):1407–1417.

Hoffman, M., Gilson, P. M., Westenburg, T. M., and Spencer, W. A. (1992). Biathlon shooting performance after exercise of different intensities. *International Journal of Sports Medicine*, 13(3):270–273.

Holmes, M. W., Tat, J., and Keir, P. J. (2015). Neuromechanical control of the forearm muscles during gripping with sudden flexion and extension wrist perturbations. *Computer Methods in Biomechanics and Biomedical Engineering*, 18(16):1826–1834.

Holzbaur, K., Murray, W. M., and Delp, S. L. (2005). A Model of the Upper Extremity for Simulating Musculoskeletal Surgery and Analyzing Neuromuscular Control. *Annals of Biomedical Engineering*, 33(6):829–840.

Hu, X., Rymer, W. Z., and Suresh, N. L. (2013). Motor unit pool organization examined via spike-triggered averaging of the surface electromyogram. *Journal of Neurophysiology*, 110(5):1205–1220.

Huffenus, A., Amarantini, D., and Forestier, N. (2006). Effects of distal and proximal arm muscles fatigue on multi-joint movement organization. *Experimental Brain Research*, 170(4):438–447.

Hug, F., Nordez, A., and Guével, A. (2009). Can the electromyographic fatigue threshold be determined from superficial elbow flexor muscles during an isometric single-joint task? *European Journal of Applied Physiology*, 107(2):193–201.

Hughes, C., Tommasino, P., Budhota, A., and Campolo, D. (2015). Upper extremity proprioception in healthy aging and stroke populations, and the effects of therapist- and robot-based rehabilitation therapies on proprioceptive function. *Frontiers in human neuroscience*, 9:120.

Huxley, A. (2000). Mechanics and models of the myosin motor. In *Philosophical Transactions of the Royal Society B: Biological Sciences*, volume 355, pages 433–440. Royal Society.

Huysmans, M., Hoozemans, M., van der Beek, A., de Looze, M., and van Dieën, J. (2006). *Fatigue effects on tracking performance*. Oxford: Elsevier.

Iandolo, R., Marini, F., Semprini, M., Laffranchi, M., Mugnosso, M., Cherif, A., De Michieli, L., Chiappalone, M., and Zenzeri, J. (2019). Perspectives and challenges in robotic neurorehabilitation. *Applied Sciences (Switzerland)*, 9(15).

Jaric, S., Blesic, S., Milanovic, S., Radovanovic, S., Ljubisavljevic, M., and Anastasijevic, R. (1999). Changes in movement final position associated with agonist and antagonist muscle fatigue. *European journal of applied physiology and occupational physiology*, 80(5):467–471.

Jeannerod and Marc (1988). *The neural and behavioural organization of goal-directed movements.* Clarendon Press/Oxford University Press.

Jebsen, R., Taylor, N., Trieschmann, R. B., Trotter, M. J., and Howard, L. A. (1969). An objective and standardized test of hand function. *Archives of physical medicine and rehabilitation*, 50(6):311–9.

Jennekens, F., Tomlinson, B., and Walton, J. N. (1972). The extensor digitorum brevis: histological and histochemical aspects. *Journal of neurology, neurosurgery, and psychiatry*, 35(1):124–32.

Jonsson, B. (1978). Kinesiology: with special reference to electromyographic kinesiology. *Electroencephalography and Clinical neurophysiology*, (34):417-428.

Ju, Y.-Y., Wang, C.-W., and Cheng, H.-Y. K. (2010). Effects of active fatiguing movement versus passive repetitive movement on knee proprioception. *Clinical Biomechanics*, 25(7):708–712.

Kahl, L. and Hofmann, U. G. (2016). Comparison of algorithms to quantify muscle fatigue in upper limb muscles based on sEMG signals. *Medical Engineering & Physics*, 38(11):1260–1269.

Karagiannopoulos, C. and Michlovitz, S. (2016). Rehabilitation strategies for wrist sensorimotor control impairment: From theory to practice. *Journal of Hand Therapy*, 29(2):154–165.

Karagiannopoulos, C., Watson, J., Kahan, S., and Lawler, D. (2019). The effect of muscle fatigue on wrist joint position sense in healthy adults. *Journal of Hand Therapy*.

Kattel, B., Fredericks, T. K., Fernandez, J. E., and Lee, D. C. (1996). The effect of upper-extremity posture on maximum grip strength. In *International Journal of Industrial Ergonomics*, volume 18, pages 423–429. Elsevier Science B.V.

Katz, B. (1939). The relation between force and speed in muscular contraction. *The Journal of Physiology*, 96(1):45–64.

Kauer, J. M. (1980). Functional anatomy of the wrist. *Clinical Orthopaedics and Related Research*, NO 149:9–20.

Kazutomo, M., Yasuyuki, I., Eiichi, T., Yoshihisa, O., Hironori, O., and Satoshi, T. (2004). The effect of local and general fatigue on knee proprioception. *Arthroscopy: The Journal of Arthroscopic & Related Surgery*, 20(4):414–418.

Kellis, E. and Baltzopoulos, V. (1998). Muscle activation differences between eccentric and concentric isokinetic exercise. *Medicine and science in sports and exercise*, 30(11):1616–23.

Kent-Braun, J., Callahan, D. M., Fay, J. L., Foulis, S. A., and Buonaccorsi, J. P. (2014). Muscle weakness, fatigue, and torque variability: Effects of age and mobility status. *Muscle & Nerve*, 49(2):209–217.

Kerkhof, F. D., van Leeuwen, T., and Vereecke, E. E. (2018). The digital human forearm and hand. *Journal of Anatomy*, 233(5):557–566.

Kijima, Y. and Viegas, S. F. (2009). Wrist Anatomy and Biomechanics. *Journal of Hand Surgery*, 34(8):1555–1563.

Knaflitz, M., Merletti, R., and De Luca, C. J. (1990). Inference of motor unit recruitment order in voluntary and electrically elicited contractions. *Journal of applied physiology (Bethesda, Md. : 1985)*, 68(4):1657–67.

Knox, J. and Hodges, P. W. (2005). Changes in head and neck position affect elbow joint position sense. *Experimental Brain Research*, 165(1):107–113.

Krnjević, K. and Miledi, R. (1959). Presynaptic failure of neuromuscular propagation in rats. *The Journal of Physiology*, 149(1):1–22.

Krupp, L., LaRocca, N. G., Muir-Nash, J., and Steinberg, A. D. (1989). The fatigue severity scale. Application to patients with multiple sclerosis and systemic lupus erythematosus. *Archives of neurology*, 46(10):1121–3.

Kupa, E. J., Roy, S. H., Kandarian, S. C., and De Luca, C. J. (1995). Effects of muscle fiber type and size on EMG median frequency and conduction velocity. *Journal of Applied Physiology*, 79(1):23–32.

Kwatny, E., Thomas, D. H., and Kwatny, H. G. (1970). An Application of Signal Processing Techniques to the Study of Myoelectric Signals. *IEEE Transaction on Biomedical Engineering*, (4).

La Delfa, N. J., Langstaff, N. M., Hodder, J. N., and Potvin, J. R. (2015). The interacting effects of forearm rotation and exertion direction on male and female wrist strength. *International Journal of Industrial Ergonomics*, 45:124–128.

Lagier-Tessonnier, F., Balzamo, E., and Jammes, Y. (1993). Comparative effects of ischemia and acute hypoxemia on muscle afferents from tibialis anterior in cats. *Muscle & Nerve*, 16(2):135–141.

Lattanzio, P. J., Petrella, R. J., Sproule, J. R., and Fowler, P. J. (1997). Effects of fatigue on knee proprioception. *Clinical journal of sport medicine : official journal of the Canadian Academy of Sport Medicine*, 7(1):22–7.

Lee, H.-M., Liau, J.-J., Cheng, C.-K., Tan, C.-M., and Shih, J.-T. (2003). Evaluation of shoulder proprioception following muscle fatigue. *Clinical biomechanics*, 18:843–847.

Lee, H.-Y., Wang, J.-D., Yao, G., and Wang, S.-F. (2008). Association between cervico-cephalic kinesthetic sensibility and frequency of subclinical neck pain. *Manual Therapy*, 13:419–425.

Letafakatar, K., Alizadeh, M. H., and Kordi, M. (2009). The effect of exhausting exercise induced muscular fatigue on functional stability.

Lewis, O. J., Hamshere, R. J., and Bucknill, T. M. (1970). The anatomy of the wrist joint. *Journal of anatomy*, 106(Pt 3):539–52.

Lexell, J. and Downham, D. (1992). What is the effect of ageing on type 2 muscle fibres? *Journal of the neurological sciences*, 107(2):250–251.

Leyk, D., Gorges, W., Ridder, D., Wunderlich, M., Rüther, T., Sievert, A., and Essfeld, D. (2007). Hand-grip strength of young men, women and highly trained female athletes. *European journal of applied physiology*, 99(4):415–421.

Lindner, O. (2008). Predictive and Discriminative Value of Shoulder Propioception Tests for Patients with Whiplash Associated Disorders. *manuelletherapie*, 12(03):137–138.

Linscheid, R. L. and Dobyns, J. H. (2002). Dynamic carpal stability. *Keio Journal of Medicine*, 51(3):140–147.

Liu, J.-X., Eriksson, P.-O., Thornell, L.-E., and Pedrosa-Domellöf, F. (2005). Fiber Content and Myosin Heavy Chain Composition of Muscle Spindles in Aged Human Biceps Brachii. *Journal of Histochemistry & Cytochemistry*, 53(4):445–454.

Lou, J.-S., Weiss, M. D., and Carter, G. T. (2010). Assessment and Management of Fatigue in Neuromuscular Disease. *American Journal of Hospice and Palliative Medicine*, 27(2):145–157.

Luc Darques, J., Decherchi, P., and Jammes, Y. (1998). Mechanisms of fatigue-induced activation of group IV muscle afferents: The roles played by lactic acid and inflammatory mediators. *Neuroscience Letters*, 257(2):109–112.

Lucidi, C. A. and Lehman, S. L. (1992). Adaptation to fatigue of long duration in human wrist movements. *Journal of applied physiology (Bethesda, Md. : 1985)*, 73(6):2596–603.

Lung, B. E. and Burns, B. (2019). Anatomy, shoulder and upper limb, hand flexor digitorum profundus muscle. In *StatPearls [Internet]*. StatPearls Publishing.

Lung, B. E. and Siwiec, R. M. (2018). Anatomy, shoulder and upper limb, forearm flexor carpi ulnaris muscle. In *StatPearls [Internet]*. StatPearls Publishing.

Luttmann, A., Jäger, M., and Laurig, W. (2000). Electromyographical indication of muscular fatigue in occupational field studies. *International Journal of Industrial Ergonomics*, 25(6):645–660.

Macefield, V. G. (2005). Physiological characteristics of low-threshold mechanoreceptors in joints, muscle and skin in human subjects. *Clinical and Experimental Pharmacology and Physiology*, 32(1-2):135–144.

Maciejasz, P., Eschweiler, J., Gerlach-Hahn, K., Jansen-Troy, A., and Leonhardt, S. (2014). A survey on robotic devices for upper limb rehabilitation. *Journal of neuroengineering and rehabilitation*, 11(1):3.

Marbini, A., Ferrari, A., Cioni, G., Bellanova, M. F., Fusco, C., and Gemignani, F. (2002). Immunohistochemical study of muscle biopsy in children with cerebral palsy. *Brain & development*, 24(2):63–6.

Marini, F., Contu, S., Morasso, P., Masia, L., and Zenzeri, J. (2017a). Codification mechanisms of wrist position sense. In *2017 International Conference on Rehabilitation Robotics (ICORR)*, pages 44–49. IEEE.

Marini, F., Ferrantino, M., and Zenzeri, J. (2018). Proprioceptive identification of joint position versus kinaesthetic movement reproduction. *Human Movement Science*, 62:1–13.

Marini, F., Squeri, V., Morasso, P., Campus, C., Konczak, J., and Masia, L. (2017b). Robot-aided developmental assessment of wrist proprioception in children. *Journal of Neuro-Engineering and Rehabilitation*, 14(1):3.

Marini, F., Squeri, V., Morasso, P., Konczak, J., and Masia, L. (2016a). Robot-Aided Mapping of Wrist Proprioceptive Acuity across a 3D Workspace. *PLOS ONE*, 11(8):e0161155.

Marini, F., Squeri, V., Morasso, P., and Masia, L. (2016b). Wrist Proprioception: Amplitude or Position Coding? *Frontiers in Neurorobotics*, 10:13.

Masia, L., Casadio, M., Giannoni, P., Sandini, G., and Morasso, P. (2009). Performance adaptive training control strategy for recovering wrist movements in stroke patients: a preliminary, feasibility study. *Journal of NeuroEngineering and Rehabilitation*, 6(1):44.

Mayhew, A., Mazzone, E. S., Eagle, M., Duong, T., Ash, M., Decostre, V., Vandenhauwe, M., Klingels, K., Florence, J., Main, M., Bianco, F., Henrikson, E., Servais, L., Campion, G., Vroom, E., Ricotti, V., Goemans, N., Mcdonald, C., and Mercuri, E. (2013). Development of the Performance of the Upper Limb module for Duchenne muscular dystrophy. *Developmental Medicine & Child Neurology*, 55(11):1038–1045.

Mazzone, E., Messina, S., Vasco, G., Main, M., Eagle, M., D'Amico, A., Doglio, L., Politano, L., Cavallaro, F., Frosini, S., et al. (2009). Reliability of the north star ambulatory assessment in a multicentric setting. *Neuromuscular Disorders*, 19(7):458–461.

Mazzone, E., Vasco, G., Palermo, C., Bianco, F., Galluccio, C., Ricotti, V., Castronovo, A. D., Mauro, M., Di Pane, M., Mayhew, A., and Mercuri, E. (2012). A critical review of functional assessment tools for upper limbs in Duchenne muscular dystrophy. *Developmental Medicine & Child Neurology*, 54(10):879–885.

McDonald, C. M., Henricson, E. K., Han, J. J., Abresch, R. T., Nicorici, A., Elfring, G. L., Atkinson, L., Reha, A., Hirawat, S., and Miller, L. L. (2010). The 6-minute walk test as a new outcome measure in Duchenne muscular dystrophy. *Muscle & Nerve*, 41(4):500–510.

McNulty, P. A., Lin, G., and Doust, C. G. (2014). Single motor unit firing rate after stroke is higher on the less-affected side during stable low-level voluntary contractions. *Frontiers in Human Neuroscience*, 8:518.

Merletti, R., Farina, D., And, M. G. J. o. E., and undefined 2003 (2003). The linear electrode array: a useful tool with many applications. *Elsevier*.

Merletti, R., Knaflitz, M., and De Luca, C. J. (1990). Myoelectric manifestations of fatigue in voluntary and electrically elicited contractions. *Journal of Applied Physiology*, 69(5).

Merletti, R. and Parker, P., editors (2004). *Electromyography*. John Wiley & Sons, Inc., Hoboken, NJ, USA.

Merletti, R. and Roy, S. (1996). Myoelectric and mechanical manifestations of muscle fatigue in voluntary contractions. *Journal of Orthopaedic and Sports Physical Therapy*, 24(6):342–353.

Meyer, T., Peters, J., Zander, T. O., Schölkopf, B., and Grosse-Wentrup, M. (2014). Predicting motor learning performance from Electroencephalographic data. *Journal of NeuroEngineering and Rehabilitation*.

Mirakhorlo, M., Visser, J. M. A., Goislard de Monsabert, B. A. A. X., van der Helm, F. C. T., Maas, H., and Veeger, H. E. J. (2016). Anatomical parameters for musculoskeletal modeling of the hand and wrist. *International Biomechanics*, 3(1):40–49.

Missenard, O., Mottet, D., and Perrey, S. (2008). Muscular fatigue increases signal-dependent noise during isometric force production. *Neuroscience Letters*, 437(2):154–157.

Mitchell, B. and Whited, L. (2019). *Anatomy, Shoulder and Upper Limb, Forearm Muscles*.

Mogk, J. and Keir, P. (2003). The effects of posture on forearm muscle loading during gripping. *Ergonomics*, 46(9):956–975.

Monjo, F., Terrier, R., and Forestier, N. (2015). Muscle fatigue as an investigative tool in motor control: A review with new insights on internal models and posture–movement coordination. *Human Movement Science*, 44:225–233.

Moore, J., Small, C., Bryant, J., Ellis, R. E., Pichora, D. R., and Hollister, A. M. (1993). A kinematic technique for describing wrist joint motion: Analysis of configuration space plots. *Proceedings of the Institution of Mechanical Engineers, Part H: Journal of Engineering in Medicine*, 207(4):211–218.

Morasso, P. (1981). Spatial control of arm movements. *Experimental Brain Research*, 42:223–227.

Mortimer, J., Magnusson, R., and Petersén, I. (1970). Conduction velocity in ischemic muscle: effect on EMG frequency spectrum. *The American journal of physiology*, 219(5):1324–1329.

Mottram, C., Heckman, C., Powers, R., Rymer, W., and Suresh, N. (2014). Disturbances of motor unit rate modulation are prevalent in muscles of spastic-paretic stroke survivors. *Journal of Neurophysiology*, 111(10):2017–2028.

Mugnosso, M., Marini, F., Gillardo, M., Morasso, P., and Zenzeri, J. (2017). A novel method for muscle fatigue assessment during robot-based tracking tasks. In *2017 International Conference on Rehabilitation Robotics (ICORR)*, pages 84–89. IEEE.

Myers, J., Guskiewicz, K. M., Schneider, R. A., and Prentice, W. E. (1999). Proprioception and neuromuscular control of the shoulder after muscle fatigue. *Journal of athletic training*, 34(4):362.

Naughton, G., Carlson, J., and Fairweather, I. (1992). Determining the Variability of Performance on Wingate Anaerobic Tests in Children Aged 6-12 Years. *International Journal of Sports Medicine*, 13(07):512–517.

Öberg, T., Sandsjö, L., and Kadefors, R. (1990). Electromyogram mean power frequency in non-fatigued trapezius muscle. *European journal of applied physiology*.

Octavia, J. R., Feys, P., and Coninx, K. (2015). Development of Activity-Related Muscle Fatigue during Robot-Mediated Upper Limb Rehabilitation Training in Persons with Multiple Sclerosis: A Pilot Trial. *Multiple sclerosis international*, 2015:650431.

Oda, S. and Kida, N. (2001). Neuromuscular fatigue during maximal concurrent hand grip and elbow flexion or extension. *Journal of Electromyography and Kinesiology*, 11(4):281–289.

Oldfield, R. (1971). The assessment and analysis of handedness: The Edinburgh inventory. *Neuropsychologia*, 9(1):97–113.

OpenStaxCollege (2013). Muscle Fiber Contraction and Relaxation. https://openstax.org/books/anatomy-and-physiology/pages/10-3-muscle-fiber-contraction-and-relaxation.

Pasquet, B., Carpentier, A., and Duchateau, J. (2006). Specific modulation of motor unit discharge for a similar change in fascicle length during shortening and lengthening contractions in humans. *Journal of Physiology*, 577(2):753–765.

Patton, J. and Mussa-Ivaldi, F. (2004). Robot-assisted adaptive training: custom force fields for teaching movement patterns. *IEEE Transactions on Biomedical*.

Pedersen, J., Ljubisavljevic, M., Bergenheim, M., and Johansson, H. (1998). Alterations in information transmission in ensembles of primary muscle spindle afferents after muscle fatigue in heteronymous muscle. *Neuroscience*, 84(3):953–959.

Phillips, B. A., Lo, S. K., and Mastaglia, F. L. (2000). Muscle force measured using "break" testing with a hand-held myometer in normal subjects aged 20 to 69 years. *Archives of Physical Medicine and Rehabilitation*, 81(5):653–661.

Popa, L. S., Hewitt, A. L., and Ebner, T. J. (2013). Purkinje cell simple spike discharge encodes error signals consistent with a forward internal model. *The Cerebellum*, 12(3):331–333.

Poyil, A. T., Amirabdollahian, F., and Steuber, V. (2017). Study of gross muscle fatigue during human-robot interactions. In *The Tenth International Conference on Advances in Computer-Human Interactions*.

Proske, U. and Morgan, D. L. (2001). Muscle damage from eccentric exercise: mechanism, mechanical signs, adaptation and clinical applications. *The Journal of Physiology*, 537(2):333–345.

Proske, U., Wise, A. K., and Gregory, J. E. (2000). The role of muscle receptors in the detection of movements. *Progress in neurobiology*, 60(1):85–96.

Ratel, S., Duché, P., and Williams, C. A. (2006). Muscle Fatigue during High-Intensity Exercise in Children. *Sports Medicine*, 36(12):1031–1065.

Refshaug, K. M. (2002). Proprioception and joint pathology. *Advances in experimental medicine and biology*, 508:95–101.

Revel, M., Andre-Deshays, C., and Minguet, M. (1991). Cervicocephalic kinesthetic sensibility in patients with cervical pain. *Archives of physical medicine and rehabilitation*, 72(5):288–291.

Ribeiro, F. and Oliveira, J. (2010). Effect of physical exercise and age on knee joint position sense. *Archives of gerontology and geriatrics*, 51(1):64–67.

Riemann, B. L. and Lephart, S. M. (2002). The sensorimotor system, part i: the physiologic basis of functional joint stability. *Journal of athletic training*, 37(1):71.

Romero-Ángeles, B., Hernández-Campos, D., Urriolagoitia-Sosa, G., Torres-San Miguel, C. R., Rodríguez-Martínez, R., Martínez-Reyes, J., Hernández-Vázquez, R. A., and Urriolagoitia-Calderón, G. (2019). Design and manufacture of a forearm prosthesis by plastic 3D impression for a patient with transradial amputation applied for strum of a guitar. In *Advanced Structured Materials*, volume 92, pages 97–121. Springer Verlag.

Romitti, P., Puzhankara, S., Mathews, K., Zamba, G., Cunniff, C., Andrews, J., Matthews, D., James, K., Miller, L., Druschel, C., Fox, D., Pandya, S., Ciafaloni, E., Adams, M., Mandel, D., Ouyang, L., Constantin, C., and Costa, P. (2009). Prevalence of Duchenne/Becker muscular dystrophy among males aged 5-24 years - four states, 2007. *Morbidity and Mortality Weekly Report*, 58(40):1119–1122.

Rossat, A., Fantino, B., Nitenberg, C., Annweiler, C., Poujol, L., Herrmann, F. R., and Beauchet, O. (2010). Risk factors for falling in community-dwelling older adults: Which of them are associated with the recurrence of falls? *The journal of nutrition, health & aging*, 14(9):787–791.

Rothwell, J. (1997). Techniques and mechanisms of action of transcranial stimulation of the human motor cortex. *Journal of Neuroscience Methods*, 74(2):113–122.

Rotto, D. and Kaufman, M. (1988). Effect of metabolic products of muscular contraction on discharge of group III and IV afferents. *Journal of Applied Physiology*, 64(6):2306–2313.

Sadler, C. M. and Cressman, E. K. (2019). Central fatigue mechanisms are responsible for decreases in hand proprioceptive acuity following shoulder muscle fatigue. *Human Movement Science*, 66:220–230.

Salmond, L. H., Davidson, A. D., and Charles, S. K. (2017). Proximal-distal differences in movement smoothness reflect differences in biomechanics. *Journal of neurophysiology*, 117(3):1239–1257.

Schmidt, R. A. and Lee, T. D. (2005). *Motor control and learning : a behavioral emphasis*. Human Kinetics.

Selen, L. P. J., Beek, P. J., and van Dieën, J. H. (2007). Fatigue-induced changes of impedance and performance in target tracking. *Experimental Brain Research*, 181(1):99–108.

Shaffer, S. and Harrison, A. L. (2007). Aging of the Somatosensory System: A Translational Perspective. *Physical Therapy*, 87(2):193–207.

Sharpe, M. and Miles, T. (1993). Position sense at the elbow after fatiguing contractions. *Experimental Brain Research*, 94(1):179–182.

Sherrington, C. S. (1907). On the proprio-ceptive system, especially in its reflex aspect. *Brain*, 29(4):467–482.

Shimizu-Motohashi, Y., Miyatake, S., Komaki, H., Takeda, S., and Aoki, Y. (2016). Recent advances in innovative therapeutic approaches for Duchenne muscular dystrophy: from discovery to clinical trials. *American journal of translational research*, 8(6):2471–89.

Sieck, G. and Prakash, Y. (1995). Fatigue at the neuromuscular junction. In *Fatigue*, pages 83–100. Springer.

Silverthorn, D. U. (2015). *Human physiology: an integrated approach*. Pearson Higher Ed.

Skinner, H. B., Wyatt, M. P., Hodgdon, J. A., Conard, D. W., and Barrack, R. L. (1986). Effect of fatigue on joint position sense of the knee. *Journal of Orthopaedic Research*, 4(1):112–118.

Smets, E., Garssen, B., Bonke, B. d., and De Haes, J. (1995). The multidimensional fatigue inventory (mfi) psychometric qualities of an instrument to assess fatigue. *Journal of psychosomatic research*, 39(3):315–325.

Snijders, C. J., Volkers, A. C., Mechelse, K., and Vleeming, A. (1987). Provocation of epicondylalgia lateralis (tennis elbow) by power grip or pinching. *Medicine and Science in Sports and Exercise*, 19(5):518–523.

Spooren, A. I., Timmermans, A. A., and Seelen, H. A. (2012). Motor training programs of arm and hand in patients with MS according to different levels of the ICF: a systematic review. *BMC Neurology*, 12(1):49.

Squeri, V., Masia, L., Casadio, M., Morasso, P., and Vergaro, E. (2010). Force-field compensation in a manual tracking task. *PLoS One*, 5(6).

Sterling, M., Jull, G., Vicenzino, B., Kenardy, J., and Darnell, R. (2003). Development of motor system dysfunction following whiplash injury. *PAIN®*, 103(1-2):65–73.

Sterner, R. L., Pincivero, D. M., and Lephart, S. M. (1998). The effects of muscular fatigue on shoulder proprioception. *Clinical journal of sport medicine : official journal of the Canadian Academy of Sport Medicine*, 8(2):96–101.

Swanik, C., Lephart, S. M., Giannantonio, F. P., and Fu, F. H. (1997). Reestablishing proprioception and neuromuscular control in the ACL-injured athlete. *Journal of Sport Rehabilitation*, 6(2):182–206.

Swash, M. and Fox, K. P. (1972). The effect of age on human skeletal muscle studies of the morphology and innervation of muscle spindles. *Journal of the Neurological Sciences*, 16(4):417–432.

Szucs, K., Navalgund, A., and Borstad, J. D. (2009). Scapular muscle activation and coactivation following a fatigue task. *Medical & Biological Engineering & Computing*, 47(5):487–495.

Tax, A. M., van der Gon, J. D., Gielen, C. A. M., and van den Tempel, C. M. (1989). Differences in the activation of m. biceps brachii in the control of slow isotonic movements and isometric contractions. *Experimental Brain Research*, 76(1):55–63.

Taylor, J., Butler, J., Allen, G., and Gandevia, S. (1996). Changes in motor cortical excitability during human muscle fatigue. *The Journal of Physiology*, 490(2):519–528.

Taylor, J. and Gandevia, S. C. (2001). Transcranial magnetic stimulation and human muscle fatigue. *Muscle & Nerve: Official Journal of the American Association of Electrodiagnostic Medicine*, 24(1):18–29.

Taylor, J. L., Amann, M., Duchateau, J., Meeusen, R., and Rice, C. L. (2016). Neural Contributions to Muscle Fatigue: From the Brain to the Muscle and Back Again. *Medicine and science in sports and exercise*, 48(11):2294–2306.

Thomas, G. D. (2013). Functional muscle ischemia in duchenne and becker muscular dystrophy. *Frontiers in physiology*, 4:381.

Tooze, J., Schoeller, D., Subar, A. F., Kipnis, V., Schatzkin, A., and Troiano, R. P. (2007). Total daily energy expenditure among middle-aged men and women: the OPEN Study. *The American journal of clinical nutrition*, 86(2):382–7.

Vafadar, A., Côté, J. N., and Archambault, P. S. (2012). The Effect of Muscle Fatigue on Position Sense in an Upper Limb Multi-joint Task. *Motor Control*, 16(2):265–283.

Viegas, S. F., Yamaguchi, S., Boyd, N. L., and Patterson, R. M. (1999). The dorsal ligaments of the wrist: Anatomy, mechanical properties, and function. *Journal of Hand Surgery*, 24(3):456–468.

Voight, M. L., Hardin, J. A., Blackburn, T. A., Tippett, S., and Canner, G. C. (1996). The effects of muscle fatigue on and the relationship of arm dominance to shoulder proprioception. *Journal of Orthopaedic & Sports Physical Therapy*, 23(6):348–352.

Vøllestad, N. K. (1997). Measurement of human muscle fatigue. *Journal of Neuroscience Methods*, 74(2):219–227.

Volz, R. G., Lieb, M., and Benjamin, J. (1980). Biomechanics of the wrist. *Clinical Orthopaedics and Related Research*, NO 149:112–117.

Wall, J., Xu, J., Reviews, X. W. B. R., and undefined 2002 (2002). Human brain plasticity: an emerging view of the multiple substrates and mechanisms that cause cortical changes and related sensory dysfunctions after injuries of. *Elsevier*.

Walsh, L. D., Hesse, C. W., Morgan, D. L., and Proske, U. (2004). Human forearm position sense after fatigue of elbow flexor muscles. *The Journal of physiology*, 558(Pt 2):705–15.

Wan, J., Qin, Z., Wang, P., and Sun, Y, X. L. (2017). Muscle fatigue: general understanding and treatment. *Experimental Molecular Medicine*.

Williams, C. and Ratel, S. (2009). *Human muscle fatigue*. Routledge.

Wolfe, F., Hawley, D. J., and Wilson, K. (1996). The prevalence and meaning of fatigue in rheumatic disease. *The Journal of rheumatology*, 23(8):1407–17.

Wright, J., McCloskey, D., and Fitzpatrick, R. C. (1999). Effects of muscle perfusion pressure on fatigue and systemic arterial pressure in human subjects. *Journal of Applied Physiology*, 86(3):845–851.

www.memorangapp.com (2019). Anatomy intercalation interview (head and neck osteology and forearm and hand anatomy) flashcards | memorang. https://www.memorangapp.com/flashcards/244195/Anatomy+Intercalation+Interview/.

www.teachmeanatomy.com (2019). Muscles of the anterior compartment of the forearm. https://teachmeanatomy.info/upper-limb/muscles/anterior-forearm/.

Yoshii, Y., Yuine, H., Kazuki, O., lin Tung, W., and Ishii, T. (2015). Measurement of wrist flexion and extension torques in different forearm positions. *BioMedical Engineering Online*, 14(1).

Zabihhosseinian, M., Holmes, M. W. R., and Murphy, B. (2015). Neck muscle fatigue alters upper limb proprioception. *Experimental Brain Research*, 233(5):1663–1675.

Zwarts, M., Bleijenberg, G., and van Engelen, B. (2008). Clinical neurophysiology of fatigue. *Clinical Neurophysiology*, 119(1):2–10.